UNIVERSITY OF TURKU

MAGNETIC RESONANCE IMAGING IN ALZHEIMER'S DISEASE, MILD COGNITIVE IMPAIRMENT AND NORMAL AGING

Multi-template tensor-based morphometry and visual rating

Terhi Tuokkola

TURUN YLIOPISTON JULKAISUJA – ANNALES UNIVERSITATIS TURKUENSIS
SARJA – SER. D OSA – TOM. 1531 | MEDICA – ODONTOLOGICA | TURKU 2021

UNIVERSITY OF TURKU

MAGNETIC RESONANCE IMAGING IN ALZHEIMER'S DISEASE, MILD COGNITIVE IMPAIRMENT AND NORMAL AGING

Multi-template tensor-based morphometry and visual rating

Terhi Tuokkola

TURUN YLIOPISTON JULKAISUJA – ANNALES UNIVERSITATIS TURKUENSIS
SARJA – SER. D OSA – TOM. 1531 | MEDICA – ODONTOLOGICA | TURKU 2021

University of Turku

Faculty of Medicine
Clinical physiology and nuclear medicine
Doctoral Program in Clinical Research
Turku PET Centre
Turku, Finland

Supervised by

Professor Juha Rinne
Turku PET Centre
Turku University Hospital
University of Turku
Turku, Finland

Professor Riitta Parkkola
Turku University Hospital
Department of Radiology
University of Turku
Turku, Finland

Reviewed by

Docent Michaela Bode
Oulu University Hospital
Department of Clinical Radiology
University of Oulu
Oulu, Finland

Docent Anna Sutela
Kuopio University Hospital
Diagnostic Imaging Centre
Department of Clinical Radiology
University of Kuopio
Kuopio, Finland

Opponent

Professor Taina Autti
University of Helsinki
Helsinki, Finland

The originality of this publication has been checked in accordance with the University of Turku quality assurance system using the Turnitin Originality Check service.

ISBN 978-951-29-8351-3 (PRINT)
ISBN 978-951-29-8352-0 (PDF)
ISSN 0355-9483 (Print)
ISSN 2343-3213 (Online)
Painosalama Oy, Turku, Finland 2021

To Antti

UNIVERSITY OF TURKU
Faculty of Medicine
Institute of Clinical Medicine
Clinical physiology and nuclear medicine
TERHI TUOKKOLA: Magnetic Resonance Imaging In Alzheimer's Disease, Mild Cognitive Impairment And Normal Aging. Multi-template tensor-based morphometry and visual rating.
Doctoral Dissertation, 135 pp.
Doctoral Program in Clinical Research
February 2021

ABSTRACT

Alzheimer's disease (AD) is the most common neurodegenerative disease preceded by a stage of mild cognitive impairment (MCI). The structural brain changes in AD can be detected more than 20 years before symptoms appear. If we are to reveal early brain changes in AD process, it is important to develop new diagnostic methods.

Magnetic resonance imaging (MRI) is an imaging technique used in the diagnosis and monitoring of neurodegenerative diseases. Magnetic resonance imaging can detect the typical signs of brain atrophy of degenerative diseases, but similar changes can also be seen in normal aging. Visual rating methods (VRM) have been developed for visual evaluation of atrophy in dementia. A computer-based tensor-based morphometry (TBM) analysis is capable of assessing the brain volume changes typically encountered in AD.

This study compared the VRM and TBM analysis in MCI and AD subjects by cross-sectional and longitudinal examination. The working hypothesis was that TBM analysis would be better than the visual methods in detecting atrophy in the brain. TBM was also used to analyze volume changes in the deep gray matter (DGM). Possible associations between TBM changes and neuropsychological tests performances were examined. This working hypothesis was that the structural DGM changes would be associated with impairments in cognitive functions.

In the cross-sectional study, TBM distinguished the MCI from controls more sensitively than VRM, but the methods were equally effective in differentiating AD from MCI and controls. In the longitudinal study, both methods were equally good in the evaluation of atrophy in MCI, if the groups were sufficiently large and the disease progressed to AD. Volume changes were found in DGM structures, and the atrophy of DGM structures was related to cognitive impairment in AD.

Based on these results, a TBM analysis is more sensitive in detecting brain changes in early AD as compared to VRM. In addition, the study produced information about the involvement of the deep gray matter in cognitive impairment in AD.

KEYWORDS: Alzheimer's disease, mild cognitive impairment, normal aging, visual rating method, tensor-based morphometry, deep gray matter, cognitive impairment

TURUN YLIOPISTO
Lääketieteen tiedekunta
Kliininen laitos
Kliininen fysiologia ja isotooppilääketiede
TERHI TUOKKOLA: Magneettikuvaus Alzheimerin taudissa, lievässä muistihäiriössä ja normaalissa ikääntymisessä: Tensoripohjainen muotoanalyysi ja visuaalinen arviointimenetelmä
Väitöskirja, 135 s.
Turun kliininen tohtoriohjelma
Helmikuu 2021

TIIVISTELMÄ

Alzheimerin tauti (AT) on yleisin dementoiva sairaus, jota edeltää yleensä lievä muistitoimintojen heikentyminen. AT:n aivomuutoksia voidaan todeta yli 20 vuotta ennen sairastumista. Jotta vielä varhaisempia AT:n aivomuutoksia voidaan todeta, on tärkeää kehittää uusia diagnostisia menetelmiä.

Magneettikuvausta (MK) käytetään rappeuttavien aivosairauksien diagnostiikassa ja seurannassa. MK:lla voidaan havaita aivorappeumasairauksille tyypillistä kutistumista, mutta samanlaisia muutoksia voi esiintyä myös normaalissa ikääntymisessä. Aivorappeuman arviointiin on kehitetty silmämääräisiä arviointimenetelmiä. Tietokoneperusteinen tensoripohjainen muotoanalyysi (TPM) laskee esimerkiksi AT:lle tyypillisiä aivojen tilavuusmuutoksia.

Tämä tutkimus vertaili silmämääräisiä arvioitimenetelmiä ja TPM:ä lievässä muistitoimintojen heikentymisessä ja AT:ssa poikittais- ja pitkittäistutkimuksella. TPM:n oletettiin olevan silmämääräisiä menetelmiä parempi tunnistamaan aivojen kutistumismuutoksia. Lisäksi TPM:llä tutkittiin AT:iin liittyviä aivojen syvän harmaan aiheen muutoksia, joita verrattiin neuropsykologisten testien tuloksiin. Syvän harmaan aineen kutistumisen oletettiin olevan yhteydessä tietojenkäsittelyn heikentymiseen.

Tulosten perustella TPM tunnisti AT:iin liittyviä aivomuutoksia silmämääräistä menetelmää paremmin jo lievän muistitoimintojen heikentymisen vaiheessa. AT:iin liittyviä aivomuutoksia löytyi myös aivojen syvästä harmaasta aineesta ja ne olivat osittain yhteydessä neuropsykologisten testien tuloksiin.

Tutkimuksen perusteella TPM voi parantaa AT:n varhaisdiagnostiikkaa verrattuna silmämääräisiin arviointimenetelmiin. Tutkimus antoi myös tietoa aivojen syvän harmaan aineen osallisuudesta ihmisen tietojenkäsittelyyn.

AVAINSANAT: Alzheimerin tauti, lievä muistitoimintojen heikentyminen, normaali ikääntyminen silmämääräinen arviointimenetelmä, tensoripohjainen muotoanalyysi, syvä harmaa aine, heikentynyt tietojenkäsittely

Table of Contents

Abbreviations

3D	three-dimensional
AD	Alzheimer's disease
AI	artificial intelligence
ALS	amyotrophic lateral sclerosis
aMCI	amnestic mild cognitive impairment
ANCOVA	analysis of covariance model
ANN	artificial neural network
ANOVA	one-way analysis of variance
APO ε4	apolipoprotein ε4 (epsilon)
AT	Alzheimerin tauti
AUC	area under curve
bvFTD	behavioral variant of frontotemporal dementia
CD	Centricity DICOM viewer
CERAD	the Consortium to Establish a Registry for Alzheimer's Disease
Cκ	Cohen's κ (Cohen's kappa coefficient)
cML	classical machine learning
CSF	cerebrospinal fluid
CT	computed tomography
Cwκ	Cohen's weighted κ (Cohen's weighted kappa coefficient)
DBL	dementia with Lewy bodies
DEM	difference of the estimated mean
DEIV	difference of the estimated index value
df	degree of freedom
DGM	deep gray matter
DL	deep learning
ED	electron density
EIV	estimated index value
EM	estimated mean
^{18}F-FDG	^{18}fluorine-fluorodeoxyglucose
FFE	fast field echo
Fκ	Fleiss' κ (Fleiss' kappa coefficient)

FLAIR	fluid attenuated inversion recovery
FOV	field of view
FSPGR	fast spoiled gradient echo
FTD	frontotemporal dementia
GE	General Electric
HC	hippocampus
IC	inner calvarium diameter
ICC	interclass correlation coefficient
IV	index values
KW	Kendall's W (Kendall's coefficient of concordance)
LAC	left anterior cingulate
LAT	left anterior temporal
LV	diameter of the lateral ventricles
MAT	mean anatomical template
MCI	mild cognitive impairment
MCIp	mild cognitive impairment progression
MCIs	mild cognitive impairment stable
ML	machine learning
MMSE	Mini-Mental State Examination
MRI	magnetic resonance imaging
MTA	medial temporal atrophy
MTL	medial temporal lobe
N.A.	not available
naMCI	non-amnestic mild cognitive impairment
NFT	neurofibrillary tangles
NINCS-ADRDA	National Institute of Neurological and Communicative Disorders and Stroke/Alzheimer's Disease and Related Disorders Association
N.S.	not statistically significant
PD	proton density
PET	positron emission tomography
PET-CT	positron emission tomography-computed tomography
PET-MRI	positron emission tomography-magnetic resonance imaging
^{11}C-PIB	^{11}carbon-Pittsburgh compound B
ρ	population Pearson's correlation coefficient (rho)
RO	ratio of coefficient
ROC	receiver operating characteristic
ROI	region of interest
SAS	Statistical Analysis Software
SD	standard deviation
SENSE	sensitivity encoding

SPSS	Statistical Package for the Social Sciences
STIR	Short tau inversion recovery, Short-TI Inversion Recovery
T	Tesla
T1, T2	relaxation times in magnetic resonance imaging
TBM	tensor-based morphometry
TH	temporal horn
TMT-A	Trail Making Test A
TPM	tensoripohjainen muotoanalyysi
TV	diameter of the third ventricle
Uκ	unspecified κ (unspecified kappa coefficient)
USA	United States of America
Wκ	weighted κ (weighted kappa coefficient)
WMS-R	Wechsler Memory Scale R
VBM	volumetric-based morphometry
VRM	visual rating method
yr	year

List of Original Publications

This dissertation is based on the following original publications, which are referred to in the text by their Roman numerals:

I. Tuokkola T., Koikkalainen J., Parkkola R., Karrasch M., Lötjönen J., Rinne J. O. Visual rating method and tensor-based morphometry in the diagnosis of mild cognitive impairment and Alzheimer's disease: a comparative magnetic resonance imaging study. *Acta Radiologica*, 2016;57(3):348–55

II. Tuokkola T., Koikkalainen J., Parkkola R., Karrasch M., Lötjönen J., Rinne J. O. Longitudinal changes in the brain in mild cognitive impairment: A magnetic resonance imaging study using the visual rating method and tensor-based morphometry. *Acta Radiologica*, 2018;59(8):973–979.

III. Tuokkola T., Karrasch M., Koikkalainen J., Parkkola R., Lötjönen J., Löyttyniemi E., Hurme S., Rinne J. O. Association between Deep Gray Matter Changes and Neurocognitive Function in Mild Cognitive Impairment and Alzheimer's Disease: A Tensor-Based Morphometric MRI Study. *Dementia and Geriatric Cognitive Disorders*, 2019;12:1–11.

1 Introduction

Alzheimer's disease (AD) is the world's most common neurodegenerative disease, causing a progressive decline in daily activities (Alzheimer's Association, 2016). AD is a degenerative brain disease, which is caused by a progressive accumulation of pathological protein products (beta-amyloid plaques and tau tangles) within the brain (Alzheimer's Association, 2016). The accumulation may begin more than two decades before the appearance of any clinical symptoms and eventually leads to neuronal damage and death (Alzheimer's Association, 2016). The most common risk factors of AD are older age, a positive family history and carrying the apolipoprotein (APO) ε4 gene (Alzheimer's Association, 2016). The prevalence of AD is 11% at the age of 65 years but it rises up to 32% at the age of 85 years. The number of new diagnoses increases also with age (Alzheimer's Association, 2016). Mild cognitive impairment (MCI) is a possible pre-condition of AD, in which cognitive abilities have declined, but do not influence activities of daily living (Alzheimer's Association, 2016; Petersen, 2016). MCI can revert back to normal cognition, remain stable or lead to other forms of dementia (Alzheimer's Association, 2016). However, almost every third MCI subject will develop AD in 5 years (Alzheimer's Association, 2016).

The diagnosis of AD is mostly clinical, but it is supplemented by a variety of diagnostic laboratory and imaging biomarkers (Alzheimer's Association, 2016). There is no curative treatment for AD and although with medication it is possible to slow down the progression of symptoms at the early stage of AD, unfortunately the therapeutic effect is only transitory (Alzheimer's Association, 2016).

Atrophy of the medial temporal lobe (MTL) is the main structural finding in the brain of subjects with AD and it has also been associated with MCI (Dubois et al., 2007; Apostolova et al., 2012). The degree of medial temporal atrophy (MTA), especially hippocampal atrophy, is associated with the degree of severity of AD (Frisoni et al., 2010; Jack Jr et al., 2002). The atrophy of MTA may also help in the differential diagnosis between healthy controls and subjects of progressive MCI, stable MCI and AD (Chételat et al., 2005; Bozzali et al., 2006; Dubois et al., 2007; Hämäläinen et al., 2007; Frisoni et al., 2010; Devanand et al., 2012; Tondelli et al., 2012; Braskie & Thompson, 2014). Atrophy of MTA has also been shown to predict

the later conversion to AD (Jack et al., 1999; Jack et al., 2000; Rusinek et al., 2004; Duara et al., 2008; Vemuri & Jack, 2010). A limitation of evaluating MTA or any gray matter atrophy is that it is not specific for any particular neurodegenerative disease as similar findings can be seen in normal aging and all neurodegenerative diseases (Fox & Freeborough, 1997; Jack Jr et al., 2002; Duara et al., 2008; Frisoni et al., 2010). However, in neurodegenerative diseases, the MTA process is stronger and more rapid than in normal aging (Driscoll et al., 2009; Chou et al., 2010; McDonald et al., 2012; Lockhart & DeCarli, 2014) and the atrophy has often a characteristic additional distribution according to the type form of neurodegenerative disease (Park & Moon, 2016).

During the neurodegenerative process, the cortical gray matter atrophy is not restricted to the MTL or to any typical areas, but spreads to the other regions of the brain as well (Thompson et al., 2003; Pini et al., 2016). In MCI and AD, the cortical atrophy spreads to other regions of the temporal lobes, and parietal and frontal lobes (Jacobs et al., 2011; Apostolova et al., 2012; McDonald et al., 2012; Trzepacz et al., 2014; Pini et al., 2016). Simultaneously with the cortical gray matter atrophy, an enlargement of cerebrospinal fluid (CSF) spaces and atrophy of deep gray matter (DGM) nuclei can be observed (de Jong et al., 2008; Liu et al., 2010; Cho et al., 2014; Pini et al., 2016; Yi et al., 2016).

Similar to the situation seen with cortical atrophy, the ventricular enlargement and DGM atrophy are progressive conditions and not specific for MCI or AD only (de Jong et al., 2008; Apostolova et al., 2012). Actually, DGM atrophy is a typical finding in diseases primarily affecting these brain structures, like Parkinson disease, vascular dementia, Huntington disease and multiple sclerosis (Kassubek et al., 2005; Batista et al., 2012; Mak et al., 2014; Debernard et al., 2015). In addition, atrophy of DGM has been shown to predict the conversion from MCI to AD, and it has also been associated with the severity of AD (Liu et al., 2010; Roh et al., 2011; Yi et al., 2016). Furthermore, DGM atrophy is related to the occurrence of dementia in healthy older subjects (de Jong et al., 2012). It has been argued that the enlargement of CSF spaces could be used in the differential diagnosis of control, MCI and AD subjects (Nestor et al., 2008), and also to predict MCI conversion to AD (Macdonald et al., 2013).

The neuronal degeneration in AD (and other neurodegenerative diseases) is associated with a progressive cognitive decline (Apostolova et al., 2012). In MCI and AD, MTA and hippocampal atrophy are associated with cognitive impairments (particularly in episodic memory functions) and predict a future cognitive decline (Du et al., 2006; Nadel & Hardt, 2011; Li et al., 2012; McDonald et al., 2012; Velayudhan et al., 2013; Pini et al., 2016). In addition, global brain atrophy and ventricular enlargement have been linked with a cognitive decline (Apostolova et al., 2012). Frontal atrophy is typically associated with impairment in executive functions

(McDonald et al., 2012). Nonetheless, to date, the reports on the possible associations between DGM atrophy and cognition in MCI and AD have been somewhat contradictory and based on only a few studies (de Jong et al., 2008; Roh et al., 2011; Cho et al., 2014; Hilal et al., 2015; Yi et al., 2016; Nie et al., 2017). However, most of the reports have found an association between DGM atrophy and a general cognitive decline (de Jong et al., 2008; Roh et al., 2011; Cho et al., 2014; Hilal et al., 2015; Yi et al., 2016; Nie et al., 2017).

Magnetic resonance imaging (MRI) is the most popular imaging method applied in MCI and AD diagnostics (Femminella et al., 2018). It is a non-invasive and radiation-free technique with excellent contrast and resolution for examining the anatomy and pathology of the brain (Symms et al., 2004; Oxtoby et al., 2017).

The visual rating method (VRM) of Scheltens et al. (1992) has been developed for the evaluation of MTA, and it is a widely used method in clinical practice. The method scores atrophy into 5 stages from 0 to 4 on the basis of MTL atrophy. Categories 0-1 represent normal stages and 2-4 pathological stages (Scheltens et al., 1992), but the score 2 indicates normal MTL in subjects above 75 years of age (Pereira et al., 2014). The VRM can separate early AD, amnestic MCI and other dementia subjects from healthy controls and can predict the conversion of healthy controls to MCI and MCI to AD (Wahlund et al., 1999; Wahlund et al., 2000; DeCarli et al., 2007; Duara et al., 2008; Appel et al., 2009; Urs et al., 2009). The general sensitivity and specificity of the VRM is approximately 80-85% in differentiating AD from controls, and approximately 80 % in differentiating MCI from controls (Scheltens et al., 1992; Dubois et al., 2007; Duara et al., 2008; Frisoni et al., 2010). In predicting the progression of MCI to AD, the sensitivity is somewhat less impressive, 51-72%, and specificity is 68-81% (Visser et al., 2002; Korf et al., 2004; DeCarli et al., 2007). The strength of VRM is that it is easy to apply, cost-effective and does not need special software. Furthermore, pathologies outside the MTL can also be observed during the analysis. The limiting element of the Scheltens' VRM is its usability for estimating the extent of the atrophy in brain areas other than in the MTA (Ferreira et al., 2009) and inter-rater reliability may be compromised when conducted by less experienced raters (Scheltens et al., 1995).

The VRM devised by Victoroff et al. (1994) was developed for the evaluation of global cortical atrophy in AD. It was divided into the categories according to the brain lobes (frontal, temporal and parietal lobes), and the rating stages were from 0 to 2. The method suffered from difficulties on reliable visual readings and in its possibilities of identifying the different dementia forms (Victoroff et al., 1994). However, it is still the only published VRM which can be utilized for evaluating the atrophy in the whole frontal area. Later, Davies et al. (2009) published their VRM for frontal subregions and Harper et al. (2016) slightly modified it in their own work.

Tensor-based method (TBM) is a fully automated voxel-based method that can objectively analyze the local expansion or shrinking of the brain tissue or CSF spaces in any brain area. TBM is based on the registration of a subject image with a template image and computing the determinant of the Jacobian matrix of the resulting deformation field (Hua et al., 2008a). This measure, termed the Jacobian, estimates the local volume change (Hua et al., 2008a). TBM has been used in cross-sectional (Lepore et al., 2008; Brun et al., 2009; Leow et al., 2009) and longitudinal studies (Apostolova et al., 2006; Teipel et al., 2007; Hua et al., 2008a; Hua et al., 2008b; Leow et al., 2009; Wolz et al., 2011), and in clinical trials (Thompson & Apostolova, 2007), but there has been rather limited exploitation in clinical imaging work. TBM is capable of separating controls, MCI subjects and AD subjects from each other and it has been used for predicting the progression of MCI and AD (Hua et al., 2008a; Hua et al., 2008a; Koikkalainen et al., 2011). The TBM results associate also with cognitive decline, genetic AD profiles and CSF markers (Hua et al., 2008a; Hua et al., 2008b; Hua et al., 2010). One benefit of TBM is that it can be used in the very early stages of dementia, before the appearance of any severe cognitive decline (Hua et al., 2008a). It is also free of subjective interpretations and the analysis extends outside the MTL. The limitations for its clinical use are the need for extra time, special expertise and computers with high computation capacity.

The aim of this thesis was to evaluate the usefulness and applicability of TBM in differentiating subjects of normal aging, MCI, progressive MCI, stable MCI and AD in both cross-sectional and longitudinal clinical settings as compared to the VRMs of Scheltens et al. (1992) and Victoroff et al. (1994). In addition, the TBM volume changes were evaluated in the area of DGM, and relationships were assessed between DGM changes and neurocognitive functions in control, MCI, and AD groups. The first hypothesis was that TBM would be more sensitive than VRMs in recognizing MCI and AD volume changes of the brain. The second hypothesis was that the TBM volume changes in DGM area would exist already in the MCI as well as in the AD groups. The third hypothesis was that DGM atrophy would be associated with impairments in cognitive functions.

2 Review of the Literature

2.1 Normal aging

2.1.1 Normal aging

In the literature, the nomenclature of advanced aging brain includes both “normal aging” (age-related differences in brain structure and function, but the absence of clinically significant impairment) and “healthy aging” (the apparent structural and functional preservation of the brain with advancing age), which is considered less common (Lockhart & DeCarli, 2014).

Aging is a normal phenomenon in the human brain. In childhood, it can be seen as a maturation process of the developing brain (Gennatas et al., 2017), but in adulthood, it is converted into a structural and functional degeneration process continuing through the rest of the individual’s life (Lockhart & DeCarli, 2014). In older age, the influence of the aging process of the brain begins to be evident both subjectively and objectively in everyday living and it is possible to detect this phenomenon in structural, functional, cognitive and metabolic studies (Lockhart & DeCarli, 2014; Goyal et al., 2017). The aetiology of these changes is still poorly understood (Goyal et al., 2017), and a confounding factor is the possibility of underlying neurodegenerative processes, which may point to an increased risk of later neurodegeneration and cognitive decline (Lockhart & DeCarli, 2014).

2.1.2 Macrostructural gray matter changes in the aging brain

The regional structural volume variation and changes in cortical thickness belong to the normal maturation of the gray matter and begin already during early years (Toga et al., 2006; Mu et al., 2017). A pure grey matter volume loss begins after the age of 20 (Terry & Katzman, 2001; Harada et al., 2013; Fleischman et al., 2014; Storsve et al., 2014) and whole-brain volume reductions are evident by age 30 (Lockhart & DeCarli, 2014). In the aging brain, the whole-brain volume reduction is about 0.45-0.52 % per year (Lockhart & DeCarli, 2014; Castellano et al., 2019). The volume loss in the aging brain is more usual in the frontal lobes or prefrontal areas than in

the temporal or parietal lobes (Lockhart & DeCarli, 2014; Minkova et al., 2017; Toepper, 2017; Pergher et al., 2019), In addition, the degeneration patterns of the aging brain are different and the decline speed is slower than encountered in neurodegenerative diseases (Lockhart & DeCarli, 2014; Minkova et al., 2017). Brain regions like the parahippocampal gyrus, cingulate cortex, or occipital brain regions have been shown to be spared from age-related changes (Toepper, 2017).

The degree of hippocampal volume loss has been demonstrated to be dependent on age (Raz et al., 2005; Du et al., 2006; Pfefferbaum et al., 2013; Lockhart & DeCarli, 2014; Toepper, 2017). In adulthood, the size of the hippocampus remains quite stable up to the age 60, but there is markedly accelerating degeneration after that time point (Long et al., 2012; Lockhart & DeCarli, 2014). In the meta-analysis conducted by Fraser et al. (2015), hippocampal atrophy rates for individuals aged under 55 years were 0.38 % per year, for age 55-70 years, 0.98 % per year and for those aged over 70 years, they were 1.12% per year. With aging, the degenerative volume changes have been observed to be clearer in the anterior part of the hippocampus (Gordon et al., 2013; Bettio et al., 2017). The hippocampal grey matter volume appears to be an important predictor for memory performance in older adults (Toepper, 2017).

There are some reports of normal aging from the basal ganglia and thalamic areas. A volume loss of the caudate nucleus has been shown to begin at puberty (Toga et al., 2006), a density loss of striatal area is already evident in young adults (Sowell et al., 1999) and a volume loss of caudate nucleus and putamen in older adults (Long et al., 2012; Castellano et al., 2019). Pfeffenbaum et al. (2013) conducted a longitudinal study and found that older age was associated with a thalamic volume loss, and furthermore the decline was faster after 60 years of age (Fama & Sullivan, 2015). There are also reports of an age-related thalamic volume loss e.g. Long et al. (2012) and Toepper (2017).

2.1.3 Neurocognitive functions and age-related changes

Cognition can be conceptualized as human information processing functions enabling the individual to adapt to changing circumstances, e.g. to learn, to focus one's attention, plan ahead, communicate with others and solve intricate problems (Kolb & Whishaw, 2015). Cognitive functions have typically been divided into separate domains, many of which are associated with the neural activity in distinct brain areas or networks (Kolb & Whishaw, 2015).

An atrophy of cortical gray matter is a common finding in older age without dementia (Sandeman et al., 2013). However, poorer cognitive performances together with age-related gray matter volume degeneration have been associated with a future cognitive decline (Lockhart & DeCarli, 2014; Dumurgier et al., 2017; Farokhian et

al., 2017) and even predicted the conversion of normal aging to incident AD (Pergher et al., 2019). On the other hand, higher volumes of the frontal and temporo-parietal cortices have been reported to confer lifelong protection of cognitive performances (Malpetti et al., 2017).

The hippocampus is a critical structure for memory, especially for episodic memory, spatial learning (Flores et al., 2015; Bettio et al., 2017) and the regulation of emotional behavior (Bettio et al., 2017). It has been reported that cognitive deficiencies are more obvious in cases in which there is bilateral hippocampal atrophy (Bettio et al., 2017). In normal aging, the hippocampal atrophy has in some studies been associated with poorer episodic memory performance and a future cognitive decline (Lockhart & DeCarli, 2014; Bettio et al., 2017; Dumurgier et al., 2017; Toepper, 2017), but on the other hand, the hippocampal atrophy is also a usual finding in normal cognitive aging (Cavallin et al., 2012).

In the area of the DGM, the thalamus mediates information transfer between the hippocampus and cortical areas (Pini et al., 2016). Thalamus directs attention and is involved in emotional, motivational and cognitive abilities (Nie et al., 2017). Thalamic atrophy has been related to the age-related cognitive decline in executive functions including attention, information processing speed, and working memory (Fama & Sullivan, 2015; Pergher et al., 2019). The caudate nucleus participates in learning and memory processes and has a supporting role in planning demanding actions and execution strategies (Liu et al., 2010; Cho et al., 2014). Atrophy of the caudate nucleus has been associated with the age-related cognitive decline such as in learning, attention and executive function (Castellano et al., 2019). It is believed that the nucleus accumbens participates in behavior and memory functions in normal aging and AD (Pini et al., 2016). A reduced volume of the nucleus accumbens has been associated with poorer global cognitive performance (de Jong et al., 2008; Pini et al., 2016; Yi et al., 2016) and this volume reduction also predicted the cognitive decline in older subjects (Pini et al., 2016; Yi et al., 2016).

The most vulnerable cognitive abilities in the aging process are the so-called fluid cognitive functions, including the domains of information processing speed and executive functions (Hedden & Gabrieli, 2004; Craik & Salthouse, 2008; Toepper, 2017). The functions most resistant to the effects of aging are crystallized cognitive abilities in the verbal domain, including vocabulary and conceptual thinking (Harada et al., 2013; Hartshorne & Germine, 2015).

2.2 Mild cognitive impairment and Alzheimer's disease

2.2.1 Mild cognitive impairment (definition, criterion, epidemiology, progression, clinical diagnosis)

MCI can be seen as a transition zone between normal cognitive aging and the cognitive decline of dementia. In MCI, an aged subject fulfills the criteria of a subjective or objective cognitive decline and impairment in one or more cognitive domains (learning and memory, social functioning, language, visuospatial function, complex attention, or executive functioning), but daily functioning is preserved and the criteria for dementia, delirium or other psychological disorders are not fulfilled (Sanford, 2017).

Cognitively normal subjects over 70 years old have a 5-6 % conversion rate per year to MCI (Petersen, 2016). It has been estimated that an overall prevalence of MCI is 3-22 % in persons over the age of 60 years and 16 % in those aged 70 years (Alzheimer's Association, 2016; Petersen, 2016; Sanford, 2017; Morley, 2018). Within 5 years, approximately 50 % of MCI subjects progress to dementia, but 20-50 % return to the cognitive performance associated with normal aging (Vega & Newhouse, 2014; Sanford, 2017; Morley, 2018). However, MCI subjects who have reverted to normal cognition still have a high risk to develop dementia, and a diagnosis of MCI can be considered as a prognostic value for later dementia (Knopman & Petersen, 2014; Vega & Newhouse, 2014; Sanford, 2017). AD is the most likely (40-60%) underlying pathology in MCI subjects (Petersen, 2016; Gillis et al., 2019). Most of the MCI subjects have an amnestic form of MCI (aMCI) (Petersen, 2016; Lo, 2017; Sanford, 2017). The typical aMCI subject has memory problems, which are a sign of an impairment in the ability to recall stored information (Knopman & Petersen, 2014; Sanford, 2017). If one considers all MCI subjects, then the aMCI subjects have the highest (nearly 10-15 % per year) possibility to progress to AD (Vega & Newhouse, 2014; Morley, 2018).

2.2.2 Alzheimer's disease (definition, criterion, epidemiology, progression, clinical diagnosis)

AD is an irreversible (Knopman & Petersen, 2014), progressive amnestic neurodegenerative disease that over time causes other cognitive, behavioral and neuropsychiatric changes, leading to difficulties in social life and abilities, even in simple activities of daily living (Dubois et al., 2010). The clinical picture of AD develops from a long-lasting asymptomatic preclinical stage AD via prodromal AD, where the subject has cognitive symptoms but does not yet fulfil the criteria of AD,

to AD dementia, where severe symptoms fulfil the AD diagnostic criteria (Dubois et al., 2007; Sperling et al., 2011; Petersen, 2016). In this categorization, MCI is included in the prodromal AD (Dubois et al., 2007).

In 2007, a proposed diagnostic criteria list for probable AD was published by Dubois et al. (2007):

- The core criterion is an observed episodic memory impairment over a period of six months or more.

In addition, at least one of the supportive features had to be positive:

a. Atrophy of medial temporal structures on MRI.
b. Abnormal cerebrospinal fluid biomarkers (amyloid-β42 peptide and total tau/phosphorylated tau).
c. Typical metabolic finding in molecular neuroimaging method, for example, in fluorodeoxyglucose (^{18}F-FDG) and Pittsburgh compound B (^{11}C-PIB) positron emission tomography (PET).
d. Familial genetic mutations (APO ε4).

The exclusion criteria are the history, clinical symptoms and findings of other diseases. In cases of definitive AD, the clinical diagnostic criterion has to be fulfilled together with either histopathological or genetic evidence of the disease.

AD is the most usual cause of dementia accounting for 50–75% of all dementias (Lane et al., 2018). The preclinical stage of AD may last for even 20 or more years (Alzheimer's Association, 2016), but the prevalence of symptomatic AD increases rapidly with age (Cornitiu, 2015). After 60 years of age, the prevalence doubles every 5 years, and in USA, 11–12% of subjects over 65 years old, 23% of subjects over 75 years old and 32–47% of subjects over 85 years old have AD (Cornitiu, 2015; Alzheimer's Association, 2016; Lane et al., 2018). The Alzheimer Europe organization website (Alzheimer Europe organization, 2013) has collated statistics about the prevalence of dementia (not only Alzheimer's disease) in different European countries in 2013: In Finland, the prevalence of dementia is somewhat lower than Alzheimer's disease in USA (5–8% in the 65–74 age group, 13–22% of those aged 75–84 and 22% in the age group of 85–89). In Sweden, the prevalence of dementia is closer to the value in USA (9–15% in the 65–74 age group, 22–38% of those aged 75–84 and 43% in individuals aged 85–89). However, after the age of 90 years, the prevalence of AD and dementia reaches a plateau (Alzheimer Europe organization, 2013; Bondi et al., 2017). The lifetime risk for AD at the age of 65 years is 17% for women and 9% for men in USA (Alzheimer's Association, 2016). The reason for the higher prevalence and incidence of AD in women may be their longer lifespan or due to a higher genetic risk (Alzheimer's Association, 2016; Riedel et al., 2016; Malpetti et al., 2017). The survival of AD after diagnosis is on average

4–8 years in subjects over 65 years old in USA and AD is the fifth leading cause of death among these patients (Alzheimer's Association, 2016).

2.2.3 Clinical examination and treatment of mild cognitive impairment and Alzheimer's disease

In the diagnostics of neurodegenerative diseases, a clinical examination is a keystone of neurologic work. European and Finnish website guidelines emphasize the importance of considering the etiology of neurodegenerative diseases in order to recognize typical dementing disorders (for example AD, Lewy body disease, and vascular and frontotemporal dementias) and to make differential diagnoses of other diseases causing memory symptoms (for example, psychiatric, metabolic and ischemic disorders, infections, and deficiency diseases) (Sorbi et al., 2012 in European academy of neurology; Suomalainen Lääkäriseura Duodecim et al., 2017). The clinical examination of memory complaining subject includes a subjective and objective evaluation of memory symptoms, cognition and the ability to cope with activities of daily living, an observation of cognition and function decline, and MRI or computer tomography (CT) study of the brain in order to examine the possible presence of atrophy and other structural changes (European academy of neurology; Suomalainen Lääkäriseura Duodecim et al., 2017). In addition, for the borderline subjects or to investigate the progression to AD, a larger neuropsychological test battery, a genetic test for APO ε4, AD biomarker (amyloid-β42 peptide and total tau/phosphorylated tau) assay of CSF, and PET studies (for example, ^{18}F-FDG, ^{11}C-PIB and tau tracer ^{18}F-flortaucipir) can be conducted (Vega & Newhouse, 2014; Counts et al., 2017).

There is no curative pharmacologic treatment for neurodegenerative diseases. The cholinesterase inhibitors (donepezil, rivastigmine, galantamine) and the glutamate receptor modulator (memantine) provide symptomatic and short-term benefits for AD subjects (Vega & Newhouse, 2014; Cornitiu, 2015; Apostolova, 2016). Cholinesterase inhibitors prevent the breakdown of acetylcholine whereas memantine is an N-methyl-D-aspartate receptor antagonist, but they do not impact on the underlying pathogenic mechanisms of AD (Vega & Newhouse, 2014; Cornitiu, 2015; Apostolova, 2016) and only delay the progression of neurodegenerative diseases (Knopman & Petersen, 2014). Memantine is only used together with cholinesterase inhibitors at the stage of AD (Apostolova, 2016).

2.2.4 Macrostructural gray matter brain changes in mild cognitive impairment and Alzheimer's disease (pathology)

In MCI and AD, the lack of specific structural brain changes is a major problem, since the progressive brain atrophy is a usual finding also in normal aging, as well as in the presymptomatic stages of neurodegenerative diseases and, in practice, all neurodegenerative diseases (Johnson et al., 2012; Tabatabaei-Jafari et al., 2015). In addition, the rate of atrophy varies widely depending on dementia risk factors, like a family history of AD and positive APO ε4 status (Flores et al., 2015; Tabatabaei-Jafari et al., 2015; Sanford, 2017). Group studies of MCI and AD have identified a typical distribution and progress rate of brain atrophy (Johnson et al., 2012; Tondelli et al., 2012; Tabatabaei-Jafari et al., 2015), although at the individual level, these results are not transferable to everyday clinical practice.

There are neuropathological hallmarks of AD i.e. extracellular amyloid deposits composed of insoluble amyloid-β42 peptide protein and intra-neuronal neurofibrillary tangles (NFTs) containing hyperphosphorylated tau protein (Flores et al., 2015). These molecular changes cannot be identified in MRI, but their presence is reflected as brain atrophy seen as decreased synaptic density, neuronal loss, and cell shrinkage (Tondelli et al., 2012). This type of atrophy is associated closely to cognitive symptoms of MCI and AD (Tondelli et al., 2012), spread of NTFs (Braak & Braak, 1991) and neuronal counts at autopsy (Bobinski et al., 2000; Jack Jr et al., 2002).

Along with NTFs, the atrophic changes begin in the entorhinal cortex and proceed to the hippocampus and limbic areas (Johnson et al., 2012; Mufson et al., 2012; Vega & Newhouse, 2014). Structurally, hippocampal atrophy is the earliest and most typical (clinical) finding in MCI and AD (Scheltens et al., 1992; Mufson et al., 2012). The hippocampal atrophy can be detected years before there is any cognitive decline and a diagnosis of neurodegenerative disease (Flores et al., 2015), as hippocampal volumes are reduced by 10–15% in aMCI subjects, by 15–30% in the early dementia stage and by 15–40% in AD subjects as compared to the healthy controls (Johnson et al., 2012; Pini et al., 2016). The hippocampal atrophy has also been seen in those cognitively healthy individuals that later developed MCI or AD (Flores et al., 2015). Based on these findings, the reduction in the hippocampal volume can be viewed as a strong predictor of dementia progression (sensitivity and specificity of 50–70%), and structural imaging with MRI as a biomarker tool for early AD detection (Johnson et al., 2012; Flores et al., 2015; Sanford, 2017).

After affecting the MTL, the atrophy extends to other cortical areas along a temporal–parietal–frontal route (Thompson et al., 2003; Whitwell et al., 2007; Tondelli et al., 2012; Teipel et al., 2013; Trzepacz et al., 2014; Vega & Newhouse, 2014; Pini et al., 2016). In general, the cortical atrophy spreading takes place at the

time of conversion MCI to AD, and cortical gray matter loss in the temporoparietal and frontal lobes has been estimated to be 14–19% at that time (Pini et al., 2016). However, in older MCI subjects or subjects in the progressive stage of MCI, the cortical atrophy has been detected earlier or it has been wider than in younger MCI subjects or subjects in the stable MCI stage (Tondelli et al., 2012). At the stage of late AD, the atrophy spreads to the sensorimotor and visual cortices, and more extensively to the frontal areas (Thompson & Apostolova, 2007; Tabatabaei-Jafari et al., 2015; Pini et al., 2016). However, even in the later affected areas of sensorimotor and visual cortices, the gray matter loss usually remains at 10% (Pini et al., 2016).

Visually, brain atrophy appears as a shrinking of the parenchyma of the brain, and the shrinking parenchyma causes an expansion of the CSF spaces. A widening of the ventral ramus of the lateral fissure and anterior temporal pole has been detected in aMCI and mild AD as compared to the controls or non-amnestic MCI (naMCI) subjects (Mufson et al., 2012). In the MCI stage, the ventricular expansion rate has been counted to be double that of healthy controls and also nearly doubled in the superior frontal and superior temporal sulcal spaces (Liu et al., 2013; Tabatabaei-Jafari et al., 2015). As a whole, 20%–25% of the whole brain shrinkage can be explained by ventricular expansion (Tabatabaei-Jafari et al., 2015). In the later AD stage, the widening of CSF spaces becomes more evident and extends to all cortical regions (Mufson et al., 2012).

Brain atrophy extends also to the DGM area in MCI and AD subjects (de Jong et al., 2008; Liu et al., 2010; Cho et al., 2014; Fama & Sullivan, 2015; Pini et al., 2016; Yi et al., 2016). The DGM can be defined to consist of the thalamus and basal ganglia. The definition of the basal ganglia is somewhat variable. According to Young and Sonne (2018), the bilateral basal ganglia are formed of corpus striatum, which contains the caudate and lenticular nuclei (the putamen, globus pallidus externus and internus), the subthalamic nucleus and the substantia nigra. Atrophy of the thalamus is a usual structural finding in MCI and AD subjects (Roh et al., 2011; Pini et al., 2016; Yi et al., 2016). The volume reduction is about 12% in AD subjects and even more in cases if the individual is an APO ε4 carrier or has positive tau levels in CSF (de Jong et al., 2008; Pini et al., 2016; Yi et al., 2016). The atrophy of thalamus is also connected to the severity of AD (Cho et al., 2014). The nucleus caudatus is also involved in AD, and at the baseline, reduced volumes in the right side are a predictor of the conversion from MCI to AD (Liu et al., 2010; Pini et al., 2016). In the later stages of AD, the volume reduction spreads to the left side (Cho et al., 2014; Pini et al., 2016). The putamen has displayed about an 11% bilateral volume reduction already in MCI stage and especially in moderate stages of AD (de Jong et al., 2008; Roh et al., 2011; Pini et al., 2016). Atrophy of the putamen has also been related to a greater severity of AD (Cho et al., 2014). The volume reduction

of the nucleus accumbens can be as much as 20% in late onset AD subjects (Pievani et al., 2013; Pini et al., 2016), but smaller volumes have also been reported in MCI subjects (Liu et al., 2010; Pini et al., 2016; Yi et al., 2016). The reduced volumes of the nucleus accumbens have been connected with the increased risk of progression from MCI to AD as well as with the severity of AD, and the volume reduction at the baseline is a predictor for MCI progression to AD (de Jong et al., 2008; Pini et al., 2016; Yi et al., 2016). The globus pallidus has not been considered to be involved in neurodegenerative diseases (de Jong et al., 2008; Pini et al., 2016; Yi et al., 2016).

2.2.5 Neurocognitive changes in mild cognitive impairment and Alzheimer's disease

MCI is usually classified into four subtypes: amnestic MCI (aMCI), non-amnestic MCI (naMCI) and multiple domain-based aMCI or naMCI (Kirova et al., 2015; Petersen, 2016). Amnestic MCI is defined as impaired episodic memory functions (both subjective and objective, as measured by episodic memory tests) in the absence of an impairment in other cognitive domains (Kirova et al., 2015; Petersen, 2016; Morley, 2018). Non-amnestic MCI, on the other hand, is defined as cognitive impairment in some cognitive domain other than episodic memory (Kirova et al., 2015; Petersen, 2016; Morley, 2018). Moreover, both aMCI and naMCI subjects can exhibit widespread impairments in more than one cognitive domain, even in the absence of a functional decline in everyday activities of living. In these cases, the labels of multiple domain aMCI or naMCI are applied (Kirova et al., 2015; Petersen, 2016; Morley, 2018). Amnestic MCI and multiple domain aMCI are the MCI subtypes that more frequently represent early, preclinical stages of AD. In the naMCI subtypes other degenerative etiologies are more likely (e.g. frontotemporal dementia and Levy body disease) (Petersen, 2016).

In aMCI and mild AD, the most impaired aspect of episodic memory function is the ability to encode and consolidate new episodic memory traces, and this impairment is most clearly seen in free recall tasks (Bennett et al., 2006; Koen & Yonelinas, 2014; Apostolova, 2016). In later stages of AD, the memory impairment becomes worse, encompassing the sense of familiarity (impaired performance in recognition tasks) as well the ability to recall old episodic memories from earlier life events (Lindeboom & Weinstein, 2004; Koen & Yonelinas, 2014; Apostolova, 2016). The explicit memory impairment is closely related to atrophy of the MTL, especially in the hippocampal-amygdala area (Whitwell et al., 2007; Liu et al., 2010; Pini et al., 2016).

In AD, the thalamic areas are atrophied and cognitive performances impaired in global cognition, attention, language, visuospatial, memory and executive functions (de Jong et al., 2008; Roh et al., 2011; Pini et al., 2016; Yi et al., 2016). The atrophy

in the caudate nucleus has been associated with memory performances and the cognitive decline in AD, and in late-onset AD in the visual memory and executive functions (Pievani et al., 2013; Pini et al., 2016; Yi et al., 2016). The putamen has been shown to have a role in language and executive function, e.g. this region is thought to be activated in learning and working memory tasks (Bellebaum et al., 2008; Dahlin et al., 2008; Pini et al., 2016). In MCI and AD, putaminal atrophy has been linked to the cognitive decline (de Jong et al., 2008; Roh et al., 2011; Cho et al., 2014; Pini et al., 2016). Atrophy of the nucleus accumbens has also been associated with the global cognitive performance in subjects complaining of memory problems, as well as in MCI and AD (de Jong et al., 2008; Pini et al., 2016; Yi et al., 2016).

2.3 Magnetic resonance imaging analyses of the brain

2.3.1 Magnetic resonance imaging

MRI is a non-invasive and radiation-free technique for examining anatomy and pathology of the brain, describing both location and morphological characteristics of the brain changes *in vivo* (Symms et al., 2004; Oxtoby et al., 2017). MRI has a superior spatial resolution with a relatively low cost, and it is easy to perform and a relatively patient-friendly examination (Teipel et al., 2013; Braskie & Thompson, 2014; Park & Moon, 2016; Femminella et al., 2018). In addition to good applicability, MRI has proved to be a reliable and validated technique in dementia diagnostics (Teipel et al., 2013; Matsuda, 2016), and it has become a popular scanning technique in dementia (Femminella et al., 2018).

MRI has potentially benefit in clinical dementia diagnostics: The diagnosis should be set as early as possible with a differential diagnosis of dementia subtypes and a prognostication of progression risk (Vemuri & Jack, 2010; Park & Moon, 2016). The information of other brain diseases is also important (Park & Moon, 2016). In addition, an evaluation of dementia progression is desirable in the follow-up stage (Vemuri & Jack, 2010). In research, MRI may be exploited in measuring the efficacy of therapeutics and as a screening method in clinical trials (Vemuri & Jack, 2010). MRI can also shed light on the disease mechanisms of dementia by helping to clarify relationships between cognition and neurodegeneration (Vemuri & Jack, 2010).

In dementia, evidence of atrophy is a typical and usually progressive finding in MRI, displaying a good correlation with cognitive deficits (Jack et al., 2004; Femminella et al., 2018). On the other hand, the atrophy of specific brain regions becomes visible years before clinical memory symptoms (Martin et al., 2010; Teipel

et al., 2013). In addition to local abnormalities in structure, changes in microstructure, function and metabolism have been postulated as MRI markers of neurodegenerative disease (Dubois et al., 2007; Oxtoby et al., 2017; Femminella et al., 2018).

The visual evaluation of MRI is still the usual diagnostic assessment method in dementia. However, digital technology has expanded from theory to clinical work as automated quantitative imaging has improved the diagnostics (Acharya et al., 2018; Femminella et al., 2018). When measuring the known pathological brain structures, region of interest (ROI)-based techniques or volumetry have been exploited (Vemuri & Jack, 2010). Several quantitative voxel-based methods have been developed for use in the analysis of whole brain atrophy (Vemuri & Jack, 2010): The most popular is voxel-based morphometry, which measures the concentration of gray matter (Ashburner & Friston, 2000; Veronese et al., 2013). Surface-based morphometry analyzes the surfaces of structural boundaries within the brain and measures not only the volume of gray matter, but also the cortical thickness (Veronese et al., 2013; Matsuda, 2016). TBM analyzes deformations in the brain by computing the determinant of the Jacobian matrix, and reveals the volume differences of the brain (Ashburner et al., 1998).

2.3.2 Visual rating methods in dementia

The basis of VRM lies in the observation that certain imaging findings can universally be connected to some underlying pathology, like the atrophy of MTL in AD (Harper et al., 2015; Pergher et al., 2019). Initially, the VRM for dementia was developed for research purposes to differentiate between dementia subjects in different stages from controls and to produce semi-quantitative data related to the degree of atrophy (Harper et al., 2015; Park & Moon, 2016). The possibility to exclude other brain illnesses was obtained as a by-product (Harper et al., 2015; Park & Moon, 2016). Later, the most reliable and practical methods have been adopted into the clinical dementia imaging work-up and even suggested to be used in diagnostics (Dubois et al., 2007; Harper et al., 2015; Park & Moon, 2016). The main emphasis of clinical dementia imaging is in the diagnostics of neurodegenerative diseases, in the exclusion of other illnesses, but also extends to the option to have preclinical or prognostic information about dementia (Harper et al., 2015; Park & Moon, 2016).

Visual rating is mainly an evaluation of cortical grey matter atrophy. In dementia, visual rating scales have been published for the evaluation of diffuse cortical atrophy, MTL atrophy, posterior cortical atrophy and frontotemporal lobar atrophy (Park & Moon, 2016). Of these, MTL atrophy and posterior cortical atrophy scales have been developed for AD diagnostics, frontotemporal lobe atrophy scales

for frontotemporal dementia diagnostics and diffuse cortical atrophy scales for all neurodegenerative diseases (Park & Moon, 2016). In addition, Fazekas et al. (1996) and Victoroff et al. (1994) have developed a visual rating method to allow an evaluation of white matter hyperintensity, where periventricular and deep white matter lesions are presumed to be of vascular-origin and related to the risk of vascular dementia and possibly to AD (Park & Moon, 2016). **Table 1** presents an overview of some of the more widely used visual rating methods.

Table 1. An overview of published visual rating methods. Modified and expanded from the publications of Park et al (2016) and Harper et al (2015).

	Publisher	Scale increments	MRI sequence	Reliability		Study Subjects	Sensitivity	Specificity
				Inter-rater	Intra-rater			
Diffuse cortical atrophy								
Global cortical atrophy scale	Pasquier et al. 1996	4	T2	>0.6 (Cwκ)	>0.7 (Cwκ)	N.A.	N.A.	N.A.
Ventricular enlargement scale	O'Donovan et al. 2013	4	T1	0.9 (ICC)	0.92 (ICC)	AD or DLB vs. controls	94 %	40 %
Victoroff (frontal, temporal, parietal atrophy)	Victoroff et al. 1994	3	T1	frontal: 0.68–0.92, temporal: N.A., parietal: 0.54–0.80 (Wκ)	frontal: 0.92, temporal: N.A., parietal: 0.87 (Wκ)	Dementia	N.A.	N.A.
Medial temporal lobe atrophy								
Scheltens	Scheltens et al. 1995	5	T1	0.72–0.84 (Cwκ)	0.83–0.94 (Cwκ)	AD	81 %	N.A.
Urs /Duara	Urs et al. 2009, Duara et al. 2008	5	T1 + software	0.75–0.94 (Uκ)	0.84–0.93 (Uκ)	Probable AD vs. controls	85 %	82 %
Modified MTA rating on axial scan	Kim et al. 2014	5	T1	0.64 (Uκ)	0.62/0.95 (Uκ)	AD vs. controls	76 %	86 %
DeLeon	DeLeon et al. 1989, 1997	4	T1	0.72 (Uκ)	N.A.	AD, MCI, controls	N.A.	N.A.
Galton	Galton et al. 2001	4	T1	0.36–0.49 (Fκ)	0.8 (Cκ)	AD, semantic dementia, FTD, controls	N.A.	N.A.
Kaneko	Kaneko et al. 2012	4	STIR + software	0.68 (Uκ)	0.79 (Uκ)	AD vs non-demended	88 %	79 %

	Publisher	Scale increments	MRI sequence	Reliability		Study Subjects	Sensitivity	Specificity
				Inter-rater	Intra-rater			
Posterior cortical atrophy								
Koedam scale	Koedam et al. 2011	4	T1, T2 FLAIR	0.65–0.84 (Cwκ)	0.93/0.95 (Cwκ)	AD vs. controls	58 %	95 %
Combined Scheltens + Koedam scales	Koedam et al. 2011					AD vs. controls	73 %	87 %
Frontotemporal lobar atrophy								
FTLA scale	Davies et al. 2009	5	T1	0.71 (Cwκ)	0.75 (Cwκ)	Semantic dementia	100 %	N.A.
FTLA scale	Davies et al. 2006, Kipps et al. 2007	5	T1	>0.7/0.62–0.71 (Cκ)	0.8/0.79–0.83 (Cκ)	bvFTD	53 %	N.A.
Ambikairajah	Ambikairajah et al. 2014	5	T1	0.91 (Uκ)	N.A.	ALS, ALS-FTD, bvFTD, controls		
Chow	Chow et al. 2011	5	T1	0.06–0.07 for LAC and 0.2 for LAT (KW)	N.A.	AD, FTD, controls	N.A.	N.A.
White matter hyperintensities								
Fazekas	Fazekas et al. 1996	4	T2	N.A.	N.A.	AD, controls	N.A.	N.A.
Victoroff	Victoroff et al. 1994	3	PD, T2 and T1	0.77–0.79 (Wκ)	0.86 (Wκ)	Dementia	N.A.	N.A.

FLAIR = fluid attenuated inversion recovery, STIR = short tau inversion recovery, PD = proton density, Cwκ = Cohen's weighted kappa coefficient, ICC = interclass correlation coefficient, Uκ = unspecified kappa coefficient, Fκ = Fleiss' kappa coefficient, Cwκ = Cohen's weighted kappa coefficient, Cκ = Cohen's kappa coefficient, LAC = left anterior cingulate, LAT= left anterior temporal, KW = Kendall's coefficient of concordance, DBL = dementia with Lewy bodies, FTD = frontotemporal dementia, bvFTD = behavioral variant of frontotemporal dementia, ALS = amyotrophic lateral sclerosis

In clinical work, the most popular visual rating scales are quick to learn, easy to use without special expertise in information technology, reliable and cost-effective, and produce an outcome of diagnostic value for clinical work (Harper et al., 2015). The most widely used MRI sequences are also suitable for routine scanning (Harper et al., 2015). The user-friendliness of the scales is inevitably a balance between a scale's complexity and reliability (Harper et al., 2015). Harper et al. (2015) have listed the factors affecting and/or improving the scale reliability and accuracy:

1. Rater-dependent: specific landmarks of the slices, training and training sets, reference images, detailed descriptions of the expected findings.
2. Technique-dependent: MRI sequence selection [contrast, resolution, three dimensional (3D)], image quality, slice positioning, validation of the sequence.
3. Scale-dependent: balance between number of scale steps (specificity, sensitivity, accuracy), age-specific cut-offs, combined scores from several rating scales, validation of the scales (correlation against other used measurement, validation against an established 'gold standard' measurement technique).

Disturbing factors decreasing the reliability of the scales are missing results of intra-rater and inter-rater differences, and understandable limitations in scale validation against a 'golden standard' measurement i.e. postmortem examination of brain tissue (Harper et al., 2015).

In the MTL rating, the scale of Scheltens et al. (1992) is the oldest and has achieved the largest success on the basis of impact number (Harper et al., 2015; Park & Moon, 2016). In this case, the subjective evaluation of the MTA is based on a reference-based five-point scale from 0 to 4 (**Table 2**, and **Figure 3** in chapter 4.2.4) (Scheltens et al., 1992; Scheltens et al., 1995). In the original publication of Scheltens et al. (1992), the scale results of the study groups were quantified and verified with the measurements of the choroid fissure width, the temporal horn width and the hippocampus formation height (**Figure 4** in chapter 4.2.4), and the MTA scores correlated well with these measurements as well as with the neuropsychological results and volumetric measurements. In the clinic, the reference-based five-point scaling is in widespread use, although its interpretation tends to be transformed into a more dichotomous form i.e. the scores 0–1 indicate normal findings and scores 2-4 point to AD pathology (Harper et al., 2015). However, the score 2 indicates normal MTL in subjects above 75 years of age (Pereira et al., 2014).

Table 2. Visual rating of medial temporal lobe atrophy of Scheltens et al 1992.

Score	Width of choroid fissure	Width of temporal horn	Height of hippocampal formation
0	normal	normal	normal
1	↑	normal	normal
2	↑↑	↑	↓
3	↑↑↑	↑↑	↓↓
4	↑↑↑	↑↑↑	↓↓↓

↑ = increase, ↓ = decrease

Since the 1980s, multiple studies with different measuring methods have demonstrated that an enlargement of the lateral ventricles and the third ventricle correlates with the severity of dementia and are indicators of generalized brain atrophy (Scheltens et al., 1992; Watson et al., 2010). O'Donovan et al. (2013) developed a visual rating scale for the evaluation of the ventricular enlargement in AD and DLB. However, despite the fact that the intra-rater and inter-rater results were very good or excellent with a sensitivity of 94%, the specificity was only 40%, suggesting that the scale was diagnostically "poor" (O'Donovan et al., 2013).

Visual rating methods have also been developed to allow the evaluation of global cortical atrophy. One is for AD subjects (Victoroff et al., 1994) and another for brain stroke patients with post-stroke dementia (Pasquier et al., 1996). In the study of Victoroff et al. (1994), the authors themselves reported major difficulties in obtaining reliable visual readings and were pessimistic for any possibilities of identifying different dementia forms. Pasquier et al. (1996) were more optimistic about the prospects of using their visual scale for assessing cortical atrophy in stroke patients. However, Scheltens et al. (1997) assessed Pasquier's rating scale as being difficult for AD evaluation with problems in reliability. Despite the faults encountered with Pasquier's scale, it has been used in research work and even in trials and multicenter studies (Harper et al., 2015). The visual atrophy rating of frontotemporal areas has later been developed by Davies et al. (2006; 2009), and Harper et al. (2016) on the basis of Davies' scale. However, Davies et al. (2006; 2009) and Harper et al. (2016) did not analyze the whole frontal lobe, but concentrated only on some of its subareas.

2.3.3 Artificial intelligence

Artificial Intelligence (AI) (**Figure 1**) is a branch of computer science and a hypernym for the development of computer algorithms, which are able to perform complicated tasks or tasks that imitate human intelligence (Hosny et al., 2018; Jarrett et al., 2019; Mazurowski et al, 2019; Zhu et al., 2019). Machine learning (ML) is a subset of AI and its goal is to develop computer algorithms in order to solve problems

by learning from experience (Jarrett et al., 2019; Lundervold & Lundervold, 2019; Mazurowski et al., 2019). Classical machine learning (cML), and artificial neural networks (ANN), with subset of deep learning (DL), are subsets of machine learning (Lundervold & Lundervold, 2019; Mazurowski et al., 2019).

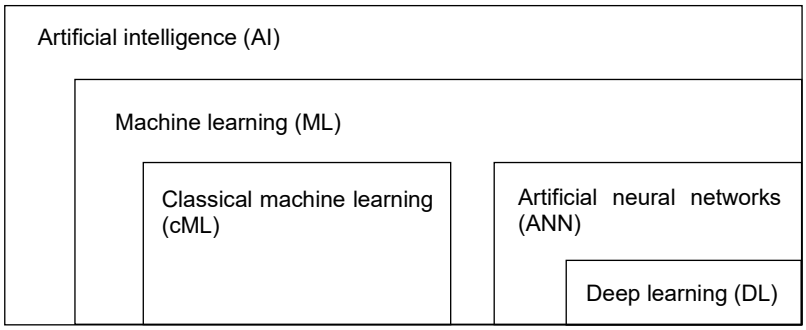

Figure 1. A schematic view of AI and its subsets.

In cML (also called radiomics in medical imaging, feature-based ML, state-of-the-art ML, handcrafted engineered feature learning or traditional ML), computers perform specific calculations supervised by human, learn from examples and replicate the programmed findings from unseen data (Suzuki, 2017; Acharya et al., 2018; Hosny et al., 2018; Langs et al., 2018; Mazurowski et al., 2019). Before all of the ML processes, there may be a need for a pre-processing step, where the data is prepared so as to be suitable for the main analysis (Despotović et al., 2015), like re-sampling the data (for example, standardization of MRI data to isotropic voxels), removal of non-brain tissue, and bias field correction to correct for intensity homogeneity (i.e. intensity normalization) (Koikkalainen et al., 2011; Min et al., 2014; Koikkalainen et al., 2016).

Depending of the characteristics of the original data and extracted features, registration or matching and segmentation steps may be needed. In registration or matching, the data from different sources (for example, image data from MRI, PET and CT), time points or scanning positions needs to be brought into one standard reference form i.e. to normalize data spatially to one stereotactic space (Wang & Summers, 2012; Veronese et al., 2013). In the segmentation, the regions of interest (ROI) or the whole study area are identified and segmented manually, semi- or fully-automatically to pinpoint the interested structures for further analyses (Suzuki, 2017; Acharya et al., 2018).

The main process of cML includes a feature extraction and selection, and ROI-analysis or classification. In the feature extraction and selection, the most relevant features are extracted from data for further characterization (Suzuki, 2017; Acharya et al., 2018), and then highly important features are selected from the extracted features in order to strengthen the performance of the feature classifier model (Acharya et al., 2018).

In the ROI-analysis or classification, the extracted and selected features are entered into the cML model with a feature classifier in order to classify new unknown data (Suzuki, 2017; Leiner et al., 2019). The training and testing of the classifier are done using separate training and validation or testing sets. During training, the feature classifier model is trained with example data, i.e. to allow the model to be taught to correctly classify the feature data (Veronese et al., 2013; Suzuki, 2017; Leiner et al., 2019). After training, the feature classifier model is tested with a validation or testing set in order to evaluate the ability of the classifier of correctly categorizing a previously unseen set of cases (Veronese et al., 2013; Suzuki, 2017; Leiner et al., 2019).

Artificial neural networks are based on the structural concept of the human brain's neuronal network, where neurons are connected to each other (Choy et al., 2018). ANN has one input (e.g. image data) layer of neurons or units, one or more "hidden layers", and one output (e.g. result of analysis) layer (Choy et al., 2018). The hidden layer is a net of units connected to all units in the previous layer (Choy et al., 2018). DL models contain more than one hidden layer, which is the reason why these models are called "deep" (Choy et al., 2018; Mazurowski et al., 2019). ANN model algorithms learn automatically without human supervision (Hosny et al., 2018). However, in DL, a theoretical understanding of analyzing process is still incomplete and therefore non-transparent, which weakens the value of the analysis results in practical scientific and clinical work (Hosny et al., 2018).

The main idea for using AI in medical imaging is to support diagnostics by recognizing findings invisible to human eyes and thus to make the clinical workflow more objective and cost-effective (Hosny et al., 2018; Langs et al., 2018). There are several potential clinical radiology applications of AI, in fact some are already implemented in a whole imaging process of modern digital imaging: scheduling and subject screening, examination protocoling, image acquisition and post-processing of data, diagnostic processing, image quality analytics, image management, display and archiving, and dose estimation (Choy et al., 2018; Mateos-Pérez et al., 2018; Zhu et al., 2019). AI has been extensively used in the MRI analysis of the brains of subjects with strokes, certain psychiatric disorders, epilepsy, neurodegenerative diseases, and demyelinating diseases (Zhu et al., 2019; Rauschecker et al., 2020). The ML algorithms are widely utilized in scientific and clinical MRI analyses, for example, in the analyses of cortical thickness, voxel-based morphometry, TBM, network analyses, functional MRI, diffusion-weighted imaging and positron emission tomography-magnetic resonance imaging (PET-MRI) (Mateos-Pérez et al., 2018; Lundervold & Lundervold, 2019).

Traditionally, electron density (ED) information of computed tomography (CT) studies has been widely used, for example in the planning of radiotherapy treatment (Andreasen et al., 2015; Hsu et al., 2015; Ranta et al., 2020) and positron emission tomography – computed tomography (PET-CT) (Roy et al., 2014). In recent years, MRI-only based studies have become more important in clinical workflow, and there has been

an evident need to solve the lack of CT-based ED information. In radiotherapy, it is now possible to transform specialized MRI sequences into pseudo-CT data (**Figure 2**) in order to produce ED information for planning radiotherapy treatment and dose calculation (Andreasen et al., 2015; Hsu et al., 2015). In PET, the attenuation correction of PET-data is critical if one wishes that the ED information can be utilized to obtain a reliable clinical analysis. In fact, several ML algorithms have been devised and are being used to calculate the density information from MRI-data (Roy et al., 2014).

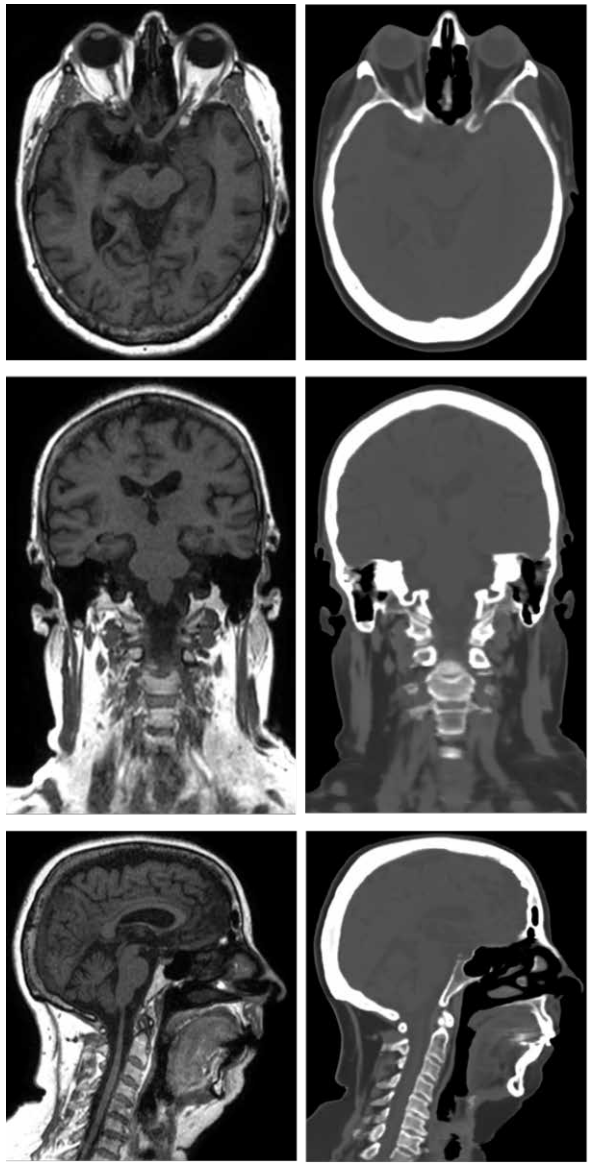

Figure 2. An example of post-processing of MRI data. T1 Dixon In-phase MRI image of the brain (left) and a pseudo-computed tomography calculated from the same MRI image (right). Picture: Courtesy of Turku University Hospital / Department of Oncology and Radiotherapy.

2.3.4 Tensor-based morphometry

TBM is a fully automated voxel-based MRI analyzing method that can identify and quantify regional structural differences in the brain (Ashburner et al., 1998). TBM is based on the deformation fields obtained when a template image is registered with

the study image. The deformation field defines for each voxel of the template image the displacements in x-, y- and z-directions needed to move the voxel to the corresponding anatomical location in the study image. The gradient of the deformation field (the Jacobian matrix) quantifies information about the non-rigid local stretching, shearing and rotation involved in the deformation (Ashburner & Friston, 2003; Lepore et al., 2008). One often-used measure in TBM is the determinant of the Jacobian matrix of the deformation field i.e. the Jacobian, which measures the local volume change on the basis of intensity differences (Ashburner & Friston, 2003; Koikkalainen et al., 2011).

An atlas-based segmentation is a common data segmentation technique (Lepore et al., 2008; Lötjönen et al., 2010), where a manually segmented atlas image is registered with the study data. In the multi-atlas segmentation, several atlases are used to improve the segmentation accuracy (Lötjönen et al., 2010). In multi-template TBM, the multi-atlas segmentation is modified to a multi-template method where study images are registered through multiple template images (Koikkalainen et al., 2011).

For example, the features computed from the TBM results can be used for further statistical analyses of size and shape differences between known study groups, as well as for classifying unseen study images to the different study groups (Koikkalainen et al., 2011). The statistical analyses and classifying do not belong to the actual tensor-based morphometry analysis, but the statistical tests can be used to achieve a visualization of the significant differences within the brain (Hua et al., 2008a).

In scientific work, there are several TBM applications, which have been widely used both in cross-sectional and longitudinal dementia studies e.g. to detect the change to progressive MCI from stable MCI (Muñoz-Ruiz et al., 2012; Hua et al., 2016), early AD to late AD (Migliaccio et al., 2015), and the progression of AD (Hua et al., 2008b; Tsao et al., 2017) and MCI (Hua et al., 2008b; Leow et al., 2009; Zhang et al., 2016 Apr). TBM applications have also been used to study other neurodegenerative diseases like Lewy body disease, frontotemporal disease and semantic dementia (Lepore et al., 2008; Muñoz-Ruiz et al., 2012; Sarro et al., 2016), and to differentiate individual neurodegenerative diseases from each other (Koikkalainen et al., 2011; Muñoz-Ruiz et al., 2012). TBM was also applied as a reference method in a post-mortem atrophy study (Josephs et al., 2017).

The usual TBM finding in neurodegenerative diseases is a gray matter atrophy at the group level (Hua et al., 2008a; Leow et al., 2009). For example, it has been reported that AD subjects have more widespread atrophy than MCI subjects and also when compared to the controls (Hua et al., 2008a; Leow et al., 2009). In the early and late onset AD, the spreading of atrophy has been noted to be similar (Migliaccio et al., 2015). The atrophy has also been localized typically according to the nature of

neurodegenerative disease. In AD subjects, the atrophy is often detected in hippocampus and the temporal lobe (Hua et al., 2008a; Koikkalainen et al., 2016). In contrast, in FTD patients, the atrophy tends to be located to the frontal areas (Muñoz-Ruiz et al., 2012; Koikkalainen et al., 2016). Another usual TBM finding is a correlation between the degree of atrophy and the severity of the cognitive decline (Hua et al., 2008a). In longitudinal studies of AD, MCI and normal subjects, atrophy detected by TBM has been associated with a future cognitive decline (Hua et al., 2008b; Leow et al., 2009; Zhang et al., 2016 Apr; Tsao et al., 2017).

Other neurodegenerative diseases, like Parkinson's disease (Tessa et al., 2014), multiple sclerosis (Datta et al., 2015; Preziosa et al., 2017), and human (Kipps et al., 2005) and a mouse model (Rattray et al., 2017) of Huntington's disease, have also been studied using TBM. Patients with migraine (Soheili-Nezhad et al., 2019), depressive disorder (Scheinost et al., 2018) and schizophrenia (Chiang et al., 2007; Lepore et al., 2008; Clifford et al., 2017; Nir et al., 2019) have also been examined with TBM applications, as have the brains of HIV/AIDS patients (Lepore et al., 2008; Clifford et al., 2017), hereditary spastic paraplegia (Sadeghi et al., 2018), pediatric traumatic brain injury (Dennis et al., 2016), Fragile X syndrome (Lee et al., 2007) and preterm neonates (Paquette et al., 2017). In addition, TBM applications have been utilized to examine healthy adults (Rocca et al., 2017), twins (Gutman et al., 2015 Apr) and to investigate human white matter pathology (Vangberg et al., 2019).

3 Aims

I. To compare the sensitivity of VRM and TBM in detecting atrophy of the medial temporal area and frontal lobe as well as assessing the enlargement of the ventricles in MCI and AD.

II. To evaluate the sensitivity of VRM and TBM in detecting atrophy of the medial temporal area and frontal lobe and the enlargement of the ventricles in stable and progressive MCI during a 2-year follow-up period.

III. To examine the possibilities of utilizing TBM in detecting the degenerative DGM changes in MCI and AD and to evaluate the relationships between DGM changes and neurocognitive function in three groups of individuals; controls, and subjects with MCI and AD.

4 Materials and Methods

4.1 Subjects

Altogether 229 participants were recruited in Turku University Hospital (PET Centre and Department of Neurology), where they underwent a standardized clinical examination and neuropsychological test battery. The participants were MCI and AD subjects, and healthy controls. In different studies (I, II and III) the number of participants was different depending on the nature of the study and available data.

MCI was diagnosed according to the criteria suggested by Petersen et al. (2001). MCI subjects had memory impairment, clinical dementia ratings of 0.5, normal global cognition, but no impairment in the activities of daily living at the baseline. None of the MCI subjects were treated with acetylcholinesterase inhibitors or memantine during the studies.

Subjects with AD fulfilled the DSM-IV criteria for dementia and the NINCS-ADRDA (National Institute of Neurological and Communicative Disorders and Stroke/Alzheimer's Disease and Related Disorders Association) criteria for probable AD (McKhann et al., 1984).

The control subjects were healthy volunteers who had no history of neurological or psychiatric disease and had scores within the age-adjusted Finnish norms in neuropsychological testing.

4.1.1 Cross-sectional study (study I)

Study I (**Table 3**) consisted of 211 subjects (109 men and 102 women). Forty-seven subjects (27 men and 20 women) had a MCI diagnosis, 80 subjects (41 men and 39 women) had AD diagnosis and 84 subjects (41 men and 43 women) were healthy controls.

The mean age was 72.9 years (SD 6.3) in the MCI group, 74.6 (SD 5.5) in the AD group and 71.0 years (SD 6.7) in the control group. Both the youngest (51.8 years) and the oldest (87.8 years) subjects were in the control group.

4.1.2 Longitudinal study (study II)

Altogether 113 Subjects (58 men and 55 women) were included in study II (**Table 4**). At baseline, there were 29 MCI subjects (17 men and 12 women), of which 11 remained stable (5 men and 6 women) and 18 progressed to AD (12 men and 16 women) during the 2-year follow-up time. The number of controls was 84 (41 men and 43 women).

At the baseline, the mean age of all MCI subjects was 70.9 years (SD 6.3). Those subjects who remained stable during the follow-up time, had a mean age of 72.1 years (SD 6.6) at the baseline. The subjects who progressed to AD were somewhat younger as their mean age was 70.1 years (SD 6.2) at the baseline.

The mean follow-up times for stable MCI subjects were 24.2 months (SD 3.2), the same as for the progressing MCI subjects (24.2 months; SD 4.5).

4.1.3 Association study between deep gray matter and neurocognitive function (study III)

Study III (**Table 5**) consisted of 154 subjects (77 men and 77 women); there were 38 MCI subjects (17 men and 21 women), 58 AD subjects (32 men and 26 women) and 58 controls (28 men and 30 women).

The mean age was 73.7 years (SD 5.8) in MCI group, 74.0 (SD 4.9) in AD group and 71.8 (SD 5.5) in control group. The youngest subjects (57.7 years) were in the control and AD groups and the oldest (87.8 years) in the control group.

4.2 Methods

4.2.1 Statistical details of the demographic of the studies

4.2.1.1 Cross-sectional study (study I)

In **study I** (**Table 3**), the groups displayed significant differences in age and education. The AD group was older than the control group and had lower education than the control and MCI groups. As expected, the groups had also significant differences in Mini-Mental State Examination (MMSE) results. The control group had higher scores in MMSE than the MCI and AD groups and the MCI group had higher scores in MMSE than the AD group. There were no significant differences between the sexes.

Table 3. Demographic details of different study groups. Study I.

Demography		Controls	MCI	AD	Stat.sign. *
Number of subjects	Total (211)	84	47	80	
Sex	males (109) / females (102)	41/43	27/20	41/39	N.S.
Age (y)	mean (SD)	71.0 (6.7)	72.9 (6.3)	74.6 (5.5)	AD > C
	median	71.4	72.6	73.7	
	min / max	51.8/87.8	59.0/85.5	57.3/85.9	
Education ([a])	mean (SD)	1.9 (0.9)	2.0 (1.2)	1.6 (0.9)	C, MCI > AD
	median	2	2	1	
	min / max	1/4	1/4	1/4	
MMSE	mean (SD)	27.8 (0.35)	26.5 (0.48)	22.3 (0.41)	C>MCI, AD; C, MCI > AD
	median	28	26	23	
	min / max	25/30	25/30	6/29	

* α < 0.05. Education (a) level was operationalized as follows: 1 = comprehensive school, 2 = vocational school, 3 = college degree and 4 = university degree. N.S. = not statistically significant

4.2.1.2 Longitudinal study (study II)

In **study II** (**Table 4**), there were no statistically significant group (controls, MCI_{all}, MCI_{stable} and $MCI_{progression}$) differences in age, education and sex at the baseline. Determination of stability or progression of MCI was assessed by repeated MMSE and neuropsychological tests (listed in **Table 6**). The MMSE results of MCI_{stable} group had remained stable after the 2-year follow-up time, whereas the MMSE results of $MCI_{progression}$ group worsened significantly as compared to control, MCI_{all}, MCI_{stable}, and also with its own baseline value.

Table 4. Demographic details of different study groups. Study II.

Demography	Controls	MCIall	MCIs		MCIp	
Subjects (113) [male (58) / female (55)]	84 (41/43)	29 (17/12)	11 (5/6)		18 (12/6)	
			year 0	year 2	year 0	year 2
Age (y), mean (SD)	71.0 (6.7)	70.9 (6.3)	72.1 (6.6)	73.4 (6.7)	70.1 (6.2)	72.5 (6.3)
Median	71.4	71.8	72.8	75.2	70.8	73.6
Min / max	51.8 / 87.8	58.5 / 80.4	58.5 / 80.4	61.1 / 82.3	59.0 / 79.0	61.2 / 81.8
Education (a), mean (SD)	1.9 (0.9)	2.3 (1.2)	2.4 (1.0)	2.7 (1.2)	2.2 (1.3)	2.3 (1.3)
Median	2	2	2	2	2	2
Min / max	1 / 4	1 / 4	1 / 4	1 / 4	1 /4	1 /4
MMSE, mean (SD)	27.7 (1.3)	27.6 (1.9)	28.1 (2.0)	26.2 (1.2)	27.3 (1.8)	*22.3 (5.4)
Median	28	28	29	26	27	23
Min / max	25 / 30	25 / 30	25 / 30	25 / 29	25 / 30	14 / 30
Months between MRI scans, mean (SD)			24.2 (3.2)		24.2 (4.5)	
Median			24.0		24.0	
Min / max			21 / 30		15 / 37	

* α < 0.05. MCIs = MCI stable group, MCIp = MCI progression group. y = year. Education (a) level was operationalized as follows: 1 = comprehensive school, 2 = vocational school, 3 = college degree, 4 = university degree. Year 0 = baseline, year 2 = after 2-year follow-up.

4.2.1.3 Association study between deep gray matter and neurocognitive function (study III)

In **study III** (**Table 5**), there were no significant group differences in age and sex, but the AD group had statistically significantly lower education than the control and MCI groups. As expected, the groups also exhibited significant differences in their MMSE results. The control group had higher scores in MMSE than the MCI and AD groups and the MCI group had higher MMSE results than the AD group.

Table 5. Demographic details of different study groups. Study III.

Demography		Controls	MCI	AD	Stat.sign.*
Number of subjects	Total (154)	58	38	58	
Sex	male (77) / female (77)	28/30	17/21	32/28	n.s.
Age (y)	mean (SD)	71.8 (5.5)	73.7 (5.8)	74.0 (4.9)	n.s.
	median	71.3	73.5	72.6	
	min / max	57.7/87.8	61.1/85.5	57.7/85.5	
Education (a)	mean (SD)	1.8 (0.9)	2.0 (1.2)	1.4 (0.6)	C, MCI > AD
	median	2	2	1	
	min / max	1/4	1/4	1/4	
MMSE	mean (SD)	27.6 (1.3)	26.4 (2.0)	21.5 (4.2)	C > MCI, AD; C, MCI > AD
	median	28	26	22	
	min / max	25/30	25/30	6/29	

* $\alpha < 0.05$. y = year. Education (a) level was operationalized as follows: 1 = comprehensive school, 2 = vocational school, 3 = college degree and 4 = university degree.

4.2.2 Neuropsychological assessments

In **all studies (I–III),** neuropsychological tests were used to ensure normal cognition in controls and the absence of a widespread cognitive impairment in MCI subjects. The neuropsychological tests were conducted at the same time with MRI scans (both at baseline and at follow-up).

In addition, in **study III,** neuropsychological tests results were used to evaluate the relationships between the changes of deep gray matter TBM index values (IV) and neurocognitive function in control, MCI and AD groups.

The neuropsychological tests included CERAD (The Consortium to Establish a Registry for Alzheimer's Disease) [(Morris et al., 1989), in Finnish (Hänninen et al., 1999)], the Logical Memory test from the Revised Wechsler Memory Scale (WMR-S) (Wechsler, 1987) and the Trail Making Test (TMT) (Reitan, 1959). These tests evaluated episodic memory and learning, language function, visuoconstructive function and visuo-motor scanning (**Table 6**).

Table 6. Cognitive functions and tests administered.

Cognitive function	Test used
Episodic memory and learning	
- Free recall	Revised WMS-R, Logical memory immediate free recall (Wenchler et al. 1987)
- Memory consolidation	Revised WMS-R, Logical memory delayed free recall (Wenchler et al. 1987)
- Learning	CERAD – Wordlist learning (Morris et al. 1989, in Finnish Hänninen et al. 1999)
Language function	
- Naming	CERAD – Naming (Morris et al. 1989, in Finnish Hänninen et al. 1999)
- Semantic processing	CERAD – Semantic fluency (Morris et al. 1989, in Finnish Hänninen et al. 1999)
Visuoconstructive function	
	CERAD – Constructional praxis (Morris et al 1989, in Finnish Hänninen et al. 1999)
Visuo-motor scanning	
	Trail making test – test A (Reitan 1959)

WMS-R = Wechsler Memory Scale, CERAD = The Consortium to Establish a Registry for Alzheimer's Disease.

4.2.3 Magnetic resonance imaging and reconstruction of the data

The MRI scanning of **all study (I–III)** subjects was collected during 9 years (1999–2008) and performed with either a 1.5T Philips Gyroscan Intera (Best, the Netherlands) or a 1.5 T MRI GE Signa Horizon LX EchoSpeed (General Electric Medical Systems, Milwaukee, Wisconsin, USA). The Philips scanner used a transaxial 3D T1/FFE (incoherent gradient echo) (voxel size 0.50 x 0.50 x 1.00 mm, FOV 256, matrix 512 x 512), a transaxial T2 and a coronal FLAIR (fluid attenuated inversion recovery) sequences in the analysis. The coil used was SENSE-head. The GE scanner used a transaxial 3D FSPGR (fast spoiled gradient echo) (voxel size 1.1 x 1.1 x 1.5 mm) and a transaxial T1 or PD (proton density) sequence in the analysis.

For the visual evaluation of the medial temporal lobe, the axial 3D T1 sequences were reconstructed manually on a GE workstation (ADW 4.4, General Electric Medical Systems, Milwaukee, Wisconsin, USA). During reconstruction, the slices were aligned with a brainstem axis (Scheltens et al., 1992). The interslice gap was 1.0 mm, the slice thickness was 5.0 mm and the number of slices ranged from 25 to 32. The reconstructed sequences were recorded on CDs (Centricity DICOM Viewer, Philips Medical Systems) and the visual evaluation itself was made on a personal computer with Windows XP as the operating system.

4.2.4 Visual magnetic resonance imaging analyses

A visual evaluation of MTL and ventricular enlargement was performed by a radiologist (TT) and a neuroradiologist (RP), and an evaluation of the frontal cortical atrophy was performed by the neuroradiologist (RP). The evaluators were blinded to the subjects' data, and the order of MRI scans was randomized. The radiologists analyzed the sequences independently. If the evaluation difference in a visual rating protocol was not more than one grade, the average of the values was calculated and rounded off to the nearest whole number (i.e. higher value was retained for the rating as there were only two evaluators in these studies). If the evaluation differences were more than one grade, the values of the scores were resolved by consensus.

The MTL evaluation in VRM was performed as described by Scheltens et al. (1992). The VRM evaluation was performed from the manually reconstructed coronal 3D T1 sequences for both sides of the MTL. MTL atrophy was staged from value 0 to 4, where a value of 0 corresponded to no atrophy and a value of 4 corresponded to severe atrophy (**Figure 3**, and **Table 2** in chapter 2.3.2). Absolute measurements (millimeters) of the largest vertical height of hippocampal formation (defined as dentate gyrus, hippocampus proper, subiculum and parahippocampal gyrus), the largest horizontal width between the hippocampal formation and brainstem, the largest vertical width of the choroid fissure and the width of temporal horn were calculated (**Figure 4**). The absolute measurements of the largest width of the lateral ventricles and third ventricle and the diameter of the inner calvarium of the skull from the level of lateral ventricles measurements were also measured in millimeters and from the same coronal slice as the MTL measurements (**Figure 5**). To calculate the indices, the absolute measurements of the lateral ventricles and third ventricle were proportioned to an absolute diameter of an inner calvarium of the skull. The purpose of the indices was to create results that would be independent of the size of the subject's skull.

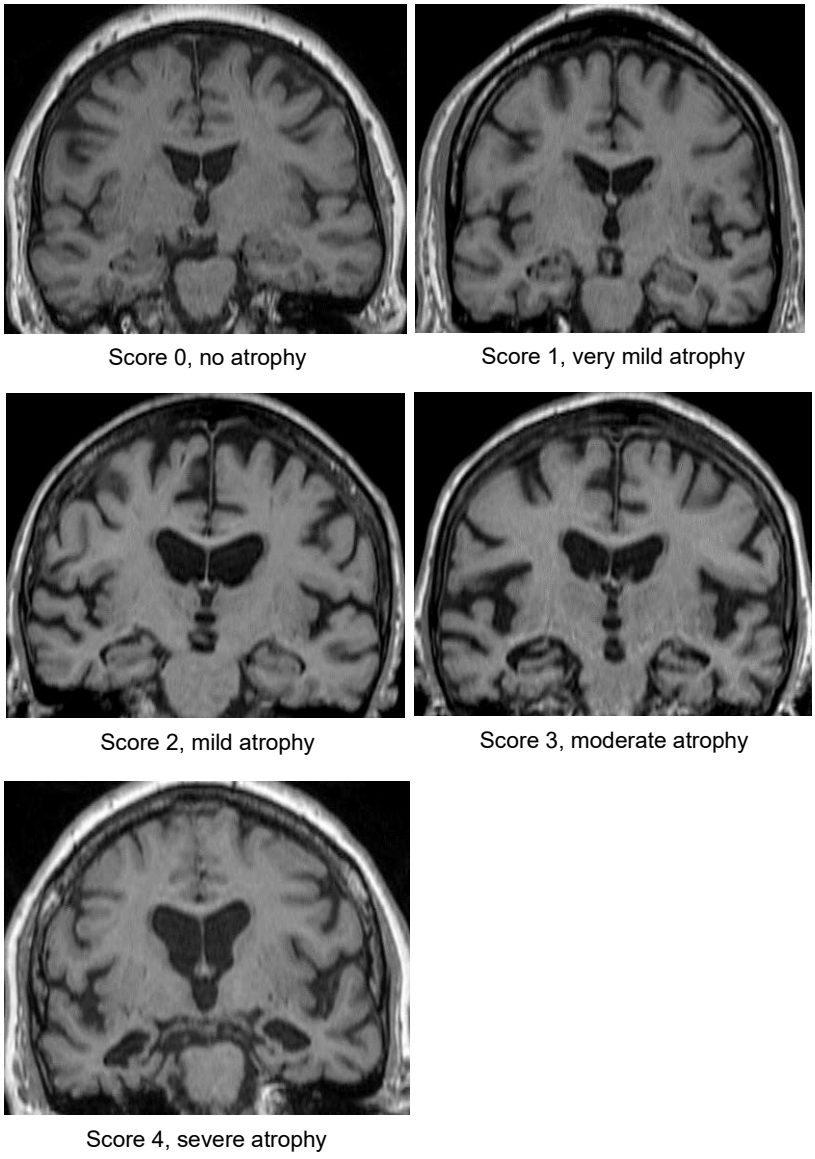

Figure 3. Visual atlas of medial temporal lobe atrophy from the study data. An adaptation from the atlas of Scheltens et al. 1995.

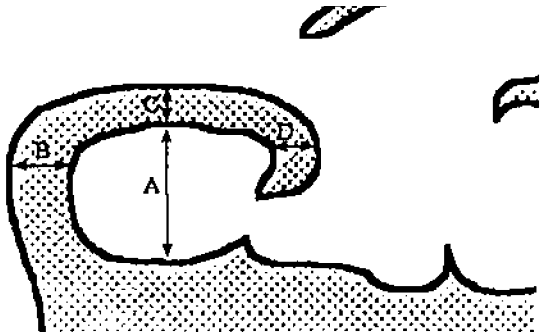

Figure 4. Linear measurements of the medial temporal lobe according to Scheltens et al. (1992).
A is the largest vertical height of hippocampal formation defined as dentate gyrus, hippocampus proper, and subiculum together with parahippocampal gyrus.
B is the largest horizontal width between hippocampal formation and brainstem.
C is the largest vertical width of choroid fissure.
D is a width of the temporal horn.

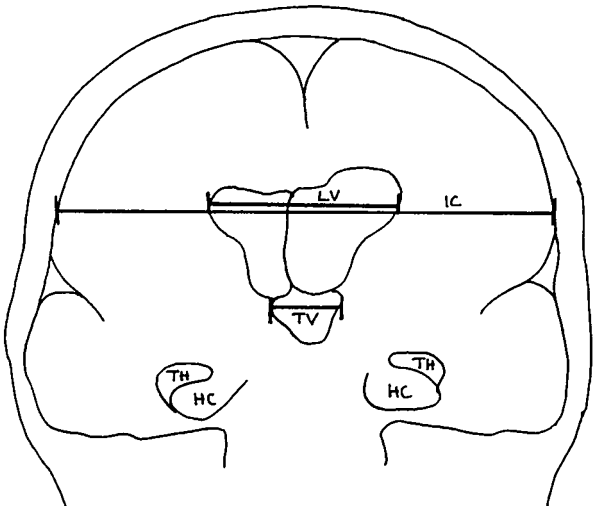

Figure 5. A schematic view of a level of the measurements of ventricles and the diameter of the inner calvarium of the skull. LV = diameter of the lateral ventricles, TV = diameter of the third ventricle, IC = inner calvarium diameter, TH = temporal horn, HC = hippocampus

The evaluation of frontal cortical atrophy was a modified form of the work Victoroff et al. (1994). The evaluation was performed from the original 3D T1 and T2 or PD sequences. The structure of the subjects' frontal lobes was visually compared to the original images of Victoroff et al. (1994) and scaled from 0–2, where 0 corresponded to no atrophy and 2 corresponded to severe atrophy. The evaluation covered the anterior prefrontal cortex to the frontal operculum. The extents of cortical atrophy in the right and left frontal lobes were rated separately. Our evaluator for the frontal atrophy was a single neuroradiologist (RP), as reliability in the frontal

lobe evaluation seemed to be remarkably dependent on the rater's experience (Victoroff et al., 1994).

In addition, visual MRI evaluation was used for detecting any structural changes of the brain, which may require a clinical treatment (i.e. tumors, fresh bleedings or infarcts). If severe structural changes were detected, the subject was excluded from the study and directed to the national health care system for possible initiation of treatment.

4.2.5 Tensor-based morphometry analysis

The original T1 3D MRI sequences were used for the TBM analysis. A multi-template method of TBM was chosen to improve the robustness of the analysis (Koikkalainen et al., 2011). The template images were a compilation of 10 AD subjects, 10 MCI subjects and 10 controls from the ADNI dataset (i.e. atlas) (Alzheimer's Disease Neuroimaging Initiative, 2017). A mean anatomical template (MAT) was constructed from the 30 templates to establish a reference space for the analysis.

For each study image, 30 separate registrations from MAT to the study image were computed. Each time, the registration was performed via a different template (MAT – template – study image registrations). From the resulting 30 deformations, the determinant of the Jacobian matrix (the Jacobian) was computed for each voxel to quantify the local volume change information. The 30 deformations were finally combined by computing the average Jacobian for each voxel. The resulting average Jacobian of the study image described the amount of local expansion or compression of the voxel compared to the corresponding voxel in the MAT.

The average Jacobians were further combined within each structure of the Hammer's brain atlas (Heckemann et al., 2006) to produce robust values for further analysis. As the structures may contain both dilating and shrinking voxels, a simple averaging within the structures may produce unsatisfactory results. Consequently, we utilized the MRI images of 100 control subjects and 100 AD subjects from the ADNI dataset to separate the voxels that typically dilate and shrink in AD. Additionally, the p-values were computed to evaluate the significance of each voxel to differentiate control subjects from AD subjects. The final TBM index was computed for each structure by measuring the similarity of the subject's Jacobians with the typical AD-related pattern of Jacobians modelled from the ADNI dataset (Koikkalainen et al., 2011). When computing this index, the dilating and shrinking voxels were processed separately, and more weight was given to the voxels with high significance. By weighting the voxels, it is possible to sharpen the calculations by giving a voxel with smaller p-value, a larger weight, and no weight is given to the statistically non-significant voxels. The index values (IVs) (range from -1,272187 to

1,27897) were used as feature values and for further analyses (Koikkalainen et al., 2011). The index values summarize all AD-type volume changes in anatomy. High index values indicate more AD-type shape changes from the shape of MAT while low IVs show similarity to the shape changes that are typical in control subjects. In the model used in this thesis, the index value zero does not mean no changes, but it does reveal about the similarity to the mean anatomical template (MAT) of the TBM analysis.

It is possible to visualize the volume changes with TBM. An example in **Figure 6** demonstrates the differences between AD, MCI and control groups as shown by color differences.

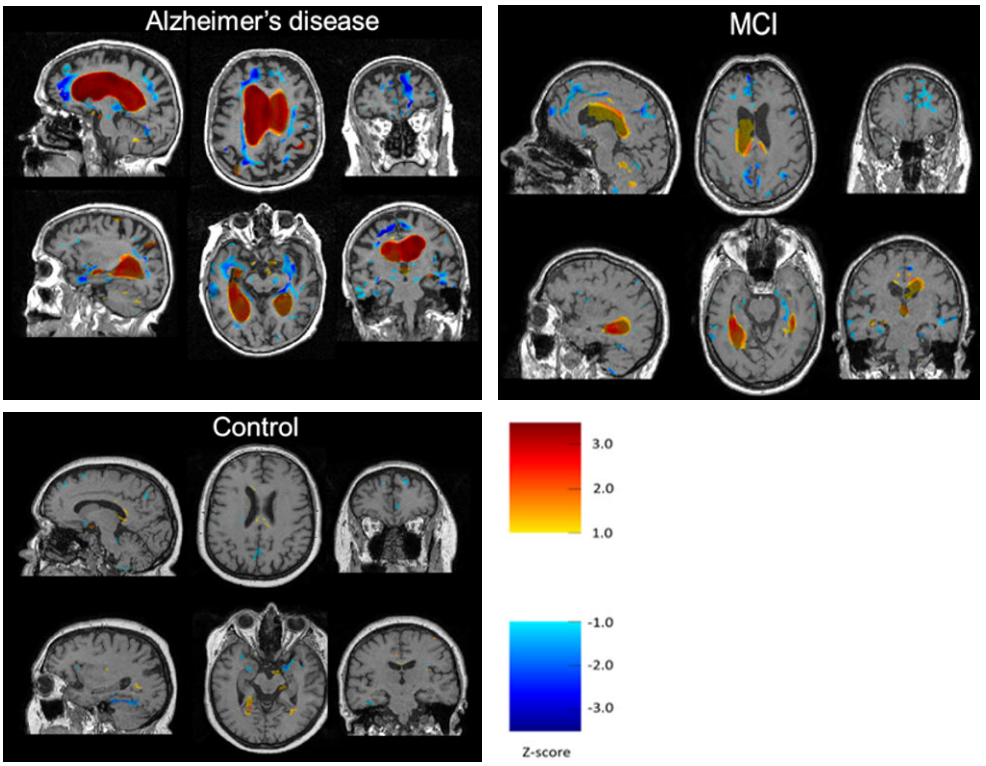

Figure 6. The visualization of the TBM results for individual AD, MCI and control subjects (Study I). The visualization is based on the z-scores of the voxel-wise Jacobians. The z-scores were computed by comparing the individual data to the entire control dataset. The red color shows the regions with AD-type brain dilation and blue color shows the regions with AD-type brain atrophy. The AD-type brain changes (i.e., locations where dilation/atrophy occurs) were computed from the AD and controls datasets. Only the regions with statistically ($p<0.05$) significant differences between AD and control groups, z-scores larger than 1.0 or smaller than -1.0, are visualized in colors.

4.2.6 Statistical analyses

In **studies I and II**, the statistical analyzes were performed using SAS 9.2 (SAS Institute Incorporation, Cary, North Carolina, USA). In study III, the statistical analyzing system was SPSS 23 (SPSS Incorporation, Chicago, Illinois, USA), except for the Cohen's d results, which were analyzed using Social Science Statistics website (Social Science Statistics, 2018).

Regardless of the analyzing system, the age differences of the groups were analyzed by one-way analysis of variance (ANOVA) with pairwise comparisons with Tukey's corrections. Differences in MMSE scores were analyzed with the Kruskal-Wallis test, continued with the Mann-Whitney U test when significant. Sex and educational differences between groups were assessed with the $\chi 2$ test. The control, MCI and AD groups were examined in **studies I and III**, and the control group and three MCI groups (stable remained, progressed and all MCI subjects) in **study II**. In **study I**, the groups displayed a significant difference in both education and age, and these were used as fixed effects in further analyses. In **studies II and III**, there were no significant group differences in age. The groups differed from each other in education levels, but the difference only trended toward statistical significance in **study II**. However, as the differences in both education and age may affect the results, they were used as covariates in the analyses of **studies II and III**. The use of covariates impacted on all other result values of the analysis. That is why the IVs of TBM were termed as estimated index values (EIVs) and the means of VRM were called the estimated means (EMs) in the results. Further, values of "difference of estimated means (DEM)" are statistically calculated differences between EMs, not simple differences between two EM values.

In **studies I and II**, analysis of covariance model (ANCOVA) was used for continuous responses. Only in the visual results of frontal atrophy was a cumulative logistic regression model (for ordinal categorical responses with more than two levels) used, because the variables had only a few values. RO was a coefficient ratio of the estimated means in the cumulative logistic regression model. In addition, ROC analysis was performed to separate the groups from each other in **study I**. The area under the ROC curve (AUC) indicated how well the test distinguished between the groups. The AUC values were classified as excellent (0.9–1.0) good (0.8–0.9) fair (0.7–0.8) poor (0.6–0.7) and failed (0.5–0.6). Furthermore, logistic regression models for categorical data, and a Spearman's nonparametric correlation analysis for hippocampi were used only in **study II**. In **studies I and II**, a p-value of 0.05 was used as the border of a statistically significant result and all the results were reported as corrected for multiple comparisons by using Tukey's p-values.

In **study III**, the values of the TBM IVs and cognitive test results of the groups were analyzed with one-way ANOVAs with pairwise comparisons with Tukey's corrections for multiple comparisons. A multiple linear regression model was used

to analyze the interactions between each neuropsychological test and TBM results. As the multiple linear regression model analyzes the results only in p-values, Pearson correlation coefficients without p-values were also calculated in order to gain an impression of the direction (negative or positive) of the correlation. Cohen's d was analyzed to measure the effect size in the group comparisons of cognitive function results. As the linear regression model with multiple correlations poses a risk of introducing a type 1 error in the statistical analysis, a p-value of 0.01 was adopted as the border of a statistically significant result in **study III**.

5 Results

5.1 Visual magnetic resonance imaging analyses

5.1.1 Cross-sectional study (study I)

The results of VRM analysis of **study I** are shown in **Table 7**.

There were statistically significant differences between the controls and the AD group with respect to the MTL, CSF space of temporal horns, and ventricular width. The negative difference in the estimated means (DEM) indicated that the AD group had higher atrophy scores in the hippocampus, wider CSF spaces around the hippocampus and larger ventricles than the control group. In turn, the positive DEM showed that the AD group had a lower height of the hippocampus and parahippocampal gyrus, which was in line with the results of the hippocampal scoring.

VRM also separated the MCI group from the AD group in most of the areas of the MTL, but not in the area of the ventricles. The positive DEM of the height of the left hippocampus and parahippocampal gyrus indicated that the control group had a higher left hippocampus value than the MCI group. A similar trend was observed on the right side.

Statistical differentiation of the MCI group from controls was only evident in the greater width of the third ventricle in the MCI group. However, a trend towards more atrophy in the areas of medial temporal lobe and ventricles in the MCI group as compared with the control group (a negative DEM) was observed.

In the frontal atrophy scores, there were no significant differences between the study subject groups in any of the comparisons.

Table 7. Results of the VRM analysis. Study I.

Visual rating analysis		Controls	MCI subjects	AD subjects	Controls vs. MCI subjects	Controls vs. AD subjects	MCI vs. AD subjects
		EM (SD)	EM (SD)	EM	DEM	DEM	DEM
Medial temporal lobe							
- Score	right	1.1 (0.12)	1.3 (0.16)	2.2 (0.14)	-0.143	****-1.056	****-0.912
	left	1.2 (0.13)	1.4 (0.18)	2.2 (0.15)	-0.251	****-1.038	***-0.786
- Indexes							
A. Height of hippocampus and	right	0.139 (0.0021)	0.139 (0.0028)	0.127 (0.0024)	0.000	****0.012	*0.012
parahippocampal gyrus	left	0.138 (0.0020)	0.134 (0.0027)	0.128 (0.0023)	0.004	***0.011	0.007
Liquor space of temporal horns							
- Indexes							
B. Distance between hippocampus	right	0.031 (0.0012)	0.031 (0.0016)	0.034 (0.0013)	-0.001	*-0.004	-0.003
and brainstem	left	0.029 (0.0011)	0.029 (0.0014)	0.034 (0.0012)	0.000	**-0.005	-0.004
C. Width of choroid fissure	right	0.021 (0.0012)	0.022 (0.0017)	0.029 (0.0014)	-0.001	****-0.009	***-0.008
	left	0.021 (0.0011)	0.021 (0.0015)	0.027 (0.0013)	0.000	****-0.006	***-0.006
D. Width of temporal horn	right	0.019 (0.0017)	0.019 (0.0022)	0.030 (0.0019)	0.000	****-0.010	***-0.010
	left (d)	-3.962 (0.0675)	-3.829 (0.0900)	-3.609 (0.0767)	-0.132	***-0.353	-0.221
E. B.+C.+D.	right	0.071 (0.0032)	0.072 (0.0043)	0.093 (0.0036)	-0.001	****-0.022	****-0.021
	left	0.072 (0.0033)	0.075 (0.0044)	0.094 (0.0037)	-0.004	****-0.022	***-0.018
Ventricles							
- Indexes							
Width of lateral ventricles		0.280 (0.0053)	0.294 (0.0071)	0.300 (0.0060)	-0.013	*-0.020	-0.007
Width of Third ventricle		0.055 (0.0022)	0.063 (0.0030)	0.067 (0.0026)	*-0.008	***-0.012	-0.004
Frontal atrophy		Mean (SD)	Mean (SD)	Mean (SD)	RO	RO	RO
- Score	right	0.52 (0.77)	0.83 (1.14)	0.64 (0.92)	0.827	1.138	0.941
	left	0.51 (0.77)	0.83 (1.14)	0.64 (0.92)	0.538	1.208	0.651

EM = estimate of the means, SD = standard deviation, DEM = difference of the estimated means, RO = ratio of coefficient. * $\alpha < 0.05$. ** $\alpha < 0.01$. *** $\alpha < 0.001$. **** $\alpha < 0.0001$. Mark (d) means conversion of logarithm.

5.1.2 Longitudinal study (study II)

The results of VRM analysis of **study II** are shown in **Table 8**.

At baseline, the MCI_{all} group showed significantly higher hippocampal atrophy scores and smaller heights of the hippocampus and parahippocampal gyrus than the controls in the bilateral medial temporal lobes (comparison A). The widths of the lateral ventricles and the right side of the combined CSF spaces were larger in the MCI_{all} group than in the control group. When the MCI_{all} group was divided into the MCI_{stable} and $MCI_{progression}$ groups, the only statistically significant difference at baseline was detected in the width of the third ventricle for the $MCI_{progression}$ group as compared to controls (comparisons B and C). Although no statistically significant differences were seen, the EM values of $MCI_{progression}$ group indicated more severe atrophy in MTL scores, right hippocampus and parahippocampal gyrus and all CSF spaces at the baseline. Only on the left side was the atrophy of hippocampus and parahippocampal gyrus stronger in the MCI_{stable} group than in the $MCI_{progression}$ group at the baseline, although the difference was statistically non-significant.

During the 2-year follow-up, the MCI_{stable} group remained stable as compared to the controls (comparison D). In contrast, the $MCI_{progression}$ group had developed significantly higher atrophy scores of the hippocampus and had wider CSF spaces than the controls (comparison E).

There were no significant differences between the MCI_{stable} and $MCI_{progression}$ groups at baseline or after follow-up (comparisons F and G). However, the positive DEM values indicated that the atrophy changes extended to include more brain areas in the $MCI_{progression}$ group than in the MCIs group at baseline and after follow-up.

When comparing the atrophy scores within the MCI groups at follow-up, the MCI_{stable} group remained stable as compared to baseline (comparison H). Within the $MCI_{progression}$ group, the positive DEM values (lines A. in **Table 8**) suggested some progression of atrophy, but this was not statistically significant (comparison J).

In the frontal atrophy scores, there were no significant differences between the study groups in any of the comparisons at any time point.

Table 8. Statistical results of the VRM analysis. Study II.

Group comparisons							
Visual rating analysis		**Controls**	**MCIall 0 yr**	**MCIs 0 yr**	**MCIs 2 yr**	**MCIp 0 yr**	**MCIp 2 yr**
		EM	**EM**	**EM**	**EM**	**EM**	**EM**
Medial temporal lobe							
- Score	right	0.9476	1.3596	1.2595	1.3094	1.4597	1.7034
	left	0.8967	1.3846	1.2424	1.5166	1.5267	1.8653
- Indexes							
A. Height of hippocampus and	right	0.1410	0.1341	0.1368	0.1437	0.1314	0.1298
parahippocampal gyrus	left	0.1407	0.1307	0.1301	0.1344	0.1313	0.1289
Liquor space of temporal horns							
- Indexes							
B. Distance between	right	0.0301	0.0334	0.0332	0.0316	0.0336	0.0348
hippocampus and brainstem	left	0.0284	0.0300	0.0286	0.0289	0.0315	0.0316
C. Width of choroid fissure	right	0.0203	0.0221	0.0210	0.0216	0.0232	0.0249
	left	0.0194	0.0213	0.0210	0.0248	0.0217	0.0233
D. Width of temporal horn	right	0.0173	0.0213	0.0195	0.0175	0.0231	0.0230
	left	0.0190	0.0237	0.0224	0.0253	0.0250	0.0325
E. B.+ C.+ D	right (c)	0.1667	0.1943	0.1870	0.1781	0.2016	0.2070
	left	0.0668	0.0751	0.0720	0.0789	0.0782	0.0874
Ventricles							
- Indexes							
Width of lateral ventricles		0.2735	0.2915	0.2822	0.2906	0.3008	0.3071
Width of third ventricle		0.0527	0.0607	0.0552	0.0592	0.0661	0.0718

Frontal atrophy		**Controls**	**MCIall 0 yr**	**MCIs 0 yr**	**MCIs 2 yr**	**MCIp 0 yr**	**MCIp 2 yr**
		Mean	**Mean**	**Mean**	**Mean**	**Mean**	**Mean**
- Score	right	0.54	1.17	1.00	1.00	1.28	0.76
	left	0.52	1.17	1.00	1.00	1.28	0.76

MCIs = MCI stable, MCIp = MCI progression, yr = year, 0 yr = baseline, 2 yr = after 2-year follow-up, EM = estimated means, DEM = difference of the estimated means, and RO = ratio of coefficient. * $\alpha < 0.05$, ** $\alpha < 0.01$, *** $\alpha < 0.001$, and **** $\alpha < 0.0001$. Mark (c) indicates a square root conversion.

	A	B	C	D	E	F	G	H	J
	C vs MCIall 0 yr	C vs MCIs 0 yr	C vs MCIp 0 yr	C vs MCIs 2 yr	C vs MCIp 2 yr	MCIs 0 yr vs MCIp 0 yr	MCIs 2 yr vs MCIp 2 yr	MCIs 0 yr vs MCIs 2 yr	MCIp 0 yr vs MCIp 2 yr
	DEM	DEM	DEM	DEM	DEM	DEM	DEM	DEM	DEM
	*-0.4120	-0.3119	-0.5121	-0.3619	*-0.7558	-0.2002	-0.3939	-0.0500	-0.2437
	*-0.4879	-0.3458	-0.6300	-0.6199	**-0.9686	-0.2842	-0.3487	-0.2741	-0.3386
	*0.0069	0.0042	0.0096	-0.0027	0.0112	0.0054	0.0139	-0.0069	0.0016
	**0.0101	0.0107	0.0095	0.0064	0.0118	-0.0012	0.0055	-0.0043	0.0024
	-0.0033	-0.0032	-0.0035	-0.0016	-0.0048	-0.0004	-0.0032	0.0016	-0.0013
	-0.0017	-0.0003	-0.0031	-0.0005	-0.0033	-0.0029	-0.0027	-0.0003	-0.0001
	-0.0017	-0.0007	-0.0028	-0.0012	-0.0045	-0.0022	-0.0033	-0.0006	-0.0017
	-0.0019	-0.0016	-0.0022	-0.0054	-0.0039	-0.0007	0.0015	-0.0038	-0.0017
	-0.0040	-0.0023	-0.0058	-0.0002	-0.0058	-0.0036	-0.0055	0.0020	0.0001
	-0.0047	-0.0033	-0.0060	-0.0062	**-0.0135	-0.0027	-0.0072	-0.0029	-0.0075
	*-0.0275	-0.0202	-0.0349	-0.0114	-0.0403	-0.0146	-0.0289	0.0089	-0.0055
	-0.0083	-0.0052	-0.0114	-0.0121	**-0.0206	-0.0062	-0.0085	-0.0070	-0.0092
	*-0.0180	-0.0087	-0.0273	-0.0171	*-0.0336	-0.0186	-0.0165	-0.0084	-0.0063
	-0.0080	-0.0025	*-0.0134	-0.0066	**-0.0191	-0.0109	-0.0125	-0.0040	-0.0057

	C vs MCIall 0 yr	C vs MCIs 0 yr	C vs MCIp 0 yr	C vs MCIs 2 yr	C vs MCIp 2 yr	MCIs 0 yr vs MCIp 0 yr	MCIs 2 yr vs MCIp 2 yr	MCIs 0 yr vs MCIs 2 yr	MCIp 0 yr vs MCIp 2 yr
	RO	RO	RO	RO	RO	RO	RO	RO	RO
	0.485	1.033	0.265	0.859	0.890	3.905	0.965	1.203	0.297
	0.456	0.956	0.250	0.787	0.842	3.822	0.934	1.214	0.297

5.2 Tensor-based morphometry analyses

5.2.1 Cross-sectional study (study I)

TBM analysis results of **study I** for the control, MCI and AD groups are shown in **Table 9**.

TBM performed best at differentiating the control group from the AD group in the areas of the medial temporal lobe and ventricles, but the differentiation was also good in the frontal area. The higher estimated index values (EIVs) in the AD group compared with the control group [negative difference of the estimated index values (DEIV)] shows a better fit to the AD type volume changes on average. In the AD group, negative DEIVs were seen in all examined brain areas except for the third ventricle and superior frontal gyrus.

When the MCI and AD groups were compared, only the hippocampus, the combined areas of MTL, temporal horns of the lateral ventricles and medial orbital gyri of the frontal area gave statistically significant results on both sides. The DEIVs were also negative. The results were also statistically significant on the left side of the parahippocampal gyrus and ambiens and in the middle frontal and straight gyri of the frontal area.

When the controls and the MCI group were compared, negative DEIVs were seen in all examined MTL brain areas. Statistically significant differences in MTL were observed in the left side of hippocampus, parahippocampal gyrus and ambiens and the combined values of the MTL. In the area of the ventricles, the third ventricle had the only statistically significant p-value. In the frontal area, the only statistically significant area was found in the right side of the superior frontal gyri. When the DEIV was examined, the negative values in the areas of MTL, ventricles and the superior frontal gyri meant that, on average, the MCI group had more AD type volume changes than the control group.

Table 9. Results of the TBM analysis. Study I.

Tensor-based morphometry analysis		Controls	MCI	AD	Controls vs. MCI subjects	Controls vs. AD subjects	MCI vs. AD subjects
		EIV	EIV	EIV	DEIV	DEIV	DEIV
Medial temporal lobe							
A. Hippocampus	right	0.0249	0.0743	0.2149	-0.049	****-0.190	**-0.141
	left (c)	0.4929	0.5747	0.6692	*-0.082	****-0.176	**-0.095
B. Anterior temporal lobe, medial part	right	0.1267	0.1636	0.2287	-0.037	***-0.102	-0.065
	left (d)	-0.5079	-0.4635	-0.3728	-0.044	***-0.135	-0.091
C. Parahippocampal gyrus and ambiens	right	0.1111	0.1510	0.1768	-0.040	***-0.066	-0.026
	left	0.1307	0.1897	0.2552	*-0.059	****-0.124	*-0.065
D. A.+B.+C.	right	0.0607	0.1203	0.2755	-0.060	****-0.215	**-0.155
	left (c)	0.5359	0.6132	0.7198	*-0.077	****-0.184	**-0.107
Ventricles							
A. Lateral ventricle (frontal and occipital horn and central part)	right	-0.0339	0.0834	0.1946	-0.1173	***-0.2285	-0.1111
	left	-0.1795	-0.0945	0.0546	-0.0850	***-0.2342	-0.1492
B. Lateral ventricle (temporal horn)	right	-0.0323	-0.0268	0.1096	-0.0055	****-0.1420	**-0.1364
	left	0.0432	0.0958	0.2131	-0.0526	****-0.1698	**-0.1172
C. Third ventricle		-0.0430	0.1050	0.0999	*-0.1480	**-0.1429	0.0050
D. A. + B. + C.	right	-0.0309	0.0839	0.1960	-0.1148	***-0.2269	-0.1121
	left	-0.1733	-0.0888	0.0623	-0.0845	***-0.2356	-0.1512
Frontal area (prefrontal)							
- Frontal lobe, (Middle frontal gyrus)	right	0.1862	0.1884	0.2417	-0.0022	*-0.0555	-0.0533
	left	0.2152	0.2153	0.2837	-0.0001	*-0.0685	*-0.0684
- Superior frontal gyrus	right (c)	0.4828	0.5346	0.5162	*-0.0518	-0.0334	0.0185
	left	0.2217	0.2599	0.2505	-0.0382	-0.0288	0.0094
- Straight gyrus	right	-0.0558	-0.0565	-0.0136	0.0007	*-0.0422	-0.0429
	left	-0.0579	-0.0837	-0.0098	0.0258	*-0.0481	**-0.0740
- Medial orbital gyrus	right	-0.0628	-0.0734	-0.0122	0.0107	**-0.0506	**-0.0613
	left	0.0134	-0.0244	0.0699	0.0378	*-0.0565	***-0.0943
- Posterior orbital gyrus	right	0.0144	0.0292	0.0623	-0.0148	-0.0479	-0.0331
	left	0.1057	0.1204	0.1673	-0.0147	**-0.0616	-0.0469
Global (the whole brain)		0.0080	0.1051	0.2459	-0.0971	****-0.2379	*-0.1408

EIV = estimated index values. DEIV = difference of the estimated index values. * α < 0,05. ** α < 0,01. *** α < 0,001. **** α < 0,0001. Mark (c) means square root conversion and (d) conversion of logarithm.

5.2.2 Longitudinal study (study II)

The results of TBM analysis of **study II** (**Table 10**) show the EIVs and DEIVs for the study groups.

Table 10. Statistical results of the TBM analysis. Study II.

Group comparisons							
Tensor-based morphometry analysis		**Controls**	**MCIall 0 yr**	**MCIs 0 yr**	**MCIs 2 yr**	**MCIp 0 yr**	**MCIp 2 yr**
		EIV	**EIV**	**EIV**	**EIV**	**EIV**	**EIV**
Medial temporal lobe							
A. Hippocampus	right	-0.011	0.035	0.039	0.106	0.030	0.190
	left	0.102	0.157	0.138	0.202	0.175	0.250
B. Anterior temporal lobe, medial part	right	0.112	0.207	0.238	0.255	0.175	0.244
	left	0.042	0.061	0.041	0.119	0.081	0.139
C. Parahippocampal gyrus and ambiens	right	0.101	0.173	0.206	0.254	0.141	0.223
	left	0.118	0.163	0.139	0.225	0.187	0.245
D. A.+ B.+ C.	right	0.020	0.092	0.099	0.198	0.084	0.250
	left	0.123	0.179	0.153	0.266	0.205	0.297
Ventricles							
A. Lateral ventricle (frontal and occipital horn and central part)	right	-0.095	0.037	-0.059	0.074	0.134	0.282
	left	-0.240	-0.154	-0.276	-0.136	-0.032	0.058
B. Lateral ventricle (temporal horn)	right	-0.062	-0.084	-0.093	-0.037	-0.076	0.019
	left	0.035	0.065	0.062	0.107	0.069	0.111
C. Third ventricle		-0.082	0.097	0.031	0.075	0.163	0.174
D. A. + B. + C.	right	-0.091	0.039	-0.056	0.076	0.134	0.280
	left	-0.233	-0.149	-0.270	-0.133	-0.027	0.060
Frontal area (prefrontal)							
- Frontal lobe, (Middle frontal gyrus)	right	0.170	0.162	0.106	0.164	0.217	0.270
	left	0.198	0.187	0.137	0.180	0.237	0.270
- Superior frontal gyrus	right	0.128	0.183	0.156	0.184	0.210	0.251
	left	0.212	0.262	0.216	0.270	0.307	0.347
- Inferior frontal gyrus	right	0.086	0.109	0.111	0.087	0.108	0.120
	left	0.093	0.108	0.097	0.069	0.119	0.140
- Anterior orbital gyrus	right	0.113	0.153	0.168	0.169	0.138	0.143
	left	0.121	0.087	0.069	0.048	0.104	0.128
Other temporal areas							
- Superior temporal gyrus, posterior part	right	0.100	0.173	0.140	0.181	0.206	0.276
	left	0.047	0.133	0.093	0.154	0.173	0.230
- Posterior temporal lobe	right	0.039	0.135	0.060	0.138	0.210	0.304
	left	0.657	0.695	0.638	0.679	0.752	0.776
- Lateral occipitotemporal gyrus, gyrus fusiformis	right	0.045	0.116	0.145	0.194	0.086	0.153
	left	0.100	0.173	0.140	0.181	0.206	0.276
Parietal lobe							
- Parietal	right	0.180	0.275	0.220	0.277	0.330	0.410
	left	0.027	0.063	0.001	0.103	0.125	0.192
Global (the whole brain)		-0.046	0.056	-0.045	0.083	0.156	0.283

MCIs = MCI stable, MCIp = MCI progression, yr = year, 0 yr = baseline, 2 yr = after 2-year follow-up, EM = estimated means, DEM = difference of the estimated means, EIV = estimated means of index values, DEIV = difference of the estimated index values, yr = year. * $\alpha < 0.05$. ** $\alpha < 0.01$. *** $\alpha < 0.001$. **** $\alpha < 0.0001$.

	A	B	C	D	E	F	G	H	J
	C vs MCIall 0 yr	C vs MCIs 0 yr	C vs MCIp 0 yr	C vs MCIs 2 yr	C vs MCIp 2 yr	MCIs 0 yr vs MCIp 0 yr	MCIs 2 yr vs MCIp 2 yr	MCIs 0 yr vs MCIs 2 yr	MCIp 0 yr vs MCIp 2 yr
	DEIV	DEIV	DEIV	DEIV	DEIV	DEIV	DEIV	DEIV	DEIV
	-0.0454	-0.0497	-0.0410	-0.1171	***-0.2011	0.0087	-0.0840	-0.0673	-0.1600
	-0.0542	-0.0355	-0.0728	-0.0995	*-0.1476	-0.0373	-0.0481	-0.0640	-0.0748
	**-0.0945	-0.1260	-0.0630	-0.1430	*-0.1318	0.0630	0.0112	-0.0169	-0.0688
	-0.0190	0.0006	-0.0386	-0.0774	-0.0974	-0.0392	-0.0200	-0.0780	-0.0588
	*-0.0720	-0.1046	-0.0395	**-0.1529	**-0.1214	0.0651	0.0315	-0.0483	-0.0819
	-0.0456	-0.0217	-0.0695	*-0.1071	**-0.1276	-0.0479	-0.0204	-0.0855	-0.0581
	-0.0714	-0.0787	-0.0641	*-0.1780	****-0.2298	0.0146	-0.0518	-0.0993	-0.1657
	-0.0565	-0.0305	-0.0824	-0.1431	**-0.1745	-0.0519	-0.0315	-0.1126	-0.0921
	-0.1321	-0.0356	-0.2286	-0.1684	**-0.3761	-0.1930	-0.2077	-0.1328	-0.1475
	-0.0860	0.0360	-0.2079	-0.1036	*-0.2973	-0.2439	-0.1937	-0.1396	-0.0894
	0.0225	0.0311	0.0139	-0.0254	-0.0808	-0.0172	-0.0554	-0.0565	-0.0947
	-0.0303	-0.0268	-0.0338	-0.0721	-0.0764	-0.0070	-0.0043	-0.0453	-0.0426
	**-0.1786	-0.1130	**-0.2441	-0.1562	**-0.2554	-0.1311	-0.0992	-0.0432	-0.0113
	-0.1296	-0.0345	-0.2247	-0.1664	**-0.3709	-0.1902	-0.2044	-0.1319	-0.1462
	-0.0840	0.0375	-0.2055	-0.1001	*-0.2931	-0.2431	-0.1930	-0.1376	-0.0876
	0.0080	0.0636	-0.0475	0.0057	-0.1003	-0.1111	-0.1060	-0.0579	-0.0528
	0.0107	0.0603	-0.0390	0.0181	-0.0725	-0.0993	-0.0906	-0.0422	-0.0335
	*-0.0549	-0.0280	-0.0818	-0.0563	**-0.1232	-0.0538	-0.0669	-0.0283	-0.0414
	*-0.0490	-0.0032	**-0.0949	-0.0574	****-0.1343	-0.0916	-0.0769	-0.0542	-0.0394
	-0.0235	-0.0248	-0.0222	-0.0009	-0.0343	0.0026	-0.0334	0.0239	-0.0121
	-0.0153	-0.0043	-0.0263	0.0238	-0.0474	-0.0220	-0.0712	0.0281	-0.0212
	*-0.0397	-0.0546	-0.0247	-0.0558	-0.0304	0.0300	0.0254	-0.0011	-0.0057
	*0.0347	0.0520	0.0174	0.0731	-0.0071	-0.0346	*-0.0803	0.0211	-0.0245
	*-0.0727	-0.0397	*-0.1056	-0.0812	****-0.1756	-0.0659	-0.0944	-0.0415	-0.0700
	**-0.0861	-0.0461	**-0.1261	-0.1070	****-0.1829	-0.0800	-0.0758	-0.0609	-0.0568
	-0.0960	-0.0212	*-0.1709	-0.0993	***-0.265	-0.1497	-0.1657	-0.0781	-0.0942
	-0.0377	0.0196	*-0.09487	-0.0215	**-0.1183	-0.1145	-0.0968	-0.0411	-0.0235
	*-0.0701	-0.0993	-0.0409	*-0.1484	*-0.1077	0.0585	0.0407	-0.0491	-0.0668
	-0.0484	-0.0259	-0.0710	-0.1023	*-0.1090	-0.0451	-0.0067	-0.0765	-0.0381
	**-0.0946	-0.0394	**-0.1498	-0.0967	****-0.2295	-0.1104	-0.1328	-0.0573	-0.0797
	-0.0359	0.0264	-0.0981	-0.0763	-0.1644	-0.1245	-0.0881	-0.1026	-0.0662
	-0.1019	**-0.0010	-0.2028	-0.1291	-0.3292	-0.2019	-0.2000	-0.1282	-0.1264

At baseline, the MCI_{all} group differed significantly from the controls (comparison A) in the right side of the MTL and in the third ventricle. When the MCI_{all} group was divided into the MCI_{stable} and $MCI_{progression}$ groups, the differences compared to controls (comparisons B and C) were smaller, and the only statistically significant difference was in the third ventricle in the $MCI_{progression}$ group. However,

the negative DEIVs indicated more AD type volume changes in both MCI groups when compared to the control group.

At the 2-year follow-up, TBM indicated that the MCI_{stable} group had developed significant changes bilaterally in the parahippocampal gyrus and ambiens, and on the right side of the combined MTL area in comparison to the controls (comparison D). At the same time, the $MCI_{progression}$ group differed significantly from the controls (comparison E) in nearly all areas.

At baseline, there were no significant differences between the MCI groups (comparison F). At follow-up, the only significant difference between MCI groups was evident in the left side of the anterior orbital gyrus (comparison G). Within the MCI_{stable} or $MCI_{progression}$ groups no significant differences were seen during follow-up (comparisons H or J). However, all DEIVs within the $MCI_{progression}$ and MCI_{stable} groups showed evidence of a progression towards the AD type of volume changes.

At baseline, the DEIV of MCI subjects showed a trend towards AD-type volume changes in the frontal areas, other temporal areas and the parietal lobes. Statistically significant differences were seen in the MCI_{all} and $MCI_{progression}$ groups in comparison to controls (comparisons A and C). At follow-up, the $MCI_{progression}$ group developed more typical AD-type volume changes and clearly differed from controls (comparison E). In the MCI_{stable} group, the only significant difference compared to controls (comparison D) was seen in the right lateral occipitotemporal area. In comparisons between or within the MCI groups, there were no statistically significant findings (comparisons E, G, H or J). However, most DEIVs showed signs of the progression towards AD-type volume changes in these comparisons.

5.2.3 Association study between deep gray matter and neurocognitive function (study III)

The descriptive TBM statistics of the groups and the p-values of the group comparisons of **study III** are shown in **Table 11**.

In all brain areas, the highest mean and median IVs were identified in the AD group. The mean and median IVs were lower in the MCI group than in the control group in the left thalamus and both sides of the putamen, whereas they were higher in the right thalamus and both sides of the caudate nucleus. There was a statistically significant difference in IV values between the study groups. When individual groups were compared with each other, the difference between the control and MCI groups was significant only in the right side of the putamen. The difference between the control and AD groups was significant in all other brain areas, with the exception of the left thalamus and right putamen. The left thalamus and both sides of the putamen were the areas in which the MCI and AD groups significantly differed from each other.

Table 11. Statistical results of the TBM differences between the groups. Study III.

Brain areas	Group	TBM results (IVs)			Test statistics F (df)	Overall p-value between the groups	Pairwise comparisons	
		Mean	Median	SD			Groups	p-value
Thalamus right	control	-0.208	-0.247	0.19	4.61 (2)	*0.011	control vs. MCI	0.914
	MCI	-0.190	-0.230	0.20			control vs. AD	*0.013
	AD	-0.094	-0.140	0.24			MCI vs. AD	0.082
Thalamus left	control	-0.282	-0.316	0.20	4.49 (2)	*0.013	control vs. MCI	0.659
	MCI	-0.319	-0.354	0.21			control vs. AD	0.078
	AD	-0.199	-0.245	0.21			MCI vs. AD	*0.015
Putamen right	control	-0.103	-0.106	0.17	8.44 (2)	****<0.0001	control vs. MCI	*0.022
	MCI	-0.195	-0.233	0.17			control vs. AD	0.251
	AD	-0.054	-0.067	0.16			MCI vs. AD	****<0.0001
Putamen left	control	-0.131	-0.111	0.15	9.81 (2)	****<0.0001	control vs. MCI	0.146
	MCI	-0.195	-0.203	0.18			control vs. AD	*0.018
	AD	-0.049	-0.055	0.15			MCI vs. AD	****<0.0001
Caudate nucleus right	control	0.011	0.001	0.23	4.75 (2)	*0.010	control vs. MCI	0.671
	MCI	0.057	0.091	0.27			control vs. AD	***0.008
	AD	0.158	0.155	0.29			MCI vs. AD	0.159
Caudate nucleus left	control	-0.154	-0.154	0.24	6.75 (2)	**0.002	control vs. MCI	0.380
	MCI	-0.079	-0.058	0.23			control vs. AD	***0.001
	AD	0.030	0.024	0.32			MCI vs. AD	0.135

* $\alpha < 0.05$, ** $\alpha < 0.01$, *** $\alpha < 0.001$, and **** $\alpha < 0.0001$. IVs = index values, SD = standard deviation, df = degree of freedom.

5.3 Receiver operating characteristic analysis

5.3.1 Cross-sectional study (study I)

In ROC analysis of **study I** (**Table 12** and **Figure 7**), the AUCs were performed to compare whether there was a sufficient difference in the hippocampal atrophy by VRM and TBM to differentiate the groups from each other. The AUCs were not significantly different between the groups with respect to any of the variables of interest, with the values of the AUCs varying between 0.564 and 0.768. In the left side, the AUC of TBM was larger than the VRM at a trend level ($p = 0.09$) when the controls were compared with the MCI subjects. In the right side, when the AUC values of the VRM was assessed, they were larger than TBM at a trend level ($p = 0.07$) when the MCI subjects were compared with the AD subjects.

Table 12. ROC analysis of study I. Comparison analysis of AUCs between the hippocampus of TMB and the hippocampus score of VRM. The hippocampus score of VRM was used as a reference.

ROC		TBM	VRM	Estimate	p-value
Controls vs. MCI subjects	Right side	0.6417	0.5642	0.0775	0.15
	Left side	0.6796	0.5877	0.0919	0.09
Controls vs. AD subjects	Right side	0.7407	0.7680	-0.0273	0.40
	Left side	0.7774	0.7609	0.0165	0.63
MCI subjects vs. AD subjects	Right side	0.6367	0.7066	-0.0699	0.07
	Left side	0.6510	0.6782	-0.0272	0.51

Estimate = difference of AUCs between TBM and VRM.

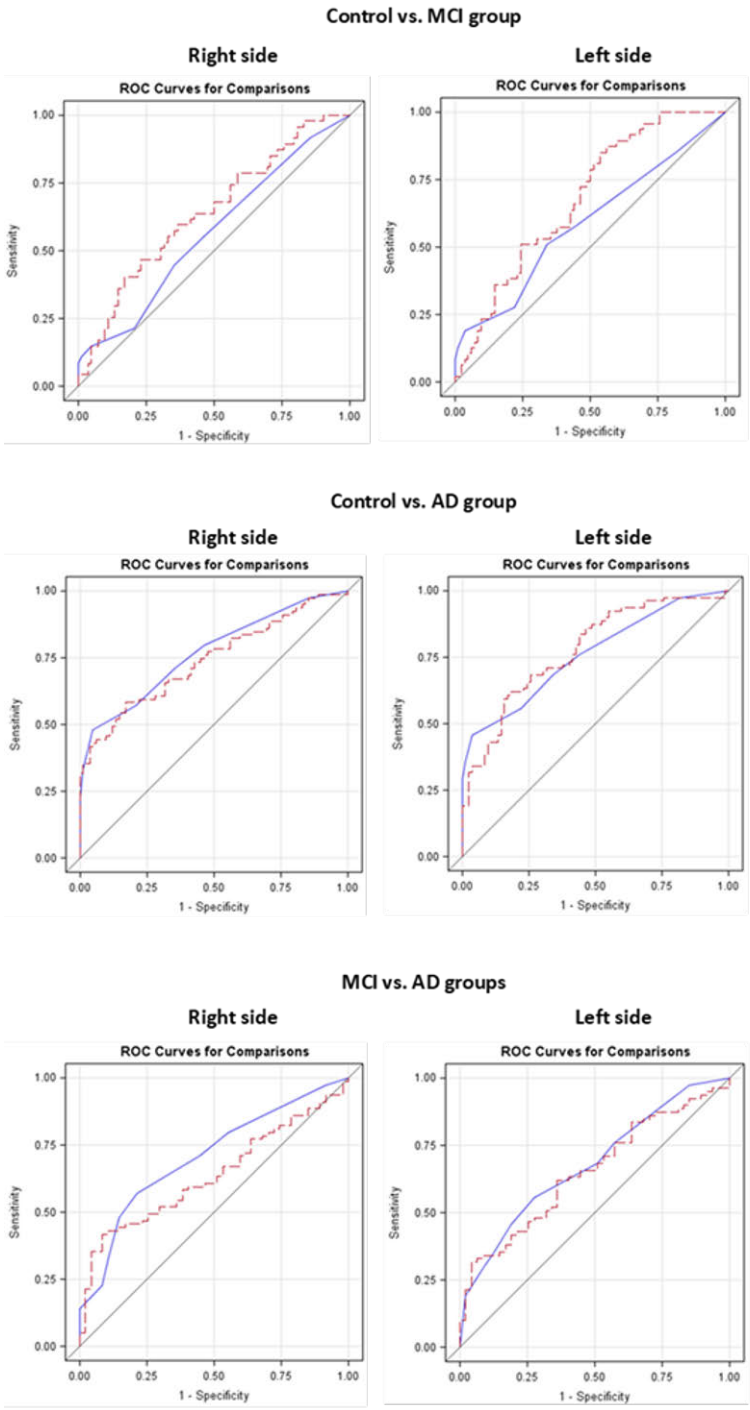

Figure 7. ROC curves for comparisons of the control and MCI groups, controls and AD groups, and MCI and AD groups from right and left sides between the hippocampus of TBM (red line) and the hippocampus score of VRM (reference, blue line).

5.4 Neuropsychological test analyses

5.4.1 Cross-sectional study (study I)

Neuropsychological characteristics of the subjects of **study I** are presented in **Table 13**.

In nearly all neuropsychological tests, the control group had better results than MCI and AD groups and MCI group had better results than the AD group. Only in the constructional praxis test had the controls somewhat worse results than the MCI group. However, the control group performed significantly better than the MCI group only in the episodic memory tests (both logical memory tests and delayed word recall test). The result demonstrates the absence of any widespread cognitive decline in the MCI subjects and indicates that the MCI subjects were of the amnestic subtype. The MCI group managed significantly better than the AD group in nearly all episodic memory and learning tests and in some language and executive tests. The AD group performed significantly worse than the control group in all tests except in constructional praxis test.

Table 13. Statistical results of the neuropsychological tests. Study I.

Analysis of neuropsychological tests	Controls	MCI subjects	AD subjects	Controls vs. MCI subjects	Controls vs. AD subjects	MCI vs. AD subjects
	EM (SD)	EM (SD)	EM (SD)	DEM	DEM	DEM
MMSE	27.8 (0.35)	26.5 (0.48)	22.3 (0.41)	*1.356	****5.497	****4.142
Neuropsychological test						
Episodic memory						
- Logic memory	20.8 (1.37)	16.4 (1.61)	12.0 (1.55)	**4.351	****8.745	**4.394
- Logic memory delayed	17.0 (1.43)	11.5 (1.68)	7.4 (1.62)	**5.477	****9.612	*4.135
- Wordlist learning (sum)	20.2 (1.00)	19.1 (1.17)	15.2 (1.14)	1.104	****5.054	***3.951
- Word delayed recall	7.3 (0.44)	6.1 (0.52)	4.4 (0.50)	*1.288	****2.933	**1.645
- Wordlist savings (%)	91.8 (5.98)	82.8 (7.04)	63.3 (6.76)	9.033	****28.549	**19.517
- Wordlist recogn. (%) (b)	97.0 (2.04)	92.9 (2.40)	86.7 (2.31)	4.105	****10.292	*6.187
- Constr. praxis savings (c)	7645.0 (682.61)	7327.5 (801.66)	5608.5 (779.82)	317.540	**2036.520	1718.990
Verbal functions						
- Semantic fluency	22.7 (1.29)	19.9 (1.51)	19.6 (1.46)	2.746	*3.052	0.305
- Naming	13.3 (0.45)	12.6 (0.53)	10.9 (0.51)	0.673	****2.370	**1.697
Visuospatial function						
- Constructional praxis (b)	9.9 (0.37)	10.1 (0.43)	9.5 (0.42)	-0.197	0.375	0.572
Executive functions						
- Clock drawing	5.4 (0.31)	5.2 (0.36)	4.1 (0.35)	0.159	****1.287	**1.128
- Trail making A	71.5 (8.43)	81.4 (9.85)	97.4 (9.36)	-9.850	**-25.854	-16.005
- Trail making B	142.6 (22.21)	172.1 (27.73)	222.6 (26.38)	-29.547	**-80.067	-50.520

EM = estimate of the means, SD = standard deviation, DEM = difference of the estimated means. * α < 0.05. ** α < 0.01. *** α < 0.001. **** α < 0.0001. Distribution of Constructional praxis and Wordlist recognition (%) task values were highly skewed (b) and they were not able to be converted normal distribution. Mark (c) means a square root conversion.

5.4.2 Longitudinal study (study II)

The neuropsychological characteristics of the subjects of **study II** are shown in **Table 14**.

At baseline, the MCI_{all} and $MCI_{progression}$ groups had significant impairments when compared to controls in the logical memory scores and delayed recognition of wordlists (comparisons A and C), confirming the amnestic form of MCI and the absence of widespread cognitive decline. At baseline and after the 2-year follow-up, the MCI_{stable} group did not differ from the controls (comparison B and D), but the MMSE results of the MCI_{stable} group were significantly worse after the 2-year follow-up as compared to the group's own baseline scores (comparison H). At baseline, MCI_{stable} and $MCI_{progression}$ groups did not differ from each other (comparison F). After the 2-year follow-up, the $MCI_{progression}$ group had highly significant impairments in almost all the cognitive domains in comparison to controls (comparison E), and the $MCI_{progression}$ group performed significantly worse on the MMSE and some episodic and executive functions when compared to the MCI_{stable} group (comparison G) or compared to the group's own baseline scores (comparison J).

These characteristics highlight the clear separation of our study population into the MCI subjects, AD (MCIp 2 yr) subjects and cognitively healthy controls.

Table 14. Statistical results of the analysis of neuropsychological tests. Study II.

Analysis of neuropsychological tests	Controls 0 yr	MCIall 0 yr	MCIs 0 yr	MCIs 2 yr	MCIp 0 yr	MCIp 2 yr
	EM	EM	EM	EM	EM	EM
MMSE	28.0	27.8	27.9	26.6	27.7	22.4
Neuropsychological test						
Episodic memory						
- Logic memory	22.0	19.1	19.3	15.4	18.9	13.7
- Logic memory delayed	18.3	13.6	14.5	10.9	12.7	10.1
- Wordlist learning (sum)	20.6	20.8	20.9	18.2	20.8	13.4
- Word delayed recall	7.6	6.7	6.9	5.8	6.5	3.5
- Wordlist savings (c)	8885.9	7283.8	7802.4	7810.0	6765.2	4291.1
- Wordlist recogn. (%) (b)	97.9	94.5	95.2	87.7	93.7	86.5
- Constr. praxis savings (c)	7301.3	6737.9	6593.2	7169.0	6882.5	3000.7
Verbal functions						
- Semantic fluency	23.7	21.1	21.3	20.8	20.9	15.6
- Naming	13.2	13.4	13.2	12.6	13.6	12.0
Visuospatial function						
- Constructional praxis (b)	10.0	10.5	10.8	10.5	10.2	9.2
Executive functions						
- Clock drawing	5.5	5.8	5.9	5.5	5.6	3.5
- Trail making A (d)	3.5	3.7	3.7	3.3	3.8	4.5
- Trail making B	138.9	151.1	130.6	143.6	171.7	279.2

MCIs = MCI stable, MCIp = MCI progression, yr = year, 0 yr = baseline, 2 yr = after 2-year follow-up, EM = estimated means, DEM = difference of the estimated means, yr = year. * $\alpha < 0.05$. ** $\alpha < 0.01$. *** $\alpha < 0.001$. **** $\alpha < 0.0001$. Distribution of wordlist recognition (%) (b) and constructional praxis (b) task values were highly skew and they were not able to change towards normal. The reliability of these marked results is not guaranteed. Mark (c) means a square root conversion and (d) means conversion of logarithm.

	A	B	C	D	E	F	G	H	J
	C vs MCIall 0 yr	C vs MCIs 0 yr	C vs MCIp 0 yr	C vs MCIs 2 yr	C vs MCIp 2 yr	MCIs 0 yr vs MCIp 0 yr	MCIs 2 yr vs MCIp 2 yr	MCIs 0 yr vs MCIs 2 yr	MCIp 0 yr vs MCIp 2 yr
	DEM	DEM	DEM	DEM	DEM	DEM	DEM	DEM	DEM
	0.2	0.2	1.5	0.3	****5.6	0.1	***4.2	****5.3	****5.3
	2.8	2.6	6.6	3.0	**8.3	0.4	1.7	4.0	5.2
	*4.7	3.8	7.4	5.6	**8.2	1.9	0.8	3.6	2.6
	-0.2	-0.3	2.4	-0.1	****7.2	0.1	4.8	2.7	**7.3
	0.9	0.7	1.8	1.1	****4.1	0.4	2.2	1.1	**3.0
	1602.1	1083.5	1075.9	2120.7	****4594.8	1037.3	3519.0	-7.6	2474.1
	3.4	2.6	**10.2	4.2	****11.4	1.5	1.1	7.6	7.2
	563.5	708.1	132.3	418.8	***4300.7	-289.3	*4168.3	-575.8	*3881.9
	2.6	2.4	2.9	2.8	****8.1	0.4	5.2	0.5	5.3
	-0.2	0.0	0.6	-0.4	1.2	-0.4	0.6	0.6	0.6
	-0.5	-0.8	-0.6	-0.2	0.8	0.7	1.3	0.3	1.0
	-0.3	-0.4	0.0	-0.2	****1.9	0.3	*2.0	0.4	**2.1
	-0.2	-0.2	0.1	-0.3	***-1.0	-0.1	**-1.2	0.3	-0.7
	-12.2	8.4	-4.6	-32.7	**-140.3	-41.1	-135.7	-13.0	-107.6

5.4.3 Association study between deep gray matter and neurocognitive function (study III)

The neuropsychological characteristics of the subjects examined in **study III** are shown in **Table 15**.

There were statistically significant differences between the controls and the AD group on all cognitive tests, and the effect sizes ranged from small in visuoconstructive function to very large in free recall, memory consolidation and naming. The MCI group performed significantly worse than the controls on measures of memory, as well as in semantic and visuo-motor processing. Effect sizes ranged from small for the latter functions (d = 0.40, 0.44) to medium/large for both memory measures (d = 0.66, 0.81). The MCI group performed significantly better than the AD group in all tests of memory and learning, as well as in the naming task. The effect sizes ranged from medium to large.

Table 15. Statistical results of cognitive function analysis. Study III.

Cognitive function (test)	Group	Neuropsychological results			Group compares	p-value	Cohen's d
		Mean	Median	SD			
Free recall (WMS-R Logical memory immediate recall)	control	20,6	20,0	7,0	control vs. MCI	**0.001	0.66
	MCI	16,2	15,0	6,3	control vs. AD	****<.0.0001	1,43
	AD	11,0	11,0	6,4	MCI vs. AD	****<.0.0001	0,82
Memory consolidation (WMS-R Logical memory delayed recall)	control	16,8	17,0	6,5	control vs. MCI	**0.001	0,81
	MCI	11,1	8,0	7,6	control vs. AD	****<.0.0001	1,57
	AD	6,3	3,0	6,9	MCI vs. AD	**0.005	0,66
Learning (CERAD wordlist learning)	control	19,8	20,0	4,4	control vs. MCI	0.340	0,21
	MCI	18,9	20,0	4,2	control vs. AD	****<.0.0001	1,11
	AD	14,2	14,0	5,6	MCI vs. AD	****<.0.0001	0,95
Naming (CERAD naming)	control	13,0	13,0	1,7	control vs. MCI	0.098	0,37
	MCI	12,3	13,0	2,1	control vs. AD	****<.0.0001	1,24
	AD	9,9	10,0	3,1	MCI vs. AD	**0.003	0,91
Semantic processing (CERAD animal fluency)	control	21,8	21,5	5,3	control vs. MCI	*0.035	0,44
	MCI	19,6	19,0	4,6	control vs. AD	**0.002	0,58
	AD	17,8	17,5	8,1	MCI vs. AD	0.240	0,27
Visuoconstructive function (CERAD Constructional praxis)	control	9,6	10,0	1,9	control vs. MCI	0.824	0,06
	MCI	9,7	10,0	1,6	control vs. AD	*0.010	0,41
	AD	8,8	9,0	2,0	MCI vs. AD	0.209	0,50
Visuo-motor function (TMT-A)	control	71,1	64,0	36,1	control vs. MCI	*0.042	0,40
	MCI	86,8	83,5	41,9	control vs. AD	**0.003	0,82
	AD	108,9	95,0	54,3	MCI vs. AD	0.362	0,46

* $\alpha < 0.05$, ** $\alpha < 0.01$, *** $\alpha < 0.001$, and **** $\alpha < 0.0001$

5.5 Correlation and association analyses

5.5.1 Correlation analysis of hippocampal visual rating method scores and tensor-based morphometry index values (study II)

As the group comparisons in **study II** were calculated separately for VRM and TBM, the aim of Spearman's nonparametric correlation analysis was to evaluate the strength of an association between hippocampal VRM scores and TBM index values. **Table 16** reveals the presence of a significant correlation between the hippocampal VRM scores and the hippocampal EIVs of TBM in the controls (right: $\rho = 0.32$, $p = 0.003$; left: $\rho = 0.32$, $p = 0004$). In the separate MCI groups, a significant positive correlation was seen in the $MCI_{progression}$ group both at baseline (right: $\rho = 0.67$, $p = 0.002$; left: $\rho = 0.60$, $p = 0.007$) and after the 2-year follow-up (right: $\rho = 0.78$, $p = 0.000$; left: $\rho = 0.81$, $p = 0.000$). In the MCI_{stable} group, there was a significant positive correlation between the hippocampal VRM score and EIVs of TBM only at

follow-up in the left hippocampus (ρ = 0.81, p = 0.005), and in addition, to a trend level correlation in the right hippocampus (ρ = 0.61, p = 0.062), but not at baseline.

Table 16. Correlations between the hippocampal VRM scores and the hippocampal EIVs of TBM in the controls at the baseline and in the MCI_{all}, MCI_{stable} and $MCI_{progression}$ groups at baseline and after the 2-year follow-up. Study II.

Correlation analysis		**VRM hippocampal score**			
		Controls		**MCIall 0 yr**	
		Right	Left	Right	Left
TBM hippocampal EIV	Right	ρ = 0,32; p = 0,003		ρ = 0,62; p = 0,000	
	Left		ρ = 0,32; p = 0,004		ρ = 0,56; p = 0,001
Correlation analysis		**VRM hippocampal score**			
		MCIs 0 yr		**MCIp 0 yr**	
		Right	Left	Right	Left
TBM hippocampal EIV	Right	ρ = 0,42; p = 0,172		ρ=0,67; p=0,002	
	Left		ρ = 0,51; p = 0,091		ρ = 0,60; p = 0,007
Correlation analysis		**VRM hippocampal score**			
		MCIs 2 yr		**MCIp 2 yr**	
		Right	Left	Right	Left
TBM hippocampal EIV	Right	ρ = 0,61; p = 0,062		ρ = 0,78; p = 0,000	
	Left		ρ = 0,81; p = 0,005		ρ = 0,81; p = 0,000

yr = year, MCIs = MCI stable group, MCIp = MCI progression group, ρ = value of Spearman's nonparametric correlation analysis, p = p-value.

5.5.2 The association analyses between neurocognitive function and tensor-based morphometry (study III)

The association analyses between the TBM IVs and cognitive test results of **study III** (**Table 17**) were conducted separately for the control, MCI and AD groups. The univariate regression model revealed multiple associations, which causes an increased risk of a type 1 error. To minimize that risk, the $p < 0.01$ α level for statistical significance was chosen. The results were focused in the AD group, as very few significant associations were identified in the control and the MCI groups, and no clear clusters emerged.

Table 17. Association results of univariate regression model (p-value), and Pearson correlations. Study III.

Associations	Controls											
	Right thalamus		Left thalamus		Right putamen		Left putamen		Right caudate nucleus		Left caudate nucleus	
	p value	Pearson	p value	Pearson	p value	Pearson	p value	Pearson	p value	Pearson	p value	Pearson
Free recall	0,192	0,23	0,109	-0,129	*0,013	-0,306	0,191	-0,162	0,822	0,047	0,406	0,171
Memory consolidation	0,265	0,206	0,172	-0,111	**0,007	-0,339	0,277	-0,144	0,95	0,007	0,459	0,16
Semantic processing	0,712	0.035	0,763	0,025	0,875	-0,144	0,492	0,017	0,594	-0,132	0,837	0,033
Naming (b)	0,245	0,134	0,781	0,041	0,923	-0,069	0,962	-0,046	0,702	-0,014	0,309	0,116
Learning (c)	0,591	0,156	0,144	-0,036	0,402	-0,119	0,708	-0,042	0,938	0,047	0,915	0,108
Visuoconstructive function (b)	0,385	-0,063	0,071	-0,177	0,137	-0,174	0,775	-0,021	*0,037	-0,257	0,249	-0,098
Visuo-motor scanning (d)	0,274	0,213	**0,005	0,302	*0,038	0,238	0,098	0,206	0,21	0,24	0,323	0,22
	MCI											
Free recall	0,116	-0,196	*0,033	-0,36	0,818	-0,069	0,306	-0,173	*0,049	-0,328	0,452	-0,162
Memory consolidation	0,21	-0,196	*0,040	-0,319	0,999	0,027	0,595	-0,065	0,064	-0,287	0,755	-0,074
Semantic processing	0,92	0,051	0,979	-0,001	0,456	0,056	0,648	-0,085	0,86	0,073	0,663	0,012
Naming (b)	0,222	-0,292	0,114	-0,34	0,283	-0,348	0,062	-0,376	0,397	-0,249	0,843	-0,173
Learning (c)	0,617	-0,029	0,384	-0,144	0,143	0,135	0,907	-0,017	0,538	0,106	0,775	0,014
Visuoconstructive function (b)	0,073	-0,249	0,36	-0,121	0,074	-0,328	0,061	-0,295	0,165	-0,192	0,363	-0,155
Visuo-motor scanning (d)	*0,033	0,388	*0,028	0,348	0,197	0,275	0,085	0,288	***0,003	0,513	0,167	0,354
	AD											
Free recall	***0,001	-0,383	0,128	-0,193	0,112	-0,201	*0,032	-0,289	***0,004	-0,343	*0,011	-0,301
Memory consolidation	***0,001	-0,375	0,105	-0,204	0,213	-0,15	0,138	-0,201	*0,026	-0,266	0,065	-0,229
Semantic processing	***0,004	-0,313	0,3	-0,134	0,273	-0,15	0,077	-0,245	**0,007	-0,301	***0,001	-0,35
Naming (b)	0,653	-0,093	0,303	0,115	0,351	0,101	0,57	-0,092	0,401	-0,133	0,502	-0,124
Learning (c)	**0,005	-0,353	0,434	-0,21	0,167	-0,211	*0,014	-0,359	*0,024	0,023	*0,025	-0,286
Visuoconstructive function (b)	0,522	-0,038	0,395	-0,046	0,614	0,035	0,256	-0,085	0,371	-0,044	0,248	-0,111
Visuo-motor scanning (d)	*0,013	0,345	*0,015	0,323	0,214	0,179	0,263	0,172	*0,012	0,347	***0,001	0,42

Mark (b) indicates cube of x (x^3), mark (c) square of x (x^2), and mark (d) natural logarithmic conversion (Ln). * $\alpha < 0.05$, ** $\alpha < 0.01$, and *** $\alpha < 0.005$.

In the AD group, the strongest association cluster was identified between the measures of episodic memory (both free recall and memory consolidation), learning and verbal function and the right thalamic TBM IV. Significant associations were also identified between semantic processing and the bilateral caudate nucleus TBM IVs. The unilateral right caudate nucleus TBM IV was associated with free recall (a trend level association was also identified in the MCI group), whereas the left caudate nucleus TBM IV was associated with visuomotor scanning. A trend level association between visuomotor scanning was also identified in the right caudate nucleus in the AD group, and this association reached statistical significance ($p = 0.003$) in the MCI group. The association between both sides of the caudate nucleus and cognitive function in AD was supported by the finding that trend level associations were identified bilaterally for learning and unilaterally for memory consolidation (left) and free recall (right). In the control group, only limited significant associations were identified: the left thalamus and visuomotor scanning ($p = 0.005$) and the right putamen and memory consolidation ($p = 0.007$).

6 Discussion

The development of dementia takes years or possibly decades; thus, an accurate diagnosis is especially important in the early stages of neurodegenerative disease when, for example, the medical treatment for AD is most beneficial. In addition, the detection of early brain changes of AD can help to develop novel diagnostic methods and treatments.

The structural diagnostic imaging of neurodegenerative diseases has centered on the MTL and especially hippocampus, the region in which the atrophy is mainly encountered in subjects with MCI and AD (Vemuri & Jack, 2010; Pini et al., 2016). However, the atrophy of MTL is not an obligatory (Kemp et al., 2003) or a specific finding for MCI or AD as it can also be observed in other neurodegenerative diseases such as the dementia of Parkinson's disease (Junqué et al., 2005; Chen et al., 2016), dementia with Lewy bodies (Chow et al., 2012; Elder et al., 2017), frontotemporal (Barnes et al., 2006; Muñoz-Ruiz et al., 2012), semantic (Chan et al., 2001) and vascular dementias (Van De Pol et al., 2006; Kim et al., 2015), and to some extent also in normal aging (Anderton, 1997; Galton et al., 2001; Apostolova et al., 2012; Cavallin et al., 2012). The major problem in clinical imaging of dementia is the need to detect MCI patients earlier than it is possible with current visual image analyzing methods. Several computer-based analyzing methods (Thompson & Apostolova, 2007; Vemuri & Jack, 2010; Rathore et al., 2017) have been developed to identify the structural neurodegenerative changes in research work and diagnostics, but in many cases, they have not displaced the visual analysis methods in daily radiology routine. In comparisons between visual rating and computer-based analyzing method in AD and FTD, the computer-based method used was volumetric-based morphometry (VBM). In MTL or hippocampus atrophy comparisons, the visual rating method was equivalent with VBM (Boutet et al., 2012; Cavallin et al., 2012; Chow et al., 2012), and correlated better to neuropsychologic test results and had better discriminatory power than VBM (Shen et al., 2011). Chow et al. (2012) also highlighted the difficulties in the translation of VBM into routine clinical work.

In scientific research, the computer-based analyzing methods make it possible to evaluate also other brain areas than MTL and hippocampus. In multiple studies, the dementia-connected atrophy has been shown to spread to other brain areas (Vemuri

& Jack, 2010; Whitwell 2010), but in the DGM, the significance for diagnostics and contribution to cognitive symptoms has remained largely unclear.

6.1 Visual magnetic resonance imaging analyses in Alzheimer's disease and mild cognitive impairment (studies I and II)

In **studies I and II**, TBM was compared to the visual methods of Scheltens et al. (1992) and Victoroff et al. (1994). Scheltens' scale is a structural-based MRI evaluation method to assess atrophy of the MTLs, especially the hippocampus (Scheltens et al., 1992; Scheltens et al., 1995), and is a widely used VRM in clinical work. A VRM for frontal atrophy evaluation has been developed by Victoroff et al. (1994), but it is rarely used in clinical work.

In the cross-sectional **study I**, when comparing the controls with the MCI group, the hippocampal atrophy values in VRM were greater in the MCI group than in the controls. The differences were not statistically significant, but the finding is in line with earlier studies which have revealed that patients with MCI or amnestic MCI have greater hippocampal atrophy scores in the VRM than controls (Duara et al., 2008; Urs et al., 2009; Shen et al., 2011). As controls and the MCI group were compared with the AD group, it was evident that the atrophy of the MTL and ventricular enlargement had progressed in the AD group, and VRM distinguished the groups from each other. As expected, controls differed from the AD group more clearly than the MCI group. Our finding of MTL atrophy is in agreement with the previous VRM results (Scheltens et al., 1995; Wahlund et al., 1999; Wahlund et al., 2000; Duara et al., 2008; Urs et al., 2009; Shen et al., 2011; Boutet et al., 2012; Duara et al., 2013). In VRM studies of ventricular enlargement, previous investigators did not detect any significant difference between AD and control groups (Scheltens et al., 1992). The ventricular evaluation method has not achieved popularity; the reason for this probably lies in the need of metric measurements of the width of the lateral and third ventricles, and to relate the results to the measurement of the inner calvarium. These calculations are time consuming, not very user-friendly and complicate distinguishing control, MCI and AD groups from each other.

In the longitudinal **study II**, VRM detected more and statistically significant hippocampal atrophy in the MCI_{all} group as compared to the control group at baseline. VRM also showed significantly higher atrophy scores in the $MCI_{progression}$ group than in the controls, but did not differentiate the MCI_{stable} group from controls at the baseline. At the 2-year follow-up, the $MCI_{progression}$ group had progressed to AD and the DEM values of VRM revealed the more progressed atrophy of the $MCI_{progression}$ group as compared to the controls, and the difference was significant.

The non-significant difference between the control and MCI_{stable} group remained unchanged.

The explanation for VRM separating the MCI_{all} group at the baseline and $MCI_{progression}$ group at both time points from the control group was most likely attributable to the large enough group sizes and large structural changes in these groups. In fact, the ability of VRM to separate heterogeneous MCI_{all} group and $MCI_{progression}$ (at baseline and after follow-up) groups from the controls was an expected result based on previous studies (Scheltens et al., 1992; Wahlund et al., 2000; Flak et al., 2018). It was disappointing that VRM did not manage to distinguish in a statistically significant manner the MCI_{stable} group from the control or $MCI_{progression}$ groups at any time points. However, as a trend of atrophy progression, MCI_{stable} group had higher scores and index values as compared to the controls, and lower scores and index values than $MCI_{progression}$ group in both time points. From this point of view, our finding is in line with earlier VRM studies, in which the MCI stable/nonconverter group differed from the MCI progressive/converter group (Bouwman et al., 2006; Persson et al., 2017). Duara et al. (2008) used a computer aided visual rating system, but they also separated controls, non-amnestic MCI, amnestic MCI and probable AD from each other. The reason for the non-significant results in MCI_{stable} group may be attributable to the small group size and an early stage of MCI disorder.

In **study II**, VRM was found to be insensitive in its ability to significantly detect structural changes in MCI_{stable} group between baseline and follow-up (comparison H in **table 8**) and in $MCI_{progression}$ group between baseline and follow-up (comparison J in **table 8**). In these comparisons, a trend towards a progressive atrophy was seen in score values of the groups, but not so clearly in the index values. There do not appear to be any other published studies which would have compared MCI_{stable} and $MCI_{progression}$ groups as conducted in comparisons H and J.

In both **studies I and II**, VRM did not detect any statistically significant differences in the frontal areas. Although there was a trend of higher atrophy scores in MCI and AD groups than in controls, we concluded that VRM was an insensitive method for frontal atrophy analysis. No previous studies of the frontal lobe atrophy evaluation by using visual rating scale of Victoroff et al. (1994) were found, and this may be result of a history of the verbal description of visual frontal atrophy evaluation rather than the application of numerical scoring.

In conclusion, **both studies** showed that VRM was not a reliable diagnostic method for revealing the early atrophy changes occurring in MCI. However, VRM can differentiate patients with progressive MCI from the controls and seems to be feasible application in the clinical evaluation of the progress of MCI patients to AD. In **both studies**, VRM was found to be an insensitive method for the analysis of frontal atrophy.

6.2 Tensor-based morphometry analysis in Alzheimer's disease and mild cognitive impairment (studies I and II)

In **studies I and II**, TBM was compared with the visual rating methods. TBM is a fully-automatic analyzing method for the whole or specific brain structures or CSF spaces. The method searches for local expansion or shrinking structures of the subject's brain and compares the changes in a large dataset. The dataset provides established diagnoses and a quantitative and visual estimate of the changes in the subject's AD type in the brain. In scientific work, there are several applications of TBM, which have been exploited both in cross-sectional and longitudinal dementia studies.

In cross-sectional **study I**, TBM revealed significant differences between controls and the MCI groups in the left hippocampus, and as a trend, the right hippocampus index values were also greater in the MCI group than in controls. When comparing the controls and the MCI group with the AD group, TBM distinguished the groups from each other as both the atrophy of the MTL and ventricular enlargement were more widespread in the AD group than in MCI group. In addition, controls differed from the AD group more clearly than the MCI group differed from the AD group. Our findings of the hippocampi, MTLs and lateral ventricles are in line with earlier studies (Hua et al., 2008a; Hua et al., 2008b; Muñoz-Ruiz et al., 2012). In the cross-sectional accuracy study, Muñoz-Ruiz et al. (2012) utilized the same TBM method as used here, but they did not analyze the left and right brain areas separately. They found a high TBM accuracy of the hippocampus and amygdala volumes and a good accuracy of the ventricular enlargement in the differentiation between the control and the AD groups (Muñoz-Ruiz et al., 2012). In the comparison of the control and $MCI_{progression}$ groups, the TBM accuracy for hippocampus and amygdala and ventricular enlargement was even better than in the comparison between the controls and the AD group (Muñoz-Ruiz et al., 2012). In comparison of the control and MCI_{stable} groups, the TBM accuracy was low for hippocampus and amygdala and ventricular enlargement (Muñoz-Ruiz et al., 2012). The modest TBM accuracy of MCI_{stable} group in the areas of hippocampus and amygdala and lateral ventriculi may be seen in our results too, as there were only a few significant findings between the control and MCI groups. A different TBM method was used in the study of Hua et al. (2008a), but they reported a significant difference between the control and AD groups in the left hippocampus, but not in the right side. In another study by Hua et al. (2008b), a significant difference of the hippocampi and MTL between the control, MCI and AD groups was found, but they did not analyze the left and right sides separately in that study.

In **study I**, the ROC analyses were performed to investigate which of the methods might be better at distinguishing the groups from each other. The ROC

analyses showed only a trend that TBM of the left hippocampus could differentiate MCI subjects from controls better than VRM. In the clinical evaluation of AD subjects, TBM displayed equal utility with VRM. On this basis, TBM and VRM seemed to be equally good at differentiating the groups from each other.

At baseline of the longitudinal **study II**, in the areas of MTL and lateral ventricles, TBM differentiated between the MCI_{all} and $MCI_{progression}$ groups and controls, but it did not separate the MCI_{stable} group from the controls. However, after the follow-up time, TBM identified some MTL differences between the MCI_{stable} and control groups, while at the same time, the MCI_{stable} group remained stable in their performance of the neuropsychological tests. This finding suggests that TBM is preconditioned to detect subtle volume changes that are not yet reflected in the cognitive status of the subjects. However, minor findings can also be variable in small study groups. It was a disappointment that TBM did not detect statistically significant results within the $MCI_{progression}$ group at follow-up, although atrophy was suggested by the index values. The small group sizes may partially explain the non-significant results in this analysis. In the previous TBM studies, temporal lobe atrophy was seen to progress significantly in the MCI group with follow-up times as short as 12 months (Hua et al., 2010), and the atrophy rate was significantly faster in $MCI_{progression}$ subjects than in MCI_{stable} subjects (Leow et al., 2009). In addition, Zhang et al. (2016 Apr) showed a significant atrophy progression of the hippocampi and lateral ventricles even in a group of basically healthy subjects who converted to MCI during a 2-years' follow-up time. Differences in the MCI populations, for instance in the severity of memory impairment, might explain the partially discrepant results between various studies.

In both **studies I and II**, statistically significant results of the frontal areas were detected only by TBM. In study I, the only significant difference in frontal areas was observed in the superior frontal gyrus between controls and the MCI group. In comparisons between MCI and AD groups and control and AD groups, the significant frontal atrophy was more apparent, but the findings were more modest as compared to the MTL and ventricular areas. Only Muñoz-Ruiz et al. (2012) have studied the accuracy of TBM in superior frontal gyrus of both sides in distinguishing between the control and AD groups; they found the accuracy to be low. The accuracy for the superior frontal gyrus in the differentiation of the control and MCI_{stable} or $MCI_{progression}$ groups was also low or good, respectively (Muñoz-Ruiz et al., 2012). The modest accuracy of TBM for the superior frontal gyrus may also explain the modest frontal results in our study.

In **study II**, the signs of atrophy in frontal, other temporal areas and right parietal findings of TBM were mainly evident in the MCI_{all} and $MCI_{progression}$ groups (in the baseline and after the follow-up time) as compared to the controls. Our results from these areas are modest, but partly in line with earlier studies as Leow et al. (2009)

found only a nearly significant atrophy of frontal lobes for the MCI group at the baseline, but after the 12 months' follow-up time, no signs of significant atrophy in the frontal lobes were found. Their results from parietal lobes were also statistically non-significant (Leow et al., 2009). The modest results of frontal and parietal lobes at the time of MCI are not unexpected as the atrophy spreads to these areas generally during the late stage of dementia (Thompson et al., 2003; Whitwell et al., 2007; Tondelli et al., 2012; Teipel et al., 2013; Trzepacz et al., 2014; Vega & Newhouse, 2014; Pini et al., 2016).

As a conclusion to **studies I and II**, TBM was found to be slightly more sensitive than VRM in MCI diagnostics, but the capability of TBM to detect the very early structural changes of MCI_{stable} group or progression of MCI groups was modest. In the frontal areas examined in **studies I and II**, the early differences were seen only by using TBM, but even in these cases, TBM was not found to be a very robust method.

6.3 Cognitive functions and tensor-based morphometry of deep gray matter structures in Alzheimer's disease and mild cognitive impairment (study III)

In dementia research there has been a growing interest in investigating the DGM areas as MRI analyzing methods have developed. Examining associations between neuropsychological test results and TBM results have made it possible to evaluate how volume changes in the DGM are related to cognitive impairment in dementia disorders.

In **study III**, TBM indicated group differences in both sides of the thalamus, putamen and caudate nucleus by showing that the AD group had more AD type changes than the control and MCI groups, although all comparisons were not statistically significant. On the right side of the thalamus and on both sides of the caudate nucleus, the MCI group had more AD type changes than the control group, even though the differences were not statistically significant. These group differences were expected on the basis of earlier DGM studies of AD and MCI subjects and healthy elderly subjects (de Jong et al., 2008; Liu et al., 2010; Roh et al., 2011; Cho et al., 2014; Hilal et al., 2015; Pini et al., 2016). In previous studies, thalamic atrophy has been shown to originate and progress bilaterally during the progression of dementia (de Jong et al., 2008; Pini et al., 2016; Yi et al., 2016). In our results, the AD type changes were slightly but insignificantly more positive on the right side than on the left side of the thalamus, and the influence of this difference was also seen in our association results as more significant neuropsychological associations were observed on the right side as compared to the left side in AD group.

Atrophy of the putamen is generally bilateral, but typically more prominent on the left lateral side of putamen during dementia progression (Cho et al., 2014; Pini et al., 2016). In our results, the AD type changes of putamen were similar on both sides. It was not possible to conduct a subregional lateralization since we analyzed only the whole putamen. Atrophy of the caudate nuclei, especially on the right side (Cho et al., 2014), has been found in the MCI and AD (Pini et al., 2016). In addition, Cho et al. (2014) found that the atrophy spreads to the left side in AD subjects. The trend was also seen in the results of the present study as AD type changes in the right caudate nucleus had higher values than on left side, although the differences between the groups were small and only partly significant.

In the AD group, right-sided thalamic and bilateral caudate nucleus brain-cognition clusters were identified, with partially overlapping cognitive associations. The right thalamic TBM index values were significantly associated with measures of learning, episodic memory and semantic processing. The reason for the finding may be that the reduced TBM index values were seen only in the right thalamus of the AD subjects. Another explanation may be in a less robust functional asymmetry at the thalamic level than at the cortical level or in the supporting role of the thalamus in the processing of episodic and semantic memory. Unfortunately, the neuropsychological test battery did not include visual memory or visuospatial tasks, thus it remains unclear whether these measures would have also been associated with thalamic changes. Our result is in contrast to a previous study (Cho et al., 2014), where no associations were found between right or left thalamic volume changes and the cognitive decline in AD. The explanation may be in the different sizes of the subject populations [36 AD subjects in Cho et al. (2014) study and 58 in our study] and in the longitudinal setting as compared to our cross-sectional study. Another explanation may also be differences in the evaluation of atrophy and statistical analyses applied. Cho et al. (2014) used a surface-based shape analysis and did not provide a detailed description of their statistical methods. Thus, it is impossible to determine whether these issues could explain the different findings.

In the AD group, the results for the caudate nucleus were relatively similar on both sides. Significant or trend level associations were identified between bilateral caudate TBM index value and measures of learning, free recall, semantic processing and visuomotor scanning, which is in line with a previous study (Cho et al., 2014). The finding that left caudate volume was also associated with visuomotor speed could support the concept that the caudate nucleus is involved in the speed aspect of the semantic fluency task. In contrast to our results, a previous study (Cho et al., 2014) did not identify associations between a decline in verbal learning and DGM structures.

In **study III**, no systematic clusters of significant brain-cognition associations appeared in the healthy controls or the MCI subjects, which is in line with previous

studies with healthy subjects (de Jong et al., 2008; Hilal et al., 2015). This is probably at least partly due to the fact that the variation in both TBM index values as well as in cognitive test results is narrower in controls and MCI subjects, thus making it less likely to find significant correlations. The only brain-cognition association that was statistically significant or showed a trend level association in all three groups was the measure of visuomotor scanning and the TBM index values of the left thalamus (significant in the controls, trend in MCI and AD). One potential explanation for this finding may be related to basic motor coordination, as most subjects were right-handed.

In conclusion, **study III** showed that TBM is a feasible tool for evaluating structural changes of the thalamus, caudate nucleus and putamen at the group level. As expected, the AD group displayed severe structural DGM changes, but differences between the control and MCI groups were mostly insignificant. In the association analyses, degenerative changes of the right thalamus and bilateral caudate nucleus were associated with the cognitive impairment in the AD subjects. The results indicate that the atrophy of DGM structures is related to the cognitive impairment evident in AD. However, no systematic clusters of significant brain-cognition associations appeared in the healthy controls or the MCI subjects.

6.4 Limitations of the studies I, II and III

In **all three studies**, the relatively low number of MCI subjects can be viewed as a limitation. This might have influenced the failure to detect changes particularly after dividing the MCI_{all} group into the MCI_{stable} and $MCI_{progression}$ groups in study II. In addition, the early stage of neurodegenerative disease may also be one reason why the MCI group did not differ from the control group in most of the analyses. Had there been larger group cohorts, then it might have been possible to reveal differences more clearly, also in the case of early-stage MCI. Furthermore, in **study II**, the 2-year follow-up period was relatively short. A longer follow-up time might have revealed differences between the MCI_{stable} and $MCI_{progression}$ groups and may have also identified those MCI_{stable} subjects who would progress later. Further, the possibility to utilize of values of dementia biomarkers from the subjects (tau, phospho-tau and beta-amyloid 42 of CSF and APO ε4) would have helped to assess the MRI results from a wider frame of reference.

Both VRMs used in **studies I and II** have limitations in objectivity and level of quality as they are dependent on the reader's experience. The methods have also limitations in how well they can detect very small anatomical changes, based on limited resolution of the human eye. In addition, the quantification ability of the methods is relatively crude and suggestive. Moreover, they lack any criteria to evaluate structures deep inside the brain. However, the VRM of Scheltens et al.

(1995) was demonstrated to have a fair-to-good inter-rater reliability. In **studies I and II**, the hippocampus scores of our raters were close to each other, but better objectivity was achieved and quality biases of evaluations were avoided by using example images and guidelines (Scheltens et al., 1992; Scheltens et al., 1995) and by co-evaluation of those MR scans in which there were clear differences in the independent evaluations.

In **all three studies**, the methodological limitations of TBM included additional time for computation work, the possible inexactness in the atlas segmentation of the structures, the inaccurate precision of the registration algorithm and the Jacobian measurement of the volume changes alone.

TBM analysis can also suffer from the quality differences in MR scanning. In **all our studies**, the voxel sizes of the T1 sequences were not similar between the scanners, which may reduce contrast in the relatively small structures and introduce difficulties in their allocation in the TBM analysis. In addition, the use of specific hippocampus or DGM sequences instead of whole brain imaging would have improved the quality of the registration accuracy of the TBM analysis.

The same MMSE and neuropsychological test battery was used in all three studies. However, in **study III**, the test battery was not optimal for the association results as it measured an overall cognitive impairment, not a specific DGM dysfunction.

6.5 General discussion

It is recognized that the earliest possible diagnostics of different dementia forms is becoming more and more important to prevent the disadvantages of the diseases for the subjects, their relatives and society. For this reason, there is a growing demand to develop more exact radiological diagnostics methods. Recently, the previous visual analyzing method has been increasingly replaced with new semi-automatic or automatic computer-based methods, especially in research work. However, the easy-to-learn and quick-to-use visual rating method of assessing the hippocampus is still widely used in clinical radiology work.

To answer these diagnostic demands, the purpose of this thesis was to estimate the suitability of applying TBM in the clinical radiological diagnostics of dementia by comparing TBM and visual raging methods in the medial temporal and frontal lobes. In addition, the possibilities of TBM differentiation were evaluated in both structural group comparisons and in an association study in the area of deep gray matter; an approach not currently included in the clinical dementia diagnostics.

On the basis of our study, we conclude that TBM is a more sensitive method than VRM in detecting structural MTL changes in very early MCI. The additional benefit of TBM over VRM is its independence of subjective interpretations and the

possibility to evaluate different areas other than MTL. This result sends a message to both neurologists and radiologists that the new technology will soon achieve a feasible level to allow it to become a part of clinical radiology work. In the future, the possible commercial analysis software for TBM will lower the threshold for clinical implementation of the technique. On the other hand, VRM still has a well-argued place in the diagnostics as TBM and VRM were equally good in the clinical evaluation of the progress of MCI subjects and diagnostics of AD. There are other advantages associated with VRM; it is easy to learn and fast to use, does not need special equipment and finally it is inexpensive.

The brain areas outside the MTL and hippocampus, like frontal lobes and DGM, will likely remain the focus of research work in the near future, and the relevance of these results for clinical work will hopefully emerge later. However, TBM has proven to be a feasible research tool for these brain areas as the structural changes of DGM were shown to be related to cognitive performances, especially in the AD group. In this respect, the visual rating method is unlikely to have a future in the evaluation of DGM atrophy.

Despite the benefits of TBM, our studies left some questions unanswered. Our cross-sectional and longitudinal studies operated at the group level, which does not reveal much about the diagnostic ability of TBM at the level of the individual subject. In the future, this kind of subject-based information analyzed by TBM will need to be assessed from the clinical diagnostic point of view. Scheltens' VRM is a simple 5 step grading system and every score quickly gives an indication of the severity of the brain atrophy. In the TBM used in this study, the situation is more complex as the quantitative volume changes are extremely small and negative or positive index values do not provide information about the direction of the volume changes. Furthermore, a single visual presentation of TBM volume changes does not provide details about the degree of the changes as compared to other MCI or AD subjects. Thus, we will need to gather more experience about the application of TBM software in clinical work. It may well be possible to adapt TBM software to make it more suitable for clinical use, for example, by creating a simple and comparable rating scale for visual/index values for AD changes from an individual patient. Subsequently, it would also be possible to evaluate whether TBM is a cost-effective technique as compared to VRM.

7 Conclusions

I. Scheltens' visual rating method is still useful for the clinical evaluation of MTL atrophy in AD and MCI patients. However, a multi-template tensor-based morphometry is more sensitive than visual evaluation at revealing early atrophic changes.

II. Scheltens' visual rating method and multi-template tensor-based morphometry are equally good in the evaluation of longitudinal structural brain changes in large MCI groups progressing to AD. Only TBM revealed minor volume changes in the stable MCI group as compared to controls at follow-up. Neither visual rating method nor multi-template tensor-based morphometry had the capability to separate the groups of stable and progress MCI from each other.

III. Scheltens' visual rating method was found to be an insensitive method for the analysis of frontal atrophy. The multi-template tensor-based morphometry was capable of revealing more atrophy in frontal areas in MCI and AD subjects as compared to controls and during the progression of MCI to AD. However, these changes were not as robust as in medial temporal lobe areas.

IV. The multi-template tensor-based morphometry was capable of detecting Alzheimer-type changes of the deep gray matter structures in MCI and AD subjects.

V. Atrophy of the deep gray matter structures, especially the thalamus and caudate nucleus, was related to cognitive impairment in AD. The deep gray matter atrophy was associated with the performance of the subjects in tests reflecting both subcortical and cortical cognitive functions.

Acknowledgements

This thesis journey started around 2007 in Turku PET Centre, when a research plan received an official authorization in Turku University Faculty of Medicine. Professor Juha Rinne had started the main PET research project years earlier, and this thesis has utilized MRI data from the main project. The MRI data was collected between the years 1999 and 2008.

The thesis has received financial support from the Turku University Hospital (personal and clinical EVO/ERVA grants and research salaries) and from grants from the Finnish Medical Society Duodecim, the Turku University Foundation, the Turku University Doctoral Programme in Clinical Research (DPCR), the Turku University Department of Clinical Medicine, and the Radiological Society of Finland. The main PET project has also paid my salary from the grants of the Academy of Finland and the Sigrid Juselius Foundation.

I am grateful that all the original supervisors have remained in place for me. Professor, neurologist, Juha Rinne has paved the way of the thesis with his excellent experience of supervising theses, knowledge of neurodegenerative diseases and endless patience. Without his main PET research project, the thesis would not exist. Professor, neuroradiologist, Riitta Parkkola offered her valuable professional skills in the visual evaluation of MRI images of the thesis. She made possible the thesis by offering her neuroradiology employees to be my deputies. An ability to focus on the essentials and give clear answers are also her admirable characteristics. A member of my guidance group, Matti Laine, Professor of Psychology in Åbo Akademi, provided a valuable perspective of psychology in the thesis. Unfortunately, my limited competence of psychology did not allow for the utilization of all his information

The official reviewers, Docent, neuroradiologist, Michaela Bode from Oulu University and Docent, neuroradiologist Anna Sutela from Kuopio University gave their valuable perspectives for the thesis by asking relevant questions which have helped me to clarify ambiguous and difficult points in the text. The content of thesis is now more understandable, and I have received good suggestions for the thesis' public defenc e.

Chief scientific officer, Docent Jyrki Lötjönen and senior imaging scientist, Docent Juha Koikkalainen of Combinostics Oy, Tampere, Finland, are the

developers of the multi-template TBM analyzing method used in the thesis. I am grateful that they were willing to participate in the thesis by analyzing MRI data with TBM, and they were able to explain the analyzing method and interpretation of the results time and time again.

Docent, neuropsychologist Mira Karrasch in Åbo Academi has been an invaluable source of neuropsychology information. I appreciate her participation in writing the third article of the thesis. I believe that without her knowledge, the article would never have been approved for publication.

Biostatisticians Eliisa Löyttyniemi and Saija Hurme in Turku University offered their valuable professional skills for counselling and solving the statistical challenges of the third article.

Marko Tättäläinen and Rami Mikkola, excellent IT professionals in Turku PET Centre have always been there to help me when I have had to make sense of my research data. They have tirelessly solved problems with my personal computer and remote access; they have a great ability to explain difficult IT terms in a comprehensible manner.

I thank my former and present heads of Turku PET Centre, and Clinical Physiology and Nuclear Medicine in Turku University: Professor Juhani Knuuti, Professor Jukka Kemppainen, Maria Saarenhovi Ph.D and Docent Tuula Janatuinen. They have granted my leaves of absence and partly arranged the finance for these absences from the clinical ERVA grants. I thank my radiology colleagues at VSKK: Most of all Teemu Paavilainen Ph.D, Jussi Kankare MD, Pirkko Sonninen MD and Docent Sami Kajander have been valuable by acting as replacements during my leaves of absence. I thank all my colleagues at Clinical Physiology and Nuclear Medicine: You have stretched yourself at work during my leaves of absence. I thank all the radiographers of Turku PET Centre, who scanned the PET and MRI data of the main research project, and all the test subjects and their close relatives, who offered their time to participate in the research.

I express my gratitude to my father Tarmo Tuokkola, my sister Jutta Lindblom and her husband Joachim Lindblom for their mental support, and to my friends Eija, Bengt, Heidi, Elina, Jyrki and Kristiina for their true friendship. I am sorry I can't arrange and invite you to a party because of the COVID-19 virus.

My husband Antti Salomaa has been there for me throughout this journey. His endless love and ability to see the sunny side of the issues have made this journey possible.

Masku, February 2021
Terhi Tuokkola

References

Acharya, U., Hagiwara, Y., Sudarshan, V., Chan, W., & Ng, K., 2018. Towards precision medicine: From quantitative imaging to radiomics. *Journal of Zhejiang University-SCIENCE B,* 19(1), 6–24. <doi:10.1631/jzus.B1700260>

Alzheimer Europe organization, 2013. Alzheimer Europe Organization. Retrieved from <https://www.alzheimer-europe.org/>

Alzheimer's Disease Neuroimaging Initiative, 2017. ADNI dataset. Retrieved from <http://adni.loni.usc.edu/>

Alzheimer's Association, 2016. 2016 Alzheimer's disease facts and figures. *Alzheimer's & Dementia: The Journal of the Alzheimer's Association,* 12(4), 459–509. <doi:S1552–5260(16)00085-6 [pii]>

Ambikairajah, A., Devenney, E., Flanagan, E., Yew, B., Mioshi, E., Kiernan, M. C., Hodges, J. R., & Hornberger, M., 2014. A visual MRI atrophy rating scale for the amyotrophic lateral sclerosis-frontotemporal dementia continuum. *Amyotrophic Lateral Sclerosis & Frontotemporal Degeneration,* 15(3–4), 226–234. <doi:10.3109/21678421.2014.880180 [doi]>

Anderton, B. H., 1997. Changes in the ageing brain in health and disease. *Philosophical Transactions of the Royal Society of London. Series B: Biological Sciences,* 352(1363), 1781–1792. <doi:10.1098/rstb.1997.0162>

Andreasen, D., Van Leemput, K., Hansen, R. H., Andersen, J. A., & Edmund, J. M., 2015. Patch-based generation of a pseudo CT from conventional MRI sequences for MRI-only radiotherapy of the brain. *Medical Physics*, 42(4), 1596–1605. <doi:10.1118/1.4914158 [doi]>

Apostolova, L. G., 2016. Alzheimer disease. *Continuum (Minneapolis, Minn.),* 22(2 Dementia), 419–434. <doi:10.1212/CON.0000000000000307 [doi]>

Apostolova, L. G., Dutton, R. A., Dinov, I. D., Hayashi, K. M., Toga, A. W., Cummings, J. L., & Thompson, P. M., 2006. Conversion of mild cognitive impairment to Alzheimer disease predicted by hippocampal atrophy maps. *Archives of Neurology,* 63(5), 693–699. <doi:10.1001/archneur.63.5.693>

Apostolova, L. G., Green, A. E., Babakchanian, S., Hwang, K. S., Chou, Y., Toga, A. W., & Thompson, P. M., 2012. Hippocampal atrophy and ventricular enlargement in normal aging, mild cognitive impairment and Alzheimer's disease. *Alzheimer Disease & Associated Disorders* 26(1), 17–27. <doi:10.1097/WAD.0b013e3182163b62>

Appel, J., Potter, E., Shen, Q., Pantol, G., Greig, M. T., Loewenstein, D., & Duara, R., 2009. A comparative analysis of structural brain MRI in the diagnosis of Alzheimer's disease. *Behavioural Neurology,* 21(1–2), 13–19. <doi:10.1155/2009/103123>

Ashburner, J., & Friston, K., 2000. Voxel-based Morphometry—The methods. *NeuroImage,* 11(6), 805–821. <doi:10.1006/nimg.2000.0582>

Ashburner, J., & Friston, K. J. (Eds.), 2003. *Human brain function (2nd ed.). Chapter 36, Morphometry.* Cambridge, Massachusetts, United states, Academic Press, U.S.

Ashburner, J., Hutton, C., Frackowiak, R., Johnsrude, I., Price, C., & Friston, K., 1998. Identifying global anatomical differences: Deformation-based morphometry. *Human Brain Mapping,* 6(5-6), 348–357. <doi:10.1002/(SICI)1097-0193(1998)6:5/63.0.CO;2-P>

Barnes, J., Whitwell, J. L., Frost, C., Josephs, K. A., Rossor, M., & Fox, N. C., 2006. Measurements of the amygdala and hippocampus in pathologically confirmed Alzheimer disease and frontotemporal lobar degeneration. *Archives of Neurology,* 63(10), 1434–1439. <doi:10.1001/archneur.63.10.1434>

Batista, S., Zivadinov, R., Hoogs, M., Bergsland, N., Heininen-Brown, M., Dwyer, M., & Weinstock-Guttman, B., 2012. Basal ganglia, thalamus and neocortical atrophy predicting slowed cognitive processing in multiple sclerosis. *Journal of Neurology,* 259(1), 139–146. <doi:10.1007/s00415-011-6147-1>

Bellebaum, C., Koch, B., Schwarz, M., & Daum, I., 2008. Focal basal ganglia lesions are associated with impairments in reward-based reversal learning. *Brain: A Journal of Neurology,* 131*(Pt 3), 829–841.* <doi:10.1093/brain/awn011 [doi]>

Bennett, I. J., Golob, E. J., Parker, E. S., & Starr, A., 2006. Memory evaluation in mild cognitive impairment using recall and recognition tests. *Journal of Clinical and Experimental Neuropsychology,* 28(8), 1408–1422. <doi:Q80L3UX366242357 [pii]>

Bettio, L. E. B., Rajendran, L., & Gil-Mohapel, J., 2017. The effects of aging in the hippocampus and cognitive decline. *Neuroscience and Biobehavioral Reviews,* 79, 66–86. <doi:10.1016/j.neubiorev.2017.04.030>

Bobinski, M., de Leon, M. J., Wegiel, J., Desanti, S., Convit, A., Saint Louis, L. A., Rusinek, H., & Wisniewski, H. M., 2000. The histological validation of post mortem magnetic resonance imaging-determined hippocampal volume in Alzheimer's disease. *Neuroscience,* 95(3), *721–725.* <doi:S0306452299004765 [pii]>

Bondi, M. W., Edmonds, E. C., & Salmon, D. P., 2017. Alzheimer's disease: Past, present, and future. *Journal of the International Neuropsychological Society: JINS,* 23(9–10), 818–831. <doi:10.1017/S135561771700100X>

Boutet, C., Chupin, M., Colliot, O., Sarazin, M., Mutlu, G., Drier, A., Pellot, A., Dormont, D., & Lehéricy, S., 2012. Is radiological evaluation as good as computer-based volumetry to assess hippocampal atrophy in Alzheimer's disease? *Neuroradiology,* 54(12), 1321–1330. <doi:10.1007/s00234-012-1058-0>

Bouwman, F. H., Schoonenboom, S. N. M., van der Flier, W. M, van Elk, E. J., Kok, A., Barkhof, F., Blankenstein, A., & Scheltens, P., 2006. CSF biomarkers and medial temporal lobe atrophy predict dementia in mild cognitive impairment. *Neurobiology of Aging,* 28(7), 1070–1074. <doi:10.1016/j.neurobiolaging.2006.05.006>

Bozzali, M., Filippi, M., Magnani, G., Cercignani, M., Franceschi, M., Schiatti, E., Castiglioni, S., Mossini, R., Falautano, M., Scotti, G., Comi, G., & Falini, A., 2006. The contribution of voxel-based morphometry in staging patients with mild cognitive impairment. *Neurology,* 67(3), 453–460. <doi:10.1212/01.wnl.0000228243.56665.c2>

Braak, H., & Braak, E., 1991. Neuropathological stageing of Alzheimer-related changes. *Acta Neuropathologica,* 82(4), 239–259. <doi:10.1007/BF00308809>

Braskie, M. N., & Thompson, P. M., 2014. A focus on structural brain imaging in the Alzheimer's disease neuroimaging initiative. *Biological Psychiatry,* 75(7), 527–533. <doi:10.1016/j.biopsych.2013.11.020>

Brun, C. C., Leporé, N., Pennec, X., Lee, A. D., Barysheva, M., Madsen, S. K., Avedissian, C., Yi-Yu, C., Zubicaray, G. I., McMahon, K. L.,Wright, M. J., Toga, A. W., & Thompson, P. M., 2009. Mapping the regional influence of genetics on brain structure variability — A tensor-based morphometry study. *Neuroimage,* 48(1), 37–49. <doi:10.1016/j.neuroimage.2009.05.022>

Castellano, C., Hudon, C., Croteau, E., Fortier, M., St-Pierre, V., Vandenberghe, C., Nugent, S., Tremblay, S., Paquet, N., Lepage, M., Fulop, T., Turcotte, E. E., Dionne, I. J., Potvin, O., Duchesne, S., & Cunnane, S. C., 2019. Links between metabolic and structural changes in the brain of cognitively normal older adults: A 4-year longitudinal follow-up. *Frontiers in Aging Neuroscience,* 11, 15. <doi:10.3389/fnagi.2019.00015>

Cavallin, L., Bronge, L., Zhang, Y., Øksengård, A., Wahlund, L., Fratiglioni, L., & Axelsson, R., 2012. Comparison between visual assessment of MTA and hippocampal volumes in an elderly, non-demented population. *Acta Radiologica,* 53(5), 573–579. <doi:10.1258/ar.2012.110664>

Chan, D., Fox, N. C., Scahill, R. I., Crum, W. R., Whitwell, J. L., Leschziner, G., Rossor, A. M., Stevens, J. M., Cipolotti. L., & Rossor, M. N., 2001. Patterns of temporal lobe atrophy in semantic dementia and Alzheimer's disease. *Annals of Neurology,* 49(4), 433–442. <doi:10.1002/ana.92>

Chen, F., Kang, D., Chen, F., Liu, Y., Wu, G., Li, X., Yu, L-H., Lin, Y-X., & Lin, Z., 2016. Gray matter atrophy associated with mild cognitive impairment in Parkinson's disease. *Neuroscience Letters,* 617, 160–165. <doi:10.1016/j.neulet.2015.12.055>

Chételat, G., Landeau, B., Eustache, F., Mézenge, F., Viader, F., de la Sayette, V., Desgranges, B., &. Baron, J-C., 2005. Using voxel-based morphometry to map the structural changes associated with rapid conversion in MCI: A longitudinal MRI study. *Neuroimage,* 27(4), 934–946. <doi:10.1016/j.neuroimage.2005.05.015>

Chiang, M., Dutton, R. A., Hayashi, K. M., Lopez, O. L., Aizenstein, H. J., Toga, A. W., Becker J. T., & Thompson, P. M., 2007. 3D pattern of brain atrophy in HIV/AIDS visualized using tensor-based morphometry. *Neuroimage,* 34(1), 44–60. <doi:10.1016/j.neuroimage.2006.08.030>

Cho, H., Kim, J., Kim, C., Ye, B. S., Kim, H. J., Yoon, C. W., Noha, Y., Kima, G. H., Kima, Y. J., Kima, J-H., Kime, C-H., Kanga, S. J., China, J., Kimf, S. T., Leeg, K-H., Naa, D. L., Seongh, J-K., & Seo, S. W., 2014. Shape changes of the basal ganglia and thalamus in Alzheimer's disease: A three-year longitudinal study. *Journal of Alzheimer's Disease: JAD,* 40(2), 285–295. <doi:10.3233/JAD-132072>

Chou, Y., Leporé, N., Saharan, P., Madsen, S. K., Hua, X., Jack, C. R., Shaw, L. M., Trojanowski, J. Q., Weiner, M. W., Toga A. W., & Thompson, P. M., 2010. Ventricular maps in 804 ADNI subjects: Correlations with CSF biomarkers and clinical decline. *Neurobiology of Aging,* 31(8), 1386–1400. <doi:10.1016/j.neurobiolaging.2010.05.001>

Chow, N., Aarsland, D., Honarpisheh, H., Beyer, M. K., Somme, J. H., Elashoff, D., Rongve, A., Tysnes, O. B., Thompson, P. M., & Apostolova, L. G., 2012. Comparing hippocampal atrophy in Alzheimer's dementia and dementia with Lewy bodies. *Dementia and Geriatric Cognitive Disorders,* 34(1), 44–50. <doi:10.1159/000339727>

Chow, T. W., Gao, F., Links, K. A., Ween, J. E., Tang-Wai, D. F., Ramirez, J., Scott, C. J., Freedman, M., Stuss, D. T., & Black, S. E., 2011. Visual rating versus volumetry to detect frontotemporal dementia. *Dementia and Geriatric Cognitive Disorders,* 31*(5), 371–378.* <doi:10.1159/000328415 [doi]>

Choy, G., Khalilzadeb, O., Michalski, M., Do, S., Samir, A. E., Pianykh, O. S., Geis. J. R., & Pandharipande, P. V., 2018. Current application and future impact of machine learning in radiology. *Radiology,* 288, 318–328. <doi:10.1148/radiol.2018171820>

Clifford, K. M., Samboju, V., Cobigo, Y., Milanini, B., Marx, G. A., Hellmuth, J. M., Rosen, H. J., Kramer, J. H., Allen, I. E., & Valcour, V. G., 2017. Progressive brain atrophy despite persistent viral suppression in HIV over age 60. *Journal of Acquired Immune Deficiency Syndromes* 76(3): 289–297. <doi:10.1097/QAI.0000000000001489>

Cornitiu, G., 2015. The epidemiological scale of Alzheimer's disease. *Journal of Clinical Medicine Research,* 7(9), 657–666. <doi:10.14740/jocmr2106w>

Counts, S., Counts, S., Ikonomovic, M., Ikonomovic, M., Mercado, N., Mercado, N., Vega, I., & Mufson, E., 2017. Biomarkers for the early detection and progression of Alzheimer's disease. *Neurotherapeutics,* 14(1), 35–53. <doi:10.1007/s13311-016-0481-z>

Craik, F., & Salthouse, T. A., 2008. *The handbook of aging and cognition* (3rd ed.). New York and Hove: Psychology Press.

Dahlin, E., Neely, A. S., Larsson, A., Backman, L., & Nyberg, L., 2008. Transfer of learning after updating training mediated by the striatum. *Science (New York, N.Y.),* 320(5882), 1510–1512. <doi:10.1126/science.1155466 [doi]>

Datta, S., Staewen, T. D., Cofield, S. S., Cutter, G. R., Lublin, F. D., Wolinsky, J. S., & Narayana, P. A., 2015. Regional gray matter atrophy in relapsing remitting multiple sclerosis: Baseline analysis of multi-center data. *Multiple Sclerosis and Related Disorders,* 4(2), 124–136. <doi:10.1016/j.msard.2015.01.004>

Davies, R. R., Kipps, C. M., Mitchell, J., Kril, J. J., Halliday, G. M., & Hodges, J. R., 2006. Progression in frontotemporal dementia: Identifying a benign behavioral variant by magnetic resonance imaging. *Archives of Neurology,* 63(11), 1627–1631. <doi:63/11/1627 [pii]>

Davies, R. R., Scahill, V. L., Graham, A., Williams, G. B., Graham, K. S., & Hodges, J. R., 2009. Development of an MRI rating scale for multiple brain regions: Comparison with volumetrics and with voxel-based morphometry. *Neuroradiology,* 51(8), 491–503. <doi:10.1007/s00234-009-0521-z [doi]>

de Jong, L. W., van der Hiele, K., Veer, I. M., Houwing, J. J., Westendorp, R. G., Bollen, E. L. E. M., & van der Grond, J., 2008. Strongly reduced volumes of putamen and thalamus in Alzheimer's disease: An MRI study. *Brain,* 131(12), 3277–3285. <doi:10.1093/brain/awn278>

de Jong, L. W., Wang, Y., White, L. R., Yu, B., van Buchem, M. A., & Launer, L. J., 2012. Ventral striatal volume is associated with cognitive decline in older people: A population based MR-study. *Neurobiology of Aging,* 33(2), 424.e1–424.e10. <doi:10.1016/j.neurobiolaging.2010.09.027>

De Leon, M. J., George, A. E., Golomb, J., Tarshish, C., Convit, A., Kluger, A., De Santi, S., McRae, T., Ferris, S. H., Reisberg, B., Ince, C., Rusinek, H., Bobinski, M., Quinn, B., Miller, D. C., & Wisniewski, H. M., 1997. Frequency of hippocampal formation atrophy in normal aging and Alzheimer's disease. *Neurobiology of Aging,* 18(1), 1–11. <doi:S0197458096002138 [pii]>

De Leon, M. J., George, A. E., Reisberg, B., Ferris, S. H., Kluger, A., Stylopoulos, L. A., Miller, J. D., La Regina, M. E., Chen, C., & Cohen, J., 1989. Alzheimer's disease: Longitudinal CT studies of ventricular change. *AJR.American Journal of Roentgenology,* 152(6), 1257–1262. <doi:10.2214/ajr.152.6.1257 [doi]>

Debernard, L., Melzer, T. R., Alla, S., Eagle, J., Van Stockum, S., Graham, C., Osborne, J. R., Dalrymple-Alford, J. C., Miller, D. H., & Mason, D. F., 2015. Deep grey matter MRI abnormalities and cognitive function in relapsing-remitting multiple sclerosis. *Psychiatry Research: Neuroimaging,* 234(3), 352–361. <doi:10.1016/j.pscychresns.2015.10.004>

DeCarli, C., Frisoni, G. B., Clark, C. M., Harvey, D., Grundman, M., Petersen, R. C., Leon J. T., Shelia J., Clifford R. J., & Scheltens, P., 2007. Qualitative estimates of medial temporal atrophy as a predictor of progression from mild cognitive impairment to dementia. *Archives of Neurology,* 64(1), 108–115. <doi:10.1001/archneur.64.1.108>

Dennis, E. L., Hua, X., Villalon-Reina, J., Moran, L. M., Kernan, C., Babikian, T., Mink, R., Babbitt, C., Johnson, J., Giza, C. C., Thompson, P. M., & Asarnow, R. F., 2016. Tensor-based morphometry reveals volumetric deficits in Moderate/Severe pediatric traumatic brain injury. *Journal of Neurotrauma,* 33(9), 84–852. <doi:10.1089/neu.2015.4012>

Despotović, I., Goossens, B., & Philips, W., 2015. MRI segmentation of the human brain: Challenges, methods, and applications. *Computational and Mathematical Methods in Medicine,* 2015, 450341-23. <doi:10.1155/2015/450341>

Devanand, D. P., Bansal, R., Liu, J., Hao, X., Pradhaban, G., & Peterson, B. S., 2012. MRI hippocampal and entorhinal cortex mapping in predicting conversion to Alzheimer's disease. *Neuroimage* 60(3), 1622–1629. <doi:10.1016/j.neuroimage.2012.01.075>

Driscoll, I., Davatzikos, C., An, Y., Wu, X., Shen, D., Kraut, M., & Resnick, S. M., 2009. Longitudinal pattern of regional brain volume change differentiates normal aging from MCI. *Neurology,* 72(22), 1906–1913. <doi:10.1212/WNL.0b013e3181a82634 [doi]>

Du, A., Schuff, N., Chao, L. L., Kornak, J., Jagust, W. J., Kramer, J. H., Reed, B. R., Miller, B. L., Norman, D., Chui, H. C., & Weiner, M. W., 2006. Age effects on atrophy rates of entorhinal cortex and hippocampus. *Neurobiology of Aging,* 27(5), 733–740. <doi:10.1016/j.neurobiolaging.2005.03.021>

Duara, R., Loewenstein, D. A., Potter, E., Appel, J., Greig, M. T., Urs, R., Shen, Q., Raj, A., Small, B., Barker, W., Schofield, E., Wu, Y., & Potter, H., 2008. Medial temporal lobe atrophy on MRI scans and the diagnosis of Alzheimer disease. *Neurology,* 71(24), 1986–1992. <doi:10.1212/01.wnl.0000336925.79704.9f>

Duara, R., Loewenstein, D. A., Shen, Q., Barker, W., Varon, D., Greig, M. T., Curiel, R., Agron, J., Santos, I., & Potter, H., 2013. The utility of age-specific cut-offs for visual rating of medial temporal atrophy in classifying Alzheimer's disease, MCI and cognitively normal elderly subjects. *Frontiers in Aging Neuroscience,* 5(47), 1–8. <doi:10.3389/fnagi.2013.00047>

Dubois, B., Feldman, H. H., Jacova, C., DeKosky, S. T., Barberger-Gateau, P., Cummings, J., Delacourte, A., Galasko, D., Gauthier, S., Jicha, G., Meguro, K., O'Brien, J., Pasquier, F., Robert, P., Rossor, M., Salloway, S., Stern, Y., Visser, P. J., & Scheltens, P., 2007. Research criteria for the diagnosis of Alzheimer's disease: Revising the NINCDS-ADRDA criteria. *Lancet neurology,* 6(8), 734–746. <doi:10.1016/S14744422(07)70178-3>

Dubois, B., Feldman, H., H, Jacova, C., Cummings, J. L., DeKosky, S. T., Barberger-Gateau, P., Delacourte, A., Frisoni, G., Fox, N. C., Galasko, D., Gauthier, S., Hampel, H., Jicha, G. A., Meguro, K., O'Brien, J., Pasquier, F., Robert, P., Rossor, M., Salloway, S., Sarazin, M., de Souza, L. C., Stern, Y., Visser, P. J., & Scheltens, P., 2010. Revising the definition of Alzheimer's disease: A new lexicon. *Lancet Neurology,* 9(11), 1118–1127. <doi:10.1016/S1474-4422(10)70223-4>

Dumurgier, J., Hanseeuw, B. J., Hatling, F. B., Judge, K. A., Schultz, A. P., Chhatwal, J. P., Blacker, D., Sperling, R. A., Johnson, K. A., Hyman, B. T., & Gómez-Isla, T., 2017. Alzheimer's biomarkers and future decline in cognitive normal older adults. *Journal of Alzheimer's disease,* 60(4), 1451–1459. <doi:10.3233/JAD-170511>

Elder, G. J., Mactier, K., Colloby, S. J., Watson, R., Blamire, A. M., O'Brien, J. T., & Taylor, J., 2017. The influence of hippocampal atrophy on the cognitive phenotype of dementia with lewy bodies. *International Journal of Geriatric Psychiatry,* 32(11), 1182–1189. doi:10.1002/gps.4719

European academy of neurology. European academy of neurology guidelines. Retrieved from <https://www.ean.org/Reference-Center.2699.0.html>

Fama, R., & Sullivan, E. V., 2015. Thalamic structures and associated cognitive functions: Relations with age and aging. *Neuroscience and Biobehavioral Reviews,* 54, 29–37. <doi:10.1016/j.neubiorev.2015.03.008>

Farokhian, F., Yang, C., Beheshti, I., Matsuda, H., & Wu, S., 2017. Age-related gray and white matter changes in normal adult brains. *Aging and Disease, 8*(6), 899–909. <doi:10.14336/AD.2017.0502>

Fazekas, F., Kapeller, P., Schmidt, R., Offenbacher, H., Payer, F., & Fazekas, G., 1996. The relation of cerebral magnetic resonance signal hyperintensities to Alzheimer's disease. *Journal of the Neurological Sciences,* 142(1–2), 121–125. <doi:10.1016/0022-510X(96)00169-4>

Femminella, G. D., Thayanandan, T., Calsolaro, V., Komici, K., Rengo, G., Corbi, G., & Ferrara, N., 2018. Imaging and molecular mechanisms of Alzheimer's disease: A review. *International Journal of Molecular Sciences,* 19(12), 10.3390/ijms19123702. <doi:E3702 [pii]>

Ferreira, L. K., Diniz, B. S., Forlenza, O. V., Busatto, G. F., & Zanetti, M. V., 2009. Neurostructural predictors of Alzheimer's disease: A meta-analysis of VBM studies. *Neurobiology of Aging,* 32(10), 1733–1741. <doi:10.1016/j.neurobiolaging.2009.11.008>

Flak, M. M., Hol, H. R., Hernes, S. S., Chang, L., Ernst, T., Engvig, A., Bjuland, K. J., Madsen, B-O., Lindland, E.M., Knapskog, A-B., Ulstein, I. D., Lona, T. E., Skranes, J., & Løhaugen, G. C., 2018. Cognitive profiles and atrophy ratings on MRI in senior patients with mild cognitive impairment. *Frontiers in Aging Neuroscience,* 10(384), 1–14. <doi:10.3389/fnagi.2018.00384>

Fleischman, D. A., Leurgans, S., Arfanakis, K., Arvanitakis, Z., Barnes, L. L., Boyle, P. A., Han, S., D., & Bennett, D. A., 2014. Gray-matter macrostructure in cognitively healthy older persons: Associations with age and cognition. *Brain Structure & Function,* 219(6), 2029–2049. <doi:10.1007/s00429-013-0622-7 [doi]>

Flores, R., Joie, R., & Chételat, G., 2015. Structural imaging of hippocampal subfields in healthy aging and Alzheimer's disease. *Neuroscience,* 309, 29–50. <doi:10.1016/j.neuroscience.2015.08.033>

Fox, N. C., & Freeborough, P. A., 1997. Brain atrophy progression measured from registered serial MRI: Validation and application to Alzheimer's disease. *Journal of Magnetic Resonance Imaging,* 7(6), 1069–1075. <doi:10.1002/jmri.1880070620>

Fraser, M. A., Shaw, M. E., & Cherbuin, N., 2015. A systematic review and meta-analysis of longitudinal hippocampal atrophy in healthy human ageing. *NeuroImage,* 112, 364–374. <doi:10.1016/j.neuroimage.2015.03.035>

Frisoni, G. B., Fox, N. C., Jack, C. R., Scheltens, P., & Thompson, P. M., 2010. The clinical use of structural MRI in Alzheimer disease. *Nature Reviews Neurology,* 6(2), 67–77. <doi:10.1038/nrneurol.2009.215>

Galton, C. J., Gomez-Anson, B., Antoun, N., Scheltens, P., Patterson, K., Graves, M., Sahakian, B. J., & Hodges, J. R., 2001. Temporal lobe rating scale: Application to Alzheimer's disease and frontotemporal dementia. *Journal of Neurology, Neurosurgery & Psychiatry,* 70(2), 165–173. <doi:10.1136/jnnp.70.2.165>

Gennatas, E. D., Avants, B. B., Wolf, D. H., Satterthwaite, T. D., Ruparel, K., Ciric, R., Hakonarson, H., Gur, R. E., & Gur, R. C., 2017. Age-related effects and sex differences in gray matter density, volume, mass, and cortical thickness from childhood to young adulthood. *The Journal of Neuroscience: The Official Journal of the Society for Neuroscience,* 37(20), 5065–5073. <doi:10.1523/JNEUROSCI.3550-16.2017>

Gillis, C., Mirzaei, F., Potashman, M., Ikram, M. A., & Maserejian, N., 2019. The incidence of mild cognitive impairment: A systematic review and data synthesis. *Alzheimer's & Dementia: Diagnosis, Assessment & Disease Monitoring,* 11(1), 248–256. <doi:10.1016/j.dadm.2019.01.004>

Gordon, B. A., Blazey, T., Benzinger, T. L. S., & Head, D., 2013. Effects of aging and Alzheimer's disease along the longitudinal axis of the hippocampus. *Journal of Alzheimer's Disease: JAD,* 37(1), 41–50. <doi:10.3233/JAD-130011>

Goyal, M. S., Vlassenko, A. G., Blazey, T. M., Su, Y., Couture, L. E., Durbin, T. J., Bateman, R. J., Benzinger, T. L-S., Morris, J., C., & Raichle, M. E., 2017. Loss of brain aerobic glycolysis in normal human aging. *Cell Metabolism,* 26(2), 353–360.e3. <doi:10.1016/j.cmet.2017.07.010>

Gutman, B. A., Jahanshad, N., Ching, C. R. K., Yalin Wang, Kochunov, P. V., Nichols, T. E., & Thompson, P. M., April 2015. Medial demons registration localizes the degree of genetic influence over subcortical shape variability: An N= 1480 meta-analysis. Paper presented at the *Proceedings of IEEE International Symposium on Biomedical Imaging,* 2015, 1402–1406. <doi:10.1109/ISBI.2015.7164138>

Hämäläinen, A., Tervo, S., Grau-Olivares, M., Niskanen, E., Pennanen, C., Huuskonen, J., Kivipelto, M., Hänninen, T., Tapiola, M., Vanhanen, M., Hallikainen, M., Helkala, E. L., Nissinen, A., Vanninen, R., & Soininen, H., 2007. Voxel-based morphometry to detect brain atrophy in progressive mild cognitive impairment. *NeuroImage,* 37(4), 1122–1131. <doi:S1053-8119(07)00535-6 [pii]>

Hänninen, T., Pulliainen, V., Salo, J., Hokkanen, L., Erkinjuntti, T., Koivisto, K., Viramo, P., Soininen, H., & Suomen muistitutkimusyksiköiden asiantuntijaryhmä, 1999. Kognitiiviset testit muistihäiriöiden ja alkavan dementian varhaisdiagnostiikassa: CERAD-tehtäväsarja. *Suomen Lääkärilehti,* 15, 1967–1975. Retrieved from <http://www.fimnet.fi/cl/pdf/1999/>

Harada, C. N., Natelson Love, M. C., & Triebel, K. L., 2013. Normal cognitive aging. *Clinics in Geriatric Medicine,* 29(4), 737–752. <doi:10.1016/j.cger.2013.07.002>

Harper, L., Fumagalli, G. G., Barkhof, F., Scheltens, P., O'Brien, J. T., Bouwman, F., E J Burton, Rohrer, J. D., Fox, N. C., Ridgway, G. R., & Schott, J. M., 2016. MRI visual rating scales in the diagnosis of dementia: Evaluation in 184 post-mortem confirmed cases. *Brain: A Journal of Neurology,* 139(Pt 4), *1211–1225.* <doi:10.1093/brain/aww005 [doi]>

Harper, L., Barkhof, F., Fox, N. C., & Schott, J. M., 2015. Using visual rating to diagnose dementia: A critical evaluation of MRI atrophy scales. *Journal of Neurology, Neurosurgery & Psychiatry,* 86(11), 1225–1233. <doi:10.1136/jnnp-2014-310090>

Hartshorne, J. K., & Germine, L. T., 2015. When does cognitive functioning peak? the asynchronous rise and fall of different cognitive abilities across the life span. *Psychological Science,* 26(4), 433–443. <doi:10.1177/0956797614567339>

Heckemann, R. A., Hajnal, J. V., Aljabar, P., Rueckert, D., & Hammers, A., 2006. Automatic anatomical brain MRI segmentation combining label propagation and decision fusion. *Neuroimage,* 33(1), 115–126. <doi:10.1016/j.neuroimage.2006.05.061>

Hedden, T., & Gabrieli, J. D. E., 2004. Insights into the ageing mind: A view from cognitive neuroscience. *Nature Reviews Neuroscience,* 5(2), 87–96. <doi:10.1038/nrn1323>

Hilal, S., Amin, S. M., Venketasubramanian, N., Niessen, W. J., Vrooman, H., Wong, T. Y., Chen, C., & Ikram, M. K., 2015. Subcortical atrophy in cognitive impairment and dementia. *Journal of Alzheimer's Disease,* 48(3), 813–823. <doi:10.3233/JAD-150473>

Hosny, A., Parmar, C., Quackenbush, J., Schwartz, L. H., & Aerts, Hugo J W L., 2018. Artificial intelligence in radiology. *Nature Reviews. Cancer,* 18(8), 500–510. <doi:10.1038/s41568-018-0016-5>

Hsu, S. H., Cao, Y., Lawrence, T. S., Tsien, C., Feng, M., Grodzki, D. M., & Balter, J. M., 2015. Quantitative characterizations of ultrashort echo (UTE) images for supporting air-bone separation in the head. *Physics in Medicine and Biology*, 60(7), 2869–2880. <doi:10.1088/0031-9155/60/7/2869 [doi]>

Hua, X., Ching, C. R. K., Mezher, A., Gutman, B. A., Hibar, D. P., Bhatt, P., Leow, A. D., Jack, C. R., Bernstein, M. A., Weiner, M. W., & Thompson, P. M., 2016. MRI-based brain atrophy rates in ADNI phase 2: Acceleration and enrichment considerations for clinical trials. *Neurobiology of Aging,* 37, 26–37. <doi:10.1016/j.neurobiolaging.2015.09.018>

Hua, X., Lee, S., Hibar, D. P., Yanovsky, I., Leow, A. D., Toga, A. W., Jack, C. R., Weiner, M. W., & Thompson, P. M., 2010. Mapping Alzheimer's disease progression in 1309 MRI scans: Power estimates for different inter-scan intervals. *Neuroimage,* 51(1), 63–75. <doi:10.1016/j.neuroimage.2010.01.104>

Hua, X., Leow, A. D., Lee, S., Klunder, A. D., Toga, A. W., Lepore, N., Chou, Y-Y., Brun, C., Chiang, M-C., Barysheva, M., Jack Jr., C. R., Bernstein, M. A., Britson, P. J., Ward, C. P., Whitwell, J. L., Borowski, B., Fleisher, A. S., Fox, N. C., Boyes, R. G., Barnes, J., Harvey, D., Kornak, J., Schuff, N., Boreta, L., Alexander, G. E., Weinerg, M. W., Thompson, P. M., & Alzheimer's Disease Neuroimaging Initiative, 2008a. 3D characterization of brain atrophy in Alzheimer's disease and mild cognitive impairment using tensor-based morphometry. *Neuroimage,* 41(1), 19–34. <doi:10.1016/j.neuroimage.2008.02.010>

Hua, X., Leow, A. D., Parikshak, N., Lee, S., Chiang, M., Toga, A. W., Jack, C. R., Weiner, M. W., & Thompson, P. M., 2008b. Tensor-based morphometry as a neuroimaging biomarker for Alzheimer's disease: An MRI study of 676 AD, MCI, and normal subjects. *Neuroimage,* 43(3), 458–469. <doi:10.1016/j.neuroimage.2008.07.013>

Jack Jr, C. R., Dickson, D. W., Parisi, J. E., Xu, Y. C., Cha, R. H., O'Brien, P. C., Edland, S. D., Smith, G. E., Boeve, B. F., Tangalos, E. G., Kokmen, E., & Petersen, R. C., 2002. Antemortem MRI findings correlate with hippocampal neuropathology in typical aging and dementia. *Neurology,* 58(5), 750–757. <doi:10.1212/WNL.58.5.750>

Jack, C. R., Petersen, R. C., Xu, Y. C., O'Brien, P. C., Smith, G. E., Ivnik, R. J., Boeve, B. F., Waring, S. C., Tangalos, E. G., & Kokmen, E., 1999. Prediction of AD with MRI-based hippocampal volume in mild cognitive impairment. *Neurology,* 52(7), 1397–1403. <doi:10.1212/wnl.52.7.1397 [doi]>

Jack, C. R., Petersen, R. C., Xu, Y., O'Brien, P. C., Smith, G. E., Ivnik, R. J., Boeve, B. F., Tangalos, E. G., & Kokmen, E., 2000. Rates of hippocampal atrophy correlate with change in clinical status in aging and AD. *Neurology,* 55(4), 484–489. <doi:10.1212/wnl.55.4.484 [doi]>

Jack, C. R., Shiung, M. M., Gunter, J. L., O'Brien, P. C., Weigand, S. D., Knopman, D. S., Boeve, R J Ivnik, Smith, G. E., Cha, R. H., Tangalos, E. G., & Petersen, R. C., 2004. Comparison of different

MRI brain atrophy rate measures with clinical disease progression in AD. *Neurology,* 62(4), 591–600. <doi:10.1212/01.wnl.0000110315.26026.ef [doi]>

Jacobs, H. I. L., Van Boxtel, M. P. J., Uylings, H. B. M., Gronenschild, E. H. B. M., Verhey, F. R., & Jolles, J., 2011. Atrophy of the parietal lobe in preclinical dementia. *Brain and Cognition, 75*(2), 154–163. <doi:10.1016/j.bandc.2010.11.003>

Jarrett, D., Stride, E., Vallis, K., & Gooding, M. J., 2019. Applications and limitations of machine learning in radiation oncology. *The British Journal of Radiology,* 92(1100), 20190001. <doi:10.1259/bjr.20190001>

Johnson, K. A., Fox, N. C., Sperling, R. A., & Klunk, W. E., 2012. Brain imaging in Alzheimer disease. *Cold Spring Harbor Perspectives in Medicine,* 2(4), a006213. <doi:10.1101/cshperspect.a006213>

Josephs, K. A., Dickson, D. W., Tosakulwong, N., Weigand, S. D., Murray, M. E., Petrucelli, L., Liesinger, A. M., Senjem, M. L., Spychalla, A. J., Knopman, D. S., Parisi, J. E., Petersen, R. C., Jack Jr, C. R., & Whitwell, J. L., 2017. Rates of hippocampal atrophy and post-mortem TDP-43 in Alzheimer's disease: A longitudinal retrospective study. *The Lancet. Neurology,* 16(11), 917–924. <doi:10.1016/S1474-4422(17)30284-3>

Junqué, C., Ramírez-Ruiz, B., Tolosa, E., Summerfield, C., Martí, M., Pastor, P., Gómez-Ansón, B., & Mercader, J. M., 2005. Amygdalar and hippocampal MRI volumetric reductions in Parkinson's disease with dementia. *Movement Disorders,* 20(5), 540–544. <doi:10.1002/mds.20371>

Kaneko, T., Kaneko, K., Matsushita, M., Kadoya, M., Ihara, N., Ryokawa, A., Ogihara, T., Inuzuka, S., & Ueda, H., 2012. New visual rating system for medial temporal lobe atrophy: A simple diagnostic tool for routine examinations. *Psychogeriatrics: The Official Journal of the Japanese Psychogeriatric Society,* 12(2), 88–92. <doi:10.1111/j.1479-8301.2011.00390.x [doi]>

Kassubek, J., Juengling, F. D., Ecker, D., & Landwehrmeyer, G. B., 2005. Thalamic atrophy in Huntington's disease co-varies with cognitive performance: A morphometric MRI analysis. *Cerebral Cortex,* 15(6), 846–853. <doi:10.1093/cercor/bhh185>

Kemp, P. M., Holmes, C., Hoffmann, S. M. A., Bolt, L., Holmes, R., Rowden, J., & Fleming, J. S., 2003. Alzheimer's disease: Differences in technetium-99m HMPAO SPECT scan findings between early onset and late onset dementia. *Journal of Neurology, Neurosurgery, and Psychiatry,* 74(6), 715–719. <doi:10.1136/jnnp.74.6.715>

Kim, G. H., Kim, J. E., Choi, K. G., Lim, S. M., Lee, J. M., Na, D. L., & Jeong, J. H., 2014. T1-weighted axial visual rating scale for an assessment of medial temporal atrophy in Alzheimer's disease. *Journal of Alzheimer's Disease: JAD,* 41(1), 169–178. <doi:10.3233/JAD-132333 [doi]>

Kim, G. H., Lee, J. H., Seo, S. W., Kim, J. H., Seong, J., Ye, B. S., Cho, H., Noh, Y., Kim, H. J., Yoon, C. W., Oh, S. J., Kim, J. S., Choe, Y. S., Lee, K. L., Kim, S. T., Hwang, J. W., Jeong, J. H., & Na, D. L., 2015. Hippocampal volume and shape in pure subcortical vascular dementia. *Neurobiology of Aging,* 36(1), 485–491. <doi:10.1016/j.neurobiolaging.2014.08.009>

Kipps, C. M., Davies, R. R., Mitchell, J., Kril, J. J., Halliday, G. M., & Hodges, J. R., 2007. Clinical significance of lobar atrophy in frontotemporal dementia: Application of an MRI visual rating scale. *Dementia and Geriatric Cognitive Disorders,* 23(5), 334–342. <doi:000100973 [pii]>

Kipps, C. M., Duggins, A. J., Mahant, N., Gomes, L., Ashburner, J., & McCusker, E. A., 2005. Progression of structural neuropathology in preclinical Huntington's disease: A tensor-based morphometry study. *Journal of Neurology, Neurosurgery, and Psychiatry,* 76(5), 650–655. <doi:10.1136/jnnp.2004.047993>

Kirova, A., Bays, R. B., & Lagalwar, S., 2015. Working memory and executive function decline across normal aging, mild cognitive impairment, and Alzheimer's disease. *BioMed Research International,* 2015, 748212. <doi:10.1155/2015/748212>

Knopman, D. S., & Petersen, R. C., 2014. Mild cognitive impairment and mild dementia: A clinical perspective. *Mayo Clinic Proceedings,* 89(10), 1452–1459. <doi:10.1016/j.mayocp.2014.06.019>

Koedam, E. L., Lehmann, M., van der Flier, W M, Scheltens, P., Pijnenburg, Y. A., Fox, N., Barkhof, F., & Wattjes, M. P., 2011. Visual assessment of posterior atrophy development of a MRI rating scale. European Radiology, 21(12), 2618–2625. <doi:10.1007/s00330-011-2205-4 [doi]>

Koen, J. D., & Yonelinas, A. P., 2014. The effects of healthy aging, amnestic mild cognitive impairment, and Alzheimer's disease on recollection and familiarity: A meta-analytic review. *Neuropsychology Review,* 24*(3), 332–354.* <doi:10.1007/s11065-014-9266-5 [doi]>

Koikkalainen, J., Lötjönen, J., Thurfjell, L., Rueckert, D., Waldemar, G., & Soininen, H., 2011. Multi-template tensor-based morphometry: Application to analysis of Alzheimer's disease. *NeuroImage,* 56(3), 1134–1144. <doi:10.1016/j.neuroimage.2011.03.029>

Koikkalainen, J., Rhodius-Meester, H., Tolonen, A., Barkhof, F., Tijms, B., Lemstra, A. W., Tong, T., Guerrero, R., Schuh, A., Ledig, C., Rueckert, D., Soininen, H., Remes, A. M., Waldemar, G., Hasselbalch, S., Mecocci, P., van der Flier, W., & Lötjönen, J., 2016. Differential diagnosis of neurodegenerative diseases using structural MRI data. *NeuroImage: Clinical,* 11(C), 435–449. <doi:10.1016/j.nicl.2016.02.019>

Kolb, B., & Whishaw, I. Q. (Eds.), 2015. *Fundamentals of human neuropsychology* (7th ed.). New York, United States: Worth Publishers Inc., U.S.

Korf, E. S. C., Wahlund, L. O., Visser, P. J., & Scheltens, P., 2004. Medial temporal lobe atrophy on MRI predicts dementia in patients with mild cognitive impairment. *Neurology,* 63(1), 94–100. <doi:10.1212/01.WNL.0000133114.92694.93>

Lane, C. A., Hardy, J., & Schott, J. M., 2018. Alzheimer's disease. *European Journal of Neurology,* 25(1), 59–70. <doi:10.1111/ene.13439 [doi]>

Langs, G., Röhrich, S., Hofmanninger, J., Prayer, F., Pan, J., Herold, C., & Prosch, H., 2018. Machine learning: From radiomics to discovery and routine. *Der Radiologe,* 58(Suppl 1), 1–6. <doi:10.1007/s00117-018-0407-3>

Lee, A. D., Leow, A. D., Lu, A., Reiss, A. L., Hall, S., Chiang, M., Toga, A. W., & Thompson, P. M., 2007. 3D pattern of brain abnormalities in fragile X syndrome visualized using tensor-based morphometry. *NeuroImage,* 34(3), 924–938. <doi:10.1016/j.neuroimage.2006.09.043>

Leiner, T., Rueckert, D., Suinesiaputra, A., Baeßler, B., Nezafat, R., Išgum, I., & Young, A. A., 2019. Machine learning in cardiovascular magnetic resonance: Basic concepts and applications. *Journal of Cardiovascular Magnetic Resonance,* 21(1), 61. <doi:10.1186/s12968-019-0575-y>

Leow, A. D., Yanovsky, I., Parikshak, N., Hua, X., Lee, S., Toga, A. W., Jack Jr., C. R., Bernstein, M. A., Britson, P. J., Gunter, J. L., Ward, C. P., Borowski, B., Shaw, L. M., Trojanowski, J. Q., Fleisher, A. S., Harvey, D., Kornak, J., Schuff, N., Alexander, G. E., Weiner, M. W., Thompson, P. M., & Alzheimer's Disease Neuroimaging Initiative, 2009. Alzheimer's disease neuroimaging initiative: A one-year follow-up study using tensor-based morphometry correlating degenerative rates, biomarkers and cognition. *Neuroimage,* 45(3), 645–655. <doi:10.1016/j.neuroimage.2009.01.004>

Lepore, N., Brun, C., Chou, Yi-Yu., Chiang, M-C., Dutton, R. A., Hayashi, K. M., Luders, E., Lopez, O. L., Aizenstein, H. J., Toga, A. W., Becker, J. T., & Thompson, P. M., 2008. Generalized tensor-based morphometry of HIV/AIDS using multivariate statistics on deformation tensors. *IEEE Transactions on Medical Imaging,* 27(1), 129–141. <doi:10.1109/TMI.2007.906091>

Li, X., Jiao, J., Shimizu, S., Jibiki, I., Watanabe, K., & Kubota, T., 2012. Correlations between atrophy of the entorhinal cortex and cognitive function in patients with Alzheimer's disease and mild cognitive impairment. *Psychiatry and Clinical Neurosciences,* 66(7), 587–593. <doi:10.1111/pcn.12002 [doi]>

Lindeboom, J., & Weinstein, H., 2004. Neuropsychology of cognitive ageing, minimal cognitive impairment, Alzheimer's disease, and vascular cognitive impairment. *European Journal of Pharmacology,* 490(1), 83–86. <doi:10.1016/j.ejphar.2004.02.046>

Liu, Y., Mattila, J., Ruiz, M. A., Paajanen, T., Koikkalainen, J., van Gils, M., Herukka, S. K., Waldemar, G., Lötjönen, J., Soininen, H., & Alzheimer's Disease Neuroimaging Initiative, 2013.

Predicting AD conversion: Comparison between prodromal AD guidelines and computer assisted PredictAD tool. *PloS One,* 8(2), e55246. <doi:10.1371/journal.pone.0055246 [doi]>

Liu, Y., Paajanen, T., Zhang, Y., Westman, E., Wahlund, L., Simmons, A., Tunnard, C., Sobow, T., Mecocci, P., Tsolaki, M., Vellas, B., Muehlboeck, S., Evans, A., Spenger, C., Lovestone, S., & Soininen, H., 2010. Analysis of regional MRI volumes and thicknesses as predictors of conversion from mild cognitive impairment to Alzheimer's disease. *Neurobiology of Aging,* 31(8), 1375–1385. <doi:10.1016/j.neurobiolaging.2010.01.022>

Lo, R. Y., 2017. The borderland between normal aging and dementia. *Tzu-Chi Medical Journal,* 29(2), 65–71. <doi:10.4103/tcmj.tcmj_18_17>

Lockhart, S., & DeCarli, C., 2014. Structural imaging measures of brain aging. *Neuropsychology Review,* 24(3), 271–289. <doi:10.1007/s11065-014-9268-3>

Long, X., Liao, W., Jiang, C., Liang, D., Qiu, B., & Zhang, L., 2012. Healthy aging: An automatic analysis of global and regional morphological alterations of human brain. *Academic Radiology,* 19(7), 785–793. <doi:10.1016/j.acra.2012.03.006 [doi]>

Lötjönen, J. M., Wolz, R., Koikkalainen, J. R., Thurfjell, L., Waldemar, G., Soininen, H., & Rueckert, D., 2010. Fast and robust multi-atlas segmentation of brain magnetic resonance images. *NeuroImage,* 49(3), 2352–2365. <doi:10.1016/j.neuroimage.2009.10.026>

Lundervold, A. S., & Lundervold, A., 2019. An overview of deep learning in medical imaging focusing on MRI. *Zeitschrift Fuer Medizinische Physik, 29*(2), 102–127. <doi:10.1016/j.zemedi.2018.11.002>

Macdonald, K. E., Bartlett, J. W., Leung, K. K., Ourselin, S., & Barnes, J., 2013. The value of hippocampal and temporal horn volumes and rates of change in predicting future conversion to AD. *Alzheimer Disease and Associated Disorders,* 27(2), 168–173. <doi:10.1097/WAD.0b013e318260a79a>

Mak, E., Bergsland, N., Dwyer, M. G., Zivadinov, R., & Kandiah, N., 2014. Subcortical atrophy is associated with cognitive impairment in mild Parkinson disease: A combined investigation of volumetric changes, cortical thickness, and vertex-based shape analysis. *American Journal of Neuroradiology,* 35(12), 2257–2264. <doi:10.3174/ajnr.A4055>

Malpetti, M., Ballarini, T., Presotto, L., Garibotto, V., Tettamanti, M., & Perani, D., 2017. Gender differences in healthy aging and Alzheimer's dementia: A 18 F-FDG-PET study of brain and cognitive reserve. *Human Brain Mapping,* 38(8), 4212–4227. <doi:10.1002/hbm.23659>

Martin, S. B., Smith, C. D., Collins, H. R., Schmitt, F. A., & Gold, B. T., 2010. Evidence that volume of anterior medial temporal lobe is reduced in seniors destined for mild cognitive impairment. *Neurobiology of Aging,* 31(7), 1099–1106. <doi:10.1016/j.neurobiolaging.2008.08.010 [doi]>

Mateos-Pérez, J. M., Dadar, M., Lacalle-Aurioles, M., Iturria-Medina, Y., Zeighami, Y., & Evans, A. C., 2018. Structural neuroimaging as clinical predictor: A review of machine learning applications. *NeuroImage. Clinical,* 20, 506–522. <doi:10.1016/j.nicl.2018.08.019>

Matsuda, H., 2016. MRI morphometry in Alzheimer's disease. *Ageing Research Reviews,* 30, 17–24. <doi:10.1016/j.arr.2016.01.003>

Mazurowski, M. A., Buda, M., Saha, A., & Bashir, M. R., 2019. Deep learning in radiology: An overview of the concepts and a survey of the state of the art with focus on MRI. *Journal of Magnetic Resonance Imaging,* 49(4), 939–954. <doi:10.1002/jmri.26534>

McDonald, C. R., Gharapetian, L., McEvoy, L. K., Fennema-Notestine, C., Hagler, D. J., Holland, D., & Dale, A. M., 2012. Relationship between regional atrophy rates and cognitive decline in mild cognitive impairment. *Neurobiology of Aging,* 33(2), 242–253. <doi:10.1016/j.neurobiolaging.2010.03.015>

McKhann, G., Drachman, D., Folstein, M., Katzman, R., Price, D., & Stadlan, E. M., 1984. Clinical diagnosis of Alzheimer's disease: Report of the NINCDS-ADRDA work group under the auspices of department of health and human services task force on Alzheimer's disease. *Neurology,* 34(7), 939–944. <doi:10.1212/wnl.34.7.939>

Migliaccio, R., Agosta, F., Possin, K. L., Canu, E., Filippi, M., Rabinovici, G. D., Rosen, H. J., Miller, B. L., & Gorno-Tempini, M. L., 2015. Mapping the progression of atrophy in early and late onset Alzheimer's disease. *Journal of Alzheimer's Disease, 46*(2), 351–364. doi:10.3233/JAD-142292

Min, R., Wu, G., Cheng, J., Wang, Q., & Shen, D., 2014. Multi-atlas-based representations for Alzheimer's disease diagnosis. *Human Brain Mapping,* 35(10), 5052–5070. <doi:10.1002/hbm.22531>

Minkova, L., Habich, A., Peter, J., Kaller, C. P., Eickhoff, S. B., & Klöppel, S., 2017. Gray matter asymmetries in aging and neurodegeneration: A review and meta-analysis. *Human Brain Mapping,* 38(12), 5890–5904. <doi:10.1002/hbm.23772>

Morley, J. E., 2018. An overview of cognitive impairment. *Clinics in Geriatric Medicine,* 34(4), 505–513. <doi:10.1016/j.cger.2018.06.003>

Morris, C., Heyman, A., Mohs, R. C., Hughes, J. P., van Belle, G., Fillenbaum, G., Mellits, E. D., & Clark, C., 1989. The consortium to establish a registry for Alzheimer's disease (CERAD). part I. clinical and neuropsychological assessment of Alzheimer's disease. *Neurology,* 39(9), 1159–1165. <doi:10.1212/wnl.39.9.1159>

Mu, S. H., Xu, M., Duan, J. X., Zhang, J., & Tan, L. H., 2017. Localizing age-related changes in brain structure using voxel-based morphometry. *Neural Plasticity,* 2017, 6303512-7. <doi:10.1155/2017/6303512>

Mufson, E., Mufson, E., Binder, L., Binder, L., Counts, S., Counts, S., DeKosky, S. T., deTolledo-Morrell, L., Ginsberg, S. D., Ikonomovic, M. D., Perez, S. E., & S. E., Scheff, S., 2012. Mild cognitive impairment: Pathology and mechanisms. *Acta Neuropathologica,* 123(1), 13–30. <doi:10.1007/s00401-011-0884-1>

Muñoz-Ruiz, M. Á, Hartikainen, P., Koikkalainen, J., Wolz, R., Julkunen, V., Niskanen, E., Herukka, S-K., Kivipelto, M., Vanninen, R., Rueckert, D., Liu, Y., Jyrki Lötjönen, J., & Soininen, H., 2012. Structural MRI in frontotemporal dementia: Comparisons between hippocampal volumetry, tensor-based morphometry and voxel-based morphometry. *PloS One,* 7(12), e52531. <doi:10.1371/journal.pone.0052531>

Nadel, L., & Hardt, O., 2011. Update on memory systems and processes. *Neuropsychopharmacology: Official Publication of the American College of Neuropsychopharmacology,* 36(1), 251–273. <doi:10.1038/npp.2010.169 [doi]>

Nestor, S. M., Rupsingh, R., Borrie, M., Smith, M., Accomazzi, V., Wells, J. L., Fogarty, J., & Bartha, R., 2008. Ventricular enlargement as a possible measure of Alzheimer's disease progression validated using the Alzheimer's disease neuroimaging initiative database. *Brain,* 131(9), 2443–2454. <doi:10.1093/brain/awn146>

Nie, X., Sun, Y., Wan, S., Zhao, H., Liu, R., Li, X., Wu, S., Nedelska, Z., Hort, J., Qing, Z., Xu, Y., & Zhang, B., 2017. Subregional structural alterations in hippocampus and nucleus accumbens correlate with the clinical impairment in patients with Alzheimer's disease clinical spectrum: Parallel combining volume and vertex-based approach. *Frontiers in Neurology,* 8, 399. <doi:10.3389/fneur.2017.00399>

Nir, T., Jahanshad, N., Ching, C., Cohen, R., Harezlak, J., Schifitto, G., Lam, H. Y., Hua, X., Zhong, J., Zhu, T., Taylor, M. J., Campbell, T. B., Daar, E. S., Singer, E. J., Alger, J. R., Thompson, P. M., & Navia, B., 2019. Progressive brain atrophy in chronically infected and treated HIV+ individuals. *Journal of NeuroVirology, 25*(3), 342–353. <doi:10.1007/s13365-019-00723-4>

O'Donovan, J., Watson, R., Colloby, S. J., Firbank, M. J., Burton, E. J., Barber, R., Blamire, A. M., & O'Brien, J. T., 2013. Does posterior cortical atrophy on MRI discriminate between Alzheimer's disease, dementia with Lewy bodies, and normal aging? *International Psychogeriatrics*, 25(1), 111–119. <doi:10.1017/S1041610212001214>

Oxtoby, N. P., Alexander, D. C., & EuroPOND consortium, 2017. Imaging plus X: Multimodal models of neurodegenerative disease. *Current Opinion in Neurology,* 30*,* 371–379. <doi:10.1097/WCO.0000000000000460>

Paquette, N., Shi, J., Wang, Y., Lao, Y., Ceschin, R., Nelson, M. D., Panigrahy, A., & Lepore, N., 2017. Ventricular shape and relative position abnormalities in preterm neonates. *NeuroImage. Clinical,* 15, 483–493. <doi:10.1016/j.nicl.2017.05.025>

Park, M., & Moon, W., 2016. Structural MR imaging in the diagnosis of Alzheimer's disease and other neurodegenerative dementia: Current imaging approach and future perspectives. *Korean Journal of Radiology,* 17(6), 827–845. <doi:10.3348/kjr.2016.17.6.827>

Pasquier, F., Leys, D., Weerts, J. G. E., Mounier-Vehier, F., Barkhof, F., & Scheltens, P., 1996. Inter- and intraobserver reproducibility of cerebral atrophy assessment on MRI scans with hemispheric infarcts. *European Neurology,* 36(5), 268–272. <doi:10.1159/000117270>

Pereira, J. B., Cavallin, L., Spulber, G., Aguilar, C., Mecocci, P., Vellas, B., Tsolaki, M., Kloszewska, I., Soininen, H., Spenger C., Aarsland, D., Lovestone, S., Simmons, A., Wahlund, L-O., Westman, E., AddNeuroMed consortium, & Alzheimer's Disease Neuroimaging Initiative, 2014. Influence of age, disease onset and ApoE4 on visual medial temporal lobe atrophy cut-offs. *Journal of Internal Medicine,* 275(3), 317–330. <doi:10.1111/joim.12148 [doi]>

Pergher, V., Demaerel, P., Soenen, O., Saarela, C., Tournoy, J., Schoenmakers, B., Karrasch, M., & Hulle, M. M., 2019. Identifying brain changes related to cognitive aging using VBM and visual rating scales. *NeuroImage: Clinical,* 22*,* 1–10. <doi:10.1016/j.nicl.2019.101697>

Persson, K., Barca, M. L., Eldholm, R. S., Cavallin, L., Šaltytė Benth, J., Selbæk, G., Brækhus, A., Saltvedt, I., & Engedal, K., 2017. Visual evaluation of medial temporal lobe atrophy as a clinical marker of conversion from mild cognitive impairment to dementia and for predicting progression in patients with mild cognitive impairment and mild Alzheimer's disease. *Dementia and Geriatric Cognitive Disorders,* 44(1–2), 12–24. <doi:10.1159/000477342>

Petersen, R. C., 2016. Mild cognitive impairment. *Continuum (Minneapolis, Minn.),* 22(2), 404–418. <doi:10.1212/CON.0000000000000313 [doi]>

Petersen, R. C., Stevens, J. C., Ganguli, M., Tangalos, E. G., Cummings, J. L., & DeKosky, S. T., 2001. Practice parameter: Early detection of dementia: Mild cognitive impairment (an evidence-based review): Report of the quality standards subcommittee of the american academy of neurology. *Neurology,* 56(9), 1133–1142. <doi:10.1212/WNL.56.9.1133>

Pfefferbaum, A., Rohlfing, T., Rosenbloom, M. J., Chu, W., Colrain, I. M., & Sullivan, E. V., 2013. Variation in longitudinal trajectories of regional brain volumes of healthy men and women (ages 10 to 85years) measured with atlas-based parcellation of MRI. *NeuroImage,* 65, 176–193. <doi:10.1016/j.neuroimage.2012.10.008>

Pievani, M., Bocchetta, M., Boccardi, M., Cavedo, E., Bonetti, M., Thompson, P. M., & Frisoni, G. B., 2013. Striatal morphology in early-onset and late-onset Alzheimer's disease: A preliminary study. *Neurobiology of Aging,* 34(7), 1728–1739. <doi:10.1016/j.neurobiolaging.2013.01.016 [doi]>

Pini, L., Pievani, M., Bocchetta, M., Altomare, D., Bosco, P., Cavedo, E., Galluzzi, S., Marizzoni. M., & Frisoni, G. B., 2016. Brain atrophy in Alzheimer's disease and aging. *Ageing Research Reviews,* 30, 25–48. <doi:10.1016/j.arr.2016.01.002>

Preziosa, P., Pagani, E., Mesaros, S., Riccitelli, G. C., Dackovic, J., Drulovic, J., Filippi, M., & Rocca, M. A., 2017. Progression of regional atrophy in the left hemisphere contributes to clinical and cognitive deterioration in multiple sclerosis: A 5-year study. *Human Brain Mapping,* 38(11), 5648–5665. <doi:10.1002/hbm.23755>

Ranta, I., Teuho, J., Linden, J., Klen, R., Teräs, M., Kapanen, M., & Keyriläinen, J., 2020. Assessment of MRI-based attenuation correction for MRI-only radiotherapy treatment planning of the brain. *Diagnostics (Basel, Switzerland),* 10(5), 10.3390/diagnostics10050299. <doi:E299 [pii]>

Rathore, S., Habes, M., Iftikhar, M. A., Shacklett, A., & Davatzikos, C., 2017. A review on neuroimaging-based classification studies and associated feature extraction methods for Alzheimer's disease and its prodromal stages. *Neuroimage* 155, 530–548. <doi:10.1016/j.neuroimage.2017.03.057>

Rattray, I., Smith, E. J., Crum, W. R., Walker, T. A., Gale, R., Bates, G. P., & Modo, M., 2017. Correlations of behavioral deficits with brain pathology assessed through longitudinal MRI and

histopathology in the HdhQ150/Q150 mouse model of Huntington's disease. *Plos One,* 12(1), e0168556. <doi:10.1371/journal.pone.0168556>

Rauschecker, A. M., Rudie, J. D., Xie, L., Wang, J., Duong, M. T., Botzolakis, E. J., Kovalovich, A. M., Egan, J., Cook, T. C., Bryan, R. N., Nasrallah, I. M., Mohan, S., & Gee, J. C., 2020. Artificial intelligence system approaching neuroradiologist-level differential diagnosis accuracy at brain MRI. *Radiology,* 295(3), 626–637. <doi:10.1148/radiol.2020190283 [doi]>

Raz, N., Lindenberger, U., Rodrigue, K. M., Kennedy, K. M., Head, D., Williamson, A., Dahle, C., Gerstorf, D., & Acker, J. D., 2005. Regional brain changes in aging healthy adults: General trends, individual differences and modifiers. *Cerebral Cortex,* 15(11), 1676–1689. <doi:10.1093/cercor/bhi044>

Reitan, R. M., 1959. *A manual for the administration and scoring of the trail making test.* Bloomington, Indiana, United States: University Press Bloomington, U.S.

Riedel, B. C., Thompson, P. M., & Brinton, R. D., 2016. Age, APOE and sex: Triad of risk of Alzheimer's disease. *Journal of Steroid Biochemistry and Molecular Biology,* 160, 134–147. <doi:10.1016/j.jsbmb.2016.03.012>

Rocca, M., Rocca, M., Fumagalli, S., Fumagalli, S., Pagani, E., Pagani, E., Gatti, R., Riccitelli, G. C., Preziosa, P., Comi, G., Falini, A., & Filippi, M., 2017. Action observation training modifies brain gray matter structure in healthy adult individuals. *Brain Imaging and Behavior,* 11(5), 1343–1352. <doi:10.1007/s11682-016-9625-3>

Roh, J. H., Qiu, A., Seo, S. W., Soon, H. W., Kim, J. H., Kim, G. H., Kim, M-J., Lee, J-M., & Na, D. L., 2011. Volume reduction in subcortical regions according to severity of Alzheimer's disease. *Journal of Neurology,* 258(6), 1013–1020. <doi:10.1007/s00415-010-5872-1>

Roy, S., Wang, W. T., Carass, A., Prince, J. L., Butman, J. A., & Pham, D. L., 2014. PET attenuation correction using synthetic CT from ultrashort echo-time MR imaging. *Journal of Nuclear Medicine: Official Publication, Society of Nuclear Medicine,* 55(12), 2071–2077. <doi:10.2967/jnumed.114.143958 [doi]>

Rusinek, H., Endo, Y., De Santi, S., Frid, D., Tsui, W., Segal, S., Convit, A., & de Leon, M. J., 2004. Atrophy rate in medial temporal lobe during progression of Alzheimer disease. *Neurology,* 63(12), 2354–2359. <doi:10.1212/01.WNL.0000148602.30175.AC>

Sadeghi, N., Arrigoni, F., D'Angelo, M. G., Thomas, C., Irfanoglu, M. O., Hutchinson, E. B., Nayak, A., Modi, P., Bassi, M. T., & Pierpaoli, C., 2018. Tensor-based morphometry using scalar and directional information of diffusion tensor MRI data (DTBM): Application to hereditary spastic paraplegia. *Human Brain Mapping,* 39(12), 4643–4651. <doi:10.1002/hbm.24278>

Sandeman, E. M., Hernandez Mdel, C., Morris, Z., Bastin, M. E., Murray, C., Gow, A. J., Corley, J., Henderson, R., Deary, I. J., Starr, J. M., & Wardlaw, J. M., 2013. Incidental findings on brain MR imaging in older community-dwelling subjects are common but serious medical consequences are rare: A cohort study. *PloS One,* 8(8), e71467. <doi:10.1371/journal.pone.0071467 [doi]>

Sanford, A. M., 2017. Mild cognitive impairment. *Clinics in Geriatric Medicine,* 33(3), 325–337. <doi:S0749-0690(17)30014-9 [pii]>

Sarro, L., Senjem, M. L., Lundt, E. S., Przybelski, S. A., Lesnick, T. G., Graff-Radford, J., Boeve, B. F., Lowe, V. J., Ferman, T. J., Knopman, D. S., Comi, G., Filippi, M., Petersen, R. C., Jack Jr., C. R., & Kantarci, K., 2016. Amyloid-β deposition and regional grey matter atrophy rates in dementia with lewy bodies. *Brain: A Journal of Neurology,* 139(Pt 10), 2740–2750. <doi:10.1093/brain/aww193>

Scheinost, D., Holmes, S. E., DellaGioia, N., Schleifer, C., Matuskey, D., Abdallah, C. G., Hampson, M., Krystal, J. H., Anticevic, A., & Esterlis, I., 2018. Multimodal investigation of network level effects using intrinsic functional connectivity, anatomical covariance, and structure-to-function correlations in unmedicated major depressive disorder. *Neuropsychopharmacology: Official Publication of the American College of Neuropsychopharmacology,* 43(5), 1119–1127. <doi:10.1038/npp.2017.229>

Scheltens, P., Launer, L. J., Barkhof, F., Weinstein, H. C., & van Gool, W. A., 1995. Visual assessment of medial temporal lobe atrophy on magnetic resonance imaging: Interobserver reliability. *Journal of Neurology,* 242(9), 557–560. <doi:10.1007/BF00868807>

Scheltens, P., Leys, D., Barkhof, F., Huglo, D., Weinstein, H. C., Vermersch, P., Kuiper, M., Steinling, M., Wolters, E.C., & Vik, J., 1992. Atrophy of medial temporal lobes on MRI in "probable" Alzheimer's disease and normal aging: Diagnostic value and neuropsychological correlates. *Journal of Neurology, Neurosurgery, and Psychiatry,* 55, 967–972.

Scheltens, P., Pasquier, F., Weerts, J. G. E., Barkhof, F., & Leys, D., 1997. Qualitative assessment of cerebral atrophy on MRI: Inter- and intra-observer reproducibility in dementia and normal aging. *European Neurology,* 37, 95–99.

Shen, Q., Loewenstein, D. A., Potter, E., Zhao, W., Appel, J., Greig, M. T., Raj, A., Acevedo, A., Schofield, E., Barker, W., Wu, Y., Potter, H., & Duara, R., 2011. Volumetric and visual rating of magnetic resonance imaging scans in the diagnosis of amnestic mild cognitive impairment and Alzheimer's disease. *Alzheimer's & Dementia,* 7(4), e101–e108. <doi:10.1016/j.jalz.2010.07.002>

Social Science Statistics, 2018. Social science statistics website, Jeremy Stangroom. Retrieved from <http://www.socscistatistics.com/Default.aspx>

Soheili-Nezhad, S., Sedghi, A., Schweser, F., Babaki, A. E. S., Jahanshad, N., Thompson, P. M., Beckmann, C. F., Sprooten, E., & Toghae, M., 2019. Structural and functional reorganization of the brain in migraine without aura. *Frontiers in Neurology,* 10, 442. <doi:10.3389/fneur.2019.00442>

Sorbi, S., Hort, J., Erkinjuntti, T., Fladby, T., Gainotti, G., Gurvit, H., Nacmias, B., Pasquier, F., Popescu, B. O., Rektorova, I., Religa, D., Rusina, R., Rossor, M., Schmidt, R., Stefanova, E., Warren, J. D., & Scheltens, P., 2012. EFNS-ENS guidelines on the diagnosis and management of disorders associated with dementia. *European Journal of Neurology,* 19(9), 1159–1179. <doi:10.1111/j.1468-1331.2012.03784.x>

Sowell, E. R., Thompson, P. M., Holmes, C. J., Jernigan, T. L., & Toga, A. W., 1999. In vivo evidence for post-adolescent brain maturation in frontal and striatal regions. *Nature Neuroscience,* 2(10), 859–861. <doi:10.1038/13154 [doi]>

Sperling, R. A., Aisen, P. S., Beckett, L. A., Bennett, D. A., Craft, S., Fagan, A. M., Iwatsubo, T., Jack Jr., C. R., Kaye, J., Montine, T. J., Park, D. C., Reiman, E. M., Rowe, C. C., Siemers, E., Stern, Y., Yaffe K., Carrillo, M. C., Thies, B., Morrison-Bogorad, M., Wagster, M. V., & Phelps, C. H., 2011. Toward defining the preclinical stages of Alzheimer's disease: Recommendations from the national institute on Aging-Alzheimer's association workgroups on diagnostic guidelines for Alzheimer's disease. *Alzheimer's & Dementia,* 7(3), 280–292. <doi:10.1016/j.jalz.2011.03.003>

Storsve, A. B., Fjell, A. M., Tamnes, C. K., Westlye, L. T., Overbye, K., Aasland, H. W., & Walhovd, K. B., 2014. Differential longitudinal changes in cortical thickness, surface area and volume across the adult life span: Regions of accelerating and decelerating change. *The Journal of Neuroscience: The Official Journal of the Society for Neuroscience,* 34(25), 8488–8498. <doi:10.1523/JNEUROSCI.0391-14.2014 [doi]>

Suomalainen Lääkäriseura Duodecim, Societas Gerontologica Fennica, Suomen Geriatrit -yhdistys, Suomen Neurologinen Yhdistys, Suomen Psykogeriatrinen Yhdistys, & Suomen Yleislääketieteen Yhdistys, 2017. Dementia diseases: Current care guidelines. Retrieved from <https://www.kaypahoito.fi/hoi50044#K1>

Suzuki, K., 2017. Overview of deep learning in medical imaging. *Radiological Physics and Technology,* 10(3), 257–273. <doi:10.1007/s12194-017-0406-5>

Symms, M., Jäger, H. R., Schmierer, K., & Yousry, T. A., 2004. A review of structural magnetic resonance neuroimaging. *Journal of Neurology, Neurosurgery & Psychiatry,* 75(9), 1235–1244. <doi:10.1136/jnnp.2003.032714>

Tabatabaei-Jafari, H., Shaw, M. E., & Cherbuin, N., 2015. Cerebral atrophy in mild cognitive impairment: A systematic review with meta-analysis. *Alzheimer's & Dementia: Diagnosis, Assessment & Disease Monitoring,* 1(4), 487–504. <doi:10.1016/j.dadm.2015.11.002>

Teipel, S. J., Born, C., Ewers, M., Bokde, A. L. W., Reiser, M. F., Möller, H., & Hampel, H., 2007. Multivariate deformation-based analysis of brain atrophy to predict Alzheimer's disease in mild cognitive impairment. *NeuroImage,* 38(1), 13–24. <doi:10.1016/j.neuroimage.2007.07.008>

Teipel, S. J., Grothe, M., Lista, S., Toschi, N., Garaci, F. G., & Hampel, H., 2013. Relevance of magnetic resonance imaging for early detection and diagnosis of Alzheimer disease. *Medical Clinics of North America*, 97(3), 399–424. <doi:10.1016/j.mcna.2012.12.013>

Terry, R. D., & Katzman, R., 2001. Life span and synapses: Will there be a primary senile dementia? *Neurobiology of Aging,* 22(3), 347–4. <doi:S0197458000002505 [pii]>

Tessa, C., Lucetti, C., Giannelli, M., Diciotti, S., Poletti, M., Danti, S., Baldacci, F., Vignali, C., Bonuccelli, U., Mascalchi. M., & Toschi, N., 2014. Progression of brain atrophy in the early stages of Parkinson's disease: A longitudinal tensor-based morphometry study in de novo patients without cognitive impairment. *Human Brain Mapping,* 35(8), 3932–3944. <doi:10.1002/hbm.22449>

Thompson, P. M., & Apostolova, L. G., 2007. Computational anatomical methods as applied to ageing and dementia. *British Journal of Radiology,* 80(S2), S78–S91. <doi:10.1259/BJR/20005470>

Thompson, P. M., Hayashi, K. M., de Zubicaray, G., Janke, A. L., Rose, S. E., Semple, J., Herman, D., Hong, M. S., Dittmer, S. S., Doddrell, D. M., & Toga, A. W., 2003. Dynamics of gray matter loss in Alzheimer's disease. *The Journal of Neuroscience: The Official Journal of the Society for Neuroscience,* 23(3), 994–1005. <doi:23/3/994 [pii]>

Toepper, M., 2017. Dissociating normal aging from Alzheimer's disease: A view from cognitive neuroscience. *Journal of Alzheimer's Disease,* 57(2), 331–352. <doi:10.3233/JAD-161099>

Toga, A. W., Thompson, P. M., & Sowell, E. R., 2006. Mapping brain maturation. *Focus, 4*(3), 378–390. <doi:10.1176/foc.4.3.378>

Tondelli, M., Wilcock, G. K., Nichelli, P., De Jager, C. A., Jenkinson, M., & Zamboni, G., 2012. Structural MRI changes detectable up to ten years before clinical Alzheimer's disease. *Neurobiology of Aging,* 33(4), 825.e25–825.e36. <doi:10.1016/j.neurobiolaging.2011.05.018>

Trzepacz, P. T., Yu, P., Sun, J., Schuh, K., Case, M., Witte, M. M., Hochstetler, H., Hake, A., & the Alzheimer's Disease Neuroimaging Initiative, 2014. Comparison of neuroimaging modalities for the prediction of conversion from mild cognitive impairment to Alzheimer's dementia. *Neurobiology of Aging,* 35(1), 143–151. <doi:10.1016/j.neurobiolaging.2013.06.018>

Tsao, S., Gajawelli, N., Zhou, J., Shi, J., Ye, J., Wang, Y., & Leporé, N., 2017. Feature selective temporal prediction of Alzheimer's disease progression using hippocampus surface morphometry. *Brain and Behavior*, 7(7), e00733-n/a. <doi:10.1002/brb3.733>

Urs, R., Potter, E., Barker, W., Appel, J., Loewenstein, D. A., Zhao, W., & Duara, R., 2009. Visual rating system for assessing magnetic resonance images: A tool in the diagnosis of mild cognitive impairment and Alzheimer disease. *Journal of Computer Assisted Tomography,* 33(1), 73–78. <doi:10.1097/RCT.0b013e31816373d8>

Van De Pol, L., Hensel, A., Van Der Flier, W M, Visser, P. J., Pijnenburg, Y. A. L., Barkhof, F., Gerte, H. J., & Scheltens, P., 2006. Hippocampal atrophy on MRI in frontotemporal lobar degeneration and Alzheimer's disease. *Journal of Neurology, Neurosurgery and Psychiatry,* 77(4), 439–442. <doi:10.1136/jnnp.2005.075341>

Vangberg, T. R., Eikenes, L., & Håberg, A. K., 2019. The effect of white matter hyperintensities on regional brain volumes and white matter microstructure, a population-based study in HUNT. *NeuroImage,* 203, 116158. <doi:10.1016/j.neuroimage.2019.116158>

Vega, J., & Newhouse, P., 2014. Mild cognitive impairment: Diagnosis, longitudinal course, and emerging treatments. *Current Psychiatry Reports,* 16(10), 1–11. <doi:10.1007/s11920-014-0490-8>

Velayudhan, L., Proitsi, P., Westman, E., Muehlboeck, J. S., Mecocci, P., Vellas, B., Tsolaki, M., Kloszewska, I., Soininen, H., Spenger. C., Hodges, A., Powell, J., Lovestone, S., Simmons, A., & AddNeuroMed Consortium, 2013. Entorhinal cortex thickness predicts cognitive decline in Alzheimer's disease. *Journal of Alzheimer's Disease: JAD,* 33(3), 755–766. <doi:10.3233/JAD-2012-121408 [doi]>

Vemuri, P., & Jack, J., Clifford R., 2010. Role of structural MRI in Alzheimer's disease. *Alzheimer's Research & Therapy,* 2(4), 23. <doi:10.1186/alzrt47>

Veronese, E., Castellani, U., Peruzzo, D., Bellani, M., & Brambilla, P., 2013. Machine learning approaches: From theory to application in schizophrenia. *Computational and Mathematical Methods in Medicine*, 2013, 867924-12. <doi:10.1155/2013/867924>

Victoroff, J., Mack, W. J., Grafton, S. T., Schreiber, S. S., & Chui, H. C., 1994. A method to improve interrater reliability of visual inspection of brain MRI scans in dementia. *Neurology,* 44, 2267–2276.

Visser, P. J., Verhey, F. R. J., Hofman, P. A. M., Scheltens, P., & Jolles, J., 2002. Medial temporal lobe atrophy predicts Alzheimer's disease in patients with minor cognitive impairment. *Journal of Neurology, Neurosurgery & Psychiatry,* 72(4), 491–497. <doi:10.1136/jnnp.72.4.491>

Wahlund, L., Julin, P., Johansson, S., & Scheltens, P., 2000. Visual rating and volumetry of the medial temporal lobe on magnetic resonance imaging in dementia: A comparative study. *Journal of Neurology, Neurosurgery & Psychiatry*, 69(5), 630–635. <doi:10.1136/jnnp.69.5.630>

Wahlund, L., Julin, P., Lindqvist, J., & Scheltens, P., 1999. Visual assessment of medial temporal lobe atrophy in demented and healthy control subjects: Correlation with volumetry. *Psychiatry Research: Neuroimaging,* 90(3), 193–199. <doi:10.1016/S0925-4927(99)00016-5>

Wang, S., & Summers, R. M., 2012. Machine learning and radiology. *Medical Image Analysis, 16*(5), 933–951. <doi:10.1016/j.media.2012.02.005>

Watson, R., Blamire, A. M., & O'Brien, J. T., 2010. Magnetic resonance imaging in lewy body dementias. *Dementia and Geriatric Cognitive Disorders,* 28(6), 493–506. <doi:10.1159/000264614>

Wechsler, D. A. (Ed.) 1987. *Wechsler memory scale-revised: Manual.* San Antonio, Texas, United States: The Psychological Corporation & Harcourt Brace Jovanovich, Inc., U.S.

Whitwell, J. L., Przybelski, S. A., Weigand, S. D., Knopman, D. S., Boeve, B. F., Petersen, R. C., & Jack, C. R., 2007. 3D maps from multiple MRI illustrate changing atrophy patterns as subjects progress from mild cognitive impairment to Alzheimer's disease. *Brain: A Journal of Neurology,* 130(Pt 7), 1777–1786. <doi:awm112 [pii]>

Whitwell, J. L., 2010. Progression of atrophy in Alzheimer's disease and related disorders. *Neurotoxicity Research,* 18(3–4), 339–346. <doi:10.1007/s12640-010-9175-1>

Wolz, R., Julkunen, V., Koikkalainen, J., Niskanen, E., Zhang, D. P., Rueckert, D., Soininen, H., & Lötjönen, J., 2011. Multi-method analysis of MRI images in early diagnostics of Alzheimer's disease. *PloS One,* 6(10), e25446. <doi:10.1371/journal.pone.0025446>

Yi, H., Möller, C., Dieleman, N., Bouwman, F. H., Barkhof, F., Scheltens, P., van der Flier, W. M., & Vrenken, H., 2016. Relation between subcortical grey matter atrophy and conversion from mild cognitive impairment to Alzheimer's disease. *Journal of Neurology, Neurosurgery & Psychiatry,* 87(4), 425–432. <doi:10.1136/jnnp-2014-309105>

Young C. B., & Sonne J., 2018. Neuroanatomy: Basal ganglia. Treasure Island, Florida, United States: StatPearls Publishing, U.S. Retrieved from <https://www.ncbi.nlm.nih.gov/books/NBK537141/>

Zhang, W., Shi, J., Stonnington, C., Bauer, R. J., Gutman, B. A., Chen, K., Reiman, E. M., Thompson, P. M., Ye, J., & Wang, Y., 2016. Morphometric analysis of hippocampus and lateral ventricle reveals regional difference between cognitively stable and declining persons. Paper presented at the *Proceedings of IEEE 13th International Symposium on Biomedical Imaging*, 2016, 14–18. <doi:10.1109/ISBI.2016.7493200>

Zhu, G., Jiang, B., Tong, L., Xie, Y., Zaharchuk, G., & Wintermark, M., 2019. Applications of deep learning to neuro-imaging techniques. *Frontiers in Neurology,* ***10*****,** 869. <doi:10.3389/fneur.2019.00869>

UNIVERSITY OF TURKU

Painosalama Oy, Turku, Finland 2021

ISBN 978-951-29-8351-3 (PRINT)
ISBN 978-951-29-8352-0 (PDF)
ISSN 0355-9483 (Print)
ISSN 2343-3213 (Online)